行 政 院 國 家 科 學 委 員 會 補 助

專 題 研 究 計 畫 成 果 報 告

Interference Suppression and Resource Allocation for TDD/CDMA Systems

計畫編號：92-2213-E-009-023

執行機關：國立交通大學電信工程學系

計畫主持人：王蒞君 副教授

中 華 民 國 九 十 三 年 七 月

摘要

本文目的主要在於希望能夠藉由適當地運用時間與空間二個不同維度上的無線資源以期在分時雙工（Time Division Duplex, TDD）分碼多工存取（Code Division Multiple Access, CDMA）系統下充分地支援非對稱性的資料傳輸並同時提高整體系統效能。隨著非對稱性傳輸需求的日益增加，分時雙工分碼多工存取系統在未來的無線網路中將扮演著一個重要的角色。然而，由於分時雙工分碼多工存取系統中的所有細胞都使用相同的頻帶來執行資料上傳和下載，使得非對稱性的資料傳輸將會導致兩個彼此相鄰但是傳輸方向相反的基地台間產生極大的交錯時槽干擾（Cross-Slot Interference）。許多的研究顯示，交錯時槽干擾不但嚴重地影響系統效能並造成龐大無線資源的浪費。

爲了解決交錯時槽干擾的問題以增進整體系統性能，我們致力於研究各種時間上的資源分配機制以及先進天線技術（Advanced Antennas）的特點。首先，我們分析在搭配三根指向性天線所形成的三區域細胞架構下分時雙工分碼多工存取系統所接受到的干擾強度。我們發現指向性天線能夠提供給我們一個額外的自由度來分配無線傳輸資源。藉由這個特性，我們採用了虛擬細胞（Virtual Cell）的

概念。虛擬細胞被定義爲由三個相鄰基地台所組成一個和一般細胞同樣涵蓋範圍的三個區域。經由這個概念，我們更進一步提出了一個虛擬細胞爲主的分散式碼和時槽分配機制以支援分時雙工分碼多工存取系統在每一個細胞涵蓋的範圍內都能提供不同程度的非對稱性資料傳輸。

在第四章中，我們由壓制上傳時交錯時槽干擾的角度來研究四種不同波束形成設計的成效。我們比較傳統波束控制（Beam-steering）技術（設計 1）和最小變異數無失真響應（Minimum Variance Distortionless Response：MVDR）波束形成器（設計 2）的上傳位元能量對干擾密度比（Bit Energy-to-Interference Density Ratio）。設計 3 中我們更進一步同時在上傳和下載的傳輸中使用波束控制技術。在設計 4 中我們在下載傳輸中使用波束控制，而使用最小變異數無失真響應波束形成器處理在基地台所接收到的上傳訊號。許多的結果顯示設計 4 比其他三種設計能更有效率的降低分時雙工分碼多工存取系統中基地台間的交錯時槽干擾。而爲了提供較低的成本考量，在區域化細胞結構下使用較爲簡單的設計 3 也能允許每一個細胞提供不同程度的非對性資料傳輸服務。

爲了更進一步同時解決上傳和下載時的交錯時槽干擾，我們在第

五章中提出一個鏈接相對性動態通道調配（Link-proportional DCA）機制搭配三區域指向性天線的優點以減緩交錯時槽干擾對分時雙工分碼多工存取系統的影響。在指向性天線的幫助下，三區域的細胞系統將會由三個不同基地台的相鄰區域來形成一個虛擬細胞。我們發現到在這種細胞架構下，交錯時槽干擾將會被限制在一個虛擬細胞中。由此，鏈接相對性動態通道調配機制能夠在虛擬細胞中藉由使用者的無線鏈結品質來做時槽的配置以達到充分降低交錯時槽干擾的需求。許多結果都顯示鏈接相對性動態通道調配機制能夠顯著的勝過其他動態通道調配機制並能提供分時雙工分碼多工存取系統一個更有效率的資源配置法。

然而，我們發現大部分的動態通道調配機制包括鏈接相對性動態通道調配都無法有效的解決上傳時的交錯時槽干擾。爲了更進一步解決這個交錯時槽干擾，我們在第六個章節更進一步提出了一個結合第四章中智慧型天線波束形成技術的交錯時槽干擾爲主的動態通道調配機制（Cross-slot Interference-based DCA）。我們所提出的交錯時槽干擾爲主的動態通道調配機制主要希望能夠降低下載時的交錯時槽干擾並利用細胞各自分散的方式調整上傳和下載的時槽數目以其在個別細胞中充分地支援非對稱性的資料傳輸。智慧型天線的波束形成技

術在這邊將被用來對付上傳時嚴重的交錯時槽干擾。許多的結果顯示我們所提出的交錯時槽干擾爲主的動態通道調配機制能夠充分的壓制交錯時槽干擾的影響，進而使得分時雙工分碼多工存取系統能夠充分地滿足不同細胞間對於非對稱資料傳輸的個別需求並同時也能達到更高更好的系統效能。

最後，我們在第七章提出一個分頻雙工（Frequency Division Duplex, FDD）分碼多工存取大細胞下涵蓋分時雙工分碼多工存取小細胞的新型階層式細胞系統。爲了利用由於非對稱性資料傳輸而未充分運用的分頻雙工上傳時的容量，分時雙工分碼多工存取小細胞運作在涵蓋其的分頻雙工分碼多工存取大細胞上傳時的頻寬。藉著應用在基地台端所提出的陣列天線以及一個新的能量調整技術，我們仔細地評估大細胞和小細胞中的運行中斷機率。從實驗結果顯示，我們證明了能夠在不影響分頻雙工分碼多工存取大細胞的效能下充分達到分時雙工分碼多工存取小細胞的全部容量。

Summary

The key idea of this thesis is to exploit two different dimensions of radio resources - time and space - to support the diverse asymmetric traffic services in the time division duplex/code division multiple access (TDD/CDMA) systems. Since the requirement for the asymmetric data services is growing, the TDD/CDMA system has been considered an important wireless network in the future. However, different asymmetric traffic loads among cells may cause the heavy cross-slot interference, which can seriously degrade the system performance.

To alleviate the impact of cross-slot interference, we investigate the different time resource allocation algorithms and advanced antenna techniques. At first, we analyze the interference of the TDD-CDMA system with a trisector cellular architecture, where three directional antennas are employed at each base station. We find that the directivity of directional antennas can provide an additional degree of freedom for allocating radio resource. Taking advantage of this property, we introduce the concept of *virtual cell*, defined as the same converge area of a cell but is composed of three sectors from the three adjacent base stations. Furthermore, we propose a new virtual cell-based distributed code/time slot allocation algorithm to enable a TDD-CDMA system to provide asymmetric services with *different* rates of asymmetry in *every* cell coverage area.

In chapter 4, we investigate the effect of four antenna beamforming schemes from the perspective of suppressing the cross-slot interference in the uplink transmission. We compare the uplink bit energy-to-interference density ratio of a traditional beam-steering technique (Scheme I) with that of the minimum variance distortionless response (MVDR) beamformer (Scheme II). Furthermore, Scheme III applies the conventional beam-steering technique for both downlink transmissions and the uplink reception. In Scheme IV we implement beam-steering for downlink transmissions, while adopting the MVDR beamformer to process the uplink signals received at base

stations. Our numerical results indicate that Scheme IV outperforms all the other three schemes, which can effectively suppress the strong base-to-base cross-slot interference in TDD/CDMA systems. While keeping low implementation costs in mind, employing the simpler Scheme III in a sectorized cellular system can also allow every cell to provide different rates of asymmetric traffic services.

To furthermore alleviate the cross-slot interference in both uplink and downlink transmissions, we propose a novel link-proportional DCA (LP-DCA) scheme combined with tri-sector directional antennas to alleviate the impact of cross-slot interference. With the help of directional antennas, the tri-sector cellular system will form a virtual cell, the cross-slot interference is restricted within it. Thus the proposed LP-DCA scheme can concentrate on combating the cross-slot interference within a virtual cell by assigning time slots to the users according to their radio link quality. Our numerical results show that LP-DCA combined with tri-sector cellular structure can significantly reduce the cross-slot interference and improve the system performance than other DCA algorithms

Nevertheless, most DCA algorithms including LP-DCA can not effectively alleviate the uplink base-to-base cross-slot interference. To further reduce this kind of base-to-base cross-slot interference, in chapter 6, we propose a cross-slot interference-based dynamic channel assignment algorithm incorporated with antenna beamforming techniques proposed in chapter 4. The proposed cross-slot interference-based DCA algorithm aims to reduce downlink cross-slot interference and distributedly assign downlink and uplink time slots to support asymmetric traffic services in each cell. The antenna beamforming techniques adopted here are mainly to avoid the impact of heavy uplink cross-slot interference. Our numerical results show that synergy of combining the cross-slot interference-based DCA algorithm and antenna beamforming can effectively suppress the cross-slot interference in both downlink and uplink, thereby enabling a TDD/CDMA system to flexibly provide various asymmetric traffic loads in different cells and achieve high system performance.

Finally, we present a new hierarchical cellular system with an underlaid TDD/CDMA microcell and overlaying FDD/CDMA macrocells in chapter 7. With an objective to exploit the underutilized FDD uplink capacity due to traffic asymmetry, the TDD/CDMA mircocell is operated within *the uplink frequency band* of the overlaying FDD/CDMA macrocells. By jointly applying the proposed antenna arrays at the cell site and a new power ratio adjustment technique, we evaluate the outage probabilities of the macrocell and the microcell. From the simulation results, we demonstrate that the full capacity of the TDD/CDMA mircocell can be obtained without degrading the performance of FDD/CDMA marcocells.

Contents

List of Tables

List of Figures

CHAPTER 1

Introduction

The increasing demands for the higher speed wireless internet applications impose many new challenges on spectrum and radio resource management in wireless networks. One of key challenges in supporting the wireless internet services is to handle the traffic asymmetry between the uplink and the downlink. That is, some services may require more radio resources in the downlink transmission, while some services may require more uplink radio resources [1]. Hence, an intelligent radio resource allocation to support asymmetric services becomes an important topic in the future wireless networks.

1.1 Mobile Radio System

Code Division multiple access (CDMA) system is a promising radio access technique for the third-generation mobile communication systems due to its high flexibility and efficiency. In the CDMA systems, there are two different operation modes, namely frequency division duplex (FDD) and time division duplex (TDD). Comparing to the FDD-CDMA system with a pair of separated frequency bands used for downlink and uplink transmissions, the uplink and downlink transmissions in the TDD/CDMA systems multiplex the uplink and downlink time slots on the same frequency band. By exploiting the inherent time division component, time division duplex (TDD) mode is very suitable to provide asymmetric traffic services. [2, 3].

However, to support the asymmetric traffic in the TDD/CDMA system, the different asymmetric traffic conditions among cells may cause heavy *cross-slot interference*, which will seriously degrade the system performance [3–5]. Take the TDD/CDMA systems specified in the Universal Mobile Telecommunications System as an example (UMTS) [6, 7]. A TDD frame has 15 time slots, where the first one is usually used for signaling, and the others can be allocated for either the uplink or the downlink traffic channels as shown in Fig. 1.1. The boundary between the uplink and downlink time slots within a transmission frame is called the switching point. When two neighboring cells have different switching points due to distinct uplink-to-downlink traffic ratios, some time slots may be used for downlink transmissions in one cell, while being used for uplink transmissions in other cells. The opposite uplink and downlink transmissions in some time slots for two neighboring cells is called the cross-slot interference in this project. Note that in Fig. 1.1, there are two kinds of cross-slot interference: base-to-base cross-slot interference in the uplink and the mobile-to-mobile cross-slot interference in the downlink. Because the transmission power of a base station is much higher than that of a mobile terminal, the base-to-base cross-slot interference is quite significant. Meanwhile, as a mobile terminal approaches to another mobile of an adjacent cell at the cell boundary, the mobile-to-mobile cross-slot interference can not be ignored. Both types of cross-slot interference will degrade the system performance seriously [8, 9], since it is usually suggested that a time slot should be used for the same transmission direction either uplink or downlink for two neighboring cells. This constraint, however, obviously wastes time slots if traffic asymmetric ratio of two neighboring cells differs significantly. Apparently, this approach may lose the key advantages of the TDD systems in supporting asymmetric traffic services [3,10]. The key to relax this restriction is to find an effective approach to overcome the cross-slot interference in the TDD/CDMA system.

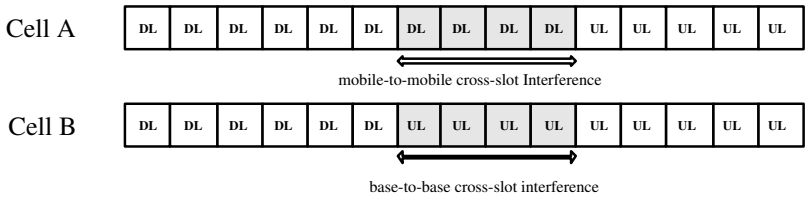

(a) TDD/CDMA frame structure

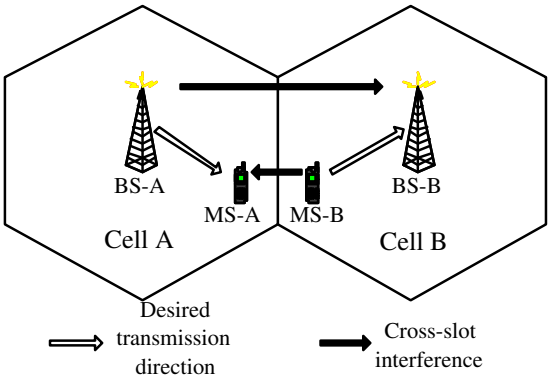

(b) cross-slot interference scenario

Figure 1.1: Frame structure and cross-slot interference in TDD/CDMA system.

In the literature, there are two research directions to avoid the cross-slot interference. The first one is to apply the dynamic channel assignment (DCA) techniques [11–13]. In [11], the authors proposed an ordered DCA algorithm to reduce the probability to use the time slot that may have a higher chance of experiencing the cross-slot interference. When the traffic load or the traffic asymmetric ratio is high, this method may have difficulty in overcoming the cross-slot interference. The authors in [12] and [13] proposed the region-based and path gain division DCA. In these algorithms, the users close to the home base station are assigned to use the time slots even having the cross-slot interference, whereas the users near the cell boundary are assigned the clean time slots without the cross-slot interference. The performance of this system will highly depend on the way of separating the inner and the outer regions. In the time-varying traffic condition, it is usually hard to accurately separate two regions with one being robust to the cross-slot interference and the other being untolerant to the cross-slot interference.

Another research direction to alleviate the impact of the opposite direction interference in TDD/CDMA systems is to apply advanced antenna techniques [14–16]. The authors in [14] proposed to adopt sector antennas combined with time slot allocation methods to suppress the opposite direction interference for the TDD/CDMA system and for the TDD/TDMA system, respectively. In [15], Choi and Murch suggested to employ a pre-rake transmitter to improve the downlink performance of the TDD/CDMA system and apply spatial diversity to improve the uplink performance. In [16], a joint space-time detection technique was presented to improve the uplink performance of the TD-SCDMA system. For overcoming the cross-slot interference in TDD/CDMA systems, we suggest combining DCA with antenna techniques to furthermore enhance the system performance.

In chapter 3, we develop an analytical framework to evaluate the interference problem of the TDD-CDMA system characterized by directional antennas and asym-

metric traffics. To our knowledge, in the context of sectorized cellular structures, the interference issues in TDD-CDMA systems with asymmetric traffic have not been fully addressed in the literature. And then we develop a resource allocation algorithm as applied to the "virtual cell" for a TDD-CDMA system. In [17], the concept of *virtual cell* was introduced, where a virtual cell consists of three neighboring sectors from three neighboring cells (e.g. sector S_1 of cell A, sector S_2 of cell C, and S_3 of cell D in Fig. 3.11). The similar concept was also proposed in [18] to reduce interference in FDD-CDMA systems. However, in the context of the TDD-CDMA system with asymmetric services, a resource allocation algorithm to explore the advantage of direction separation in the trisector cellular architecture has not been found in the literature. In this chapter, we extend the work in [17, 18] to develop such a resource allocation algorithm to resolve the cross-slot interference for the TDD-CDMA system. The basic idea of the proposed algorithm can be described in two folds. On the one hand, by employing simple sector antennas at base stations (as shown in Figure 3.11), we restrict the cross-slot interference within a cell coverage area. Applying the developed interference analysis framework, we will show that the interference between virtual cells can be suppressed due to the directivity of directional antennas. On the other hand, the cross-slot interference within a virtual cell can be resolved by a simple time slot allocation method. Hence, with trisector cellular architecture, the switching points of neighboring virtual cells can differ arbitrarily. In brief, taking advantage of this additional orthogonality from the direction separation of sector antennas, we propose a virtual cell-based interference-resolving algorithm to support asymmetric traffic services in TDD-CDMA systems.

In chapter 4, we focus on the uplink performance of TDD/CDMA systems. Compared with other categories of smart antenna technology, beamforming is known for its capability of suppressing strong interference [19, 20]. In addition, beamforming can easily exploit the reciprocity of TDD channels to leverage the benefit of

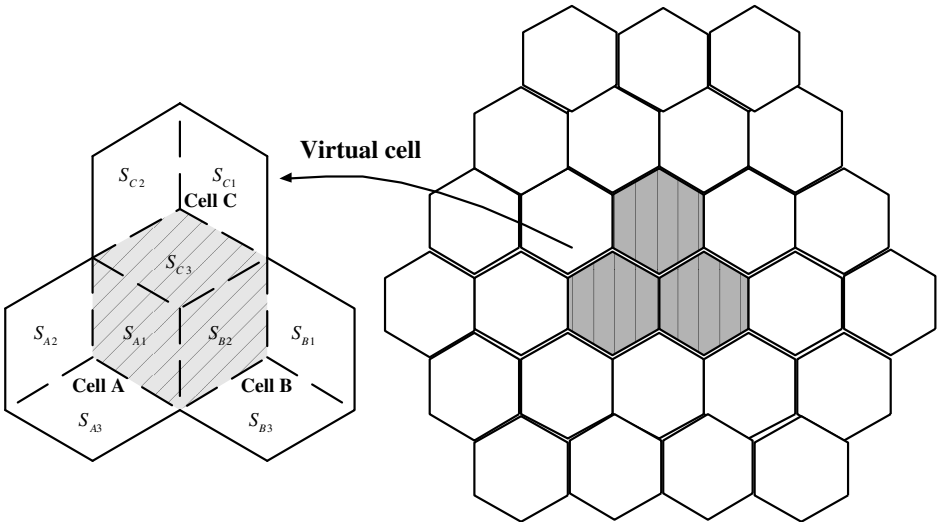

Figure 1.2: A trisector cellular system with the virtual cell.

joint downlink and uplink beamforming. Thus, beamforming is a promising technology in resolving the opposite direction interference of TDD/CDMA systems. The application of beamforming technique in FDD/CDMA systems has been studied extensively [21–23]. To our knowledge, in the context of the TDD/CDMA system with consideration of asymmetric traffic, the performance improvements by adopting antenna beamforming techniques have not been studied fully in the literature yet. The goal of this chapter is, from a system perspective of the TDD/CDMA cellular network, to investigate how to effectively apply antenna beamforming techniques to suppress the opposite direction interference. To this end, we evaluate two types of antenna beamformers: the conventional beam-steering technique and the minimum variance distortionless response (MVDR) beamformer. We will derive the received bit energy-to-interference density ratio of TDD/CDMA signals in the presence of opposite direction interference, and evaluate how these two antenna beamforming techniques can improve the performance. In addition, we exploit the channel reciprocity of TDD systems and propose to incorporate downlink transmitting beamforming at base stations. Although downlink transmitting beamforming can significantly enhance the downlink capacity of a cellular system [23, 24], it is still a challenging task to implement the optimal downlink beamforming solution. Specifically, the optimal downlink beamforming solution requires sophisticated calculations for the beamformer weights of all users and the transmission power levels of all base stations in the entire network [23, 24]. In order to get the insight of how to leverage the synergy of combining transmitting and receiving beamforming, we adopt a simpler downlink beam-steering technique in this work. We believe that the concept of simultaneously using transmitting and receiving beamformers is new in the TDD/CDMA system because the synergy of combining the downlink transmitting and uplink receiving beamforming has not been fully investigated from a system perspective, i.e., from the angle of suppressing the opposite direction interference.

Aiming to alleviate the cross-slot interference, we propose a link-proportional dynamic channel assignment scheme (LP-DCA) with sectorized antennas in Chap. 5. With the assistant of directional antennas, we utilize the concept of virtual cell composed from three neighboring sectors with the same coverage area of a cell [17]. By taking the advantages of virtual cell, we propose a effective DCA algorithm to flexibly alleviate the co-channel interference, especially for the cross-slot interference. The key idea of LP-DCA scheme is to classify the cross-slot interference and allocate the radio resource according to the users' received signal quality. The total users of a sector are sorted based on their received signal strength. We partition these sorted users into some different groups and allocate the time slots with the consideration of alleviating the cross-clot interference. Specifically, the sector with the largest downlink traffic load will allocate both the downlink and uplink groups in a ascending order from the left side of available time slots. The sector with largest uplink traffic load will allocate both the downlink and uplink groups in a ascending order from the right side of the available time slots. The sector with similar uplink and downlink traffic load will allocate the downlink groups in ascending order from left side of the available time slots and uplink groups in ascending order from right side of the available time slots. By properly allocating users, LP-DCA outperforms other DCA algorithms with high ability to alleviate the co-channel interference. Nevertheless, we find that most DCA algorithms including the LP-DCA can not effectively alleviate the base-to-base cross-slot interference [11].

To furthermore alleviate the cross-slot interference, we propose a cross-slot interference-based dynamic channel assignment scheme combined with the MVDR beamformer in chap. 6. In the proposed scheme, the DCA is focused on reducing the mobile-to-mobile cross-slot interference, while the MVDR beamformer is aiming to suppress the base-to-base cross-slot interference. To alleviate the mobile-to-mobile cross-slot interference, the basic idea of the cross-slot interference-based DCA is to

allocate time slots to users in a specific order. Specifically, for reducing the base-to-base cross-slot interference, both receiving and transmitting beamforming weights are designed according to the MVDR beamformer criterion and the fourier beamformer criterion, respectively. According to our numerical results, the cross-slot interference-based DCA can improve system performance in both downlink and uplink, while providing asymmetric traffic services with a great deal of flexibility.

Finally, we present a new hierarchical cellular system with an underlaid TDD/CDMA microcell and overlaying FDD/CDMA macrocells. With an objective to exploit the underutilized FDD uplink capacity due to traffic asymmetry, the TDD/CDMA mircocell is operated within *the uplink frequency band* of the overlaying FDD/CDMA macrocells. By jointly applying the proposed antenna arrays at the cell site and a new power ratio adjustment technique, we evaluate the outage probabilities of the macrocell and the microcell. From the simulation results, we demonstrate that the full capacity of the TDD/CDMA mircocell can be obtained without degrading the performance of FDD/CDMA marcocells.

1.2 Project Outline

The rest of this project is organized as follows. Chapter 2 reviews the document of TDD-CDMA wireless cellular systems. In chapter 3, we analyze the interference scenario in the TDD-CDMA system and evaluates the interference level with the effect of non-uniform antenna gain. Furthermore, we propose a virtual cell-based interference-resolving algorithm to take advantage of directional antennas and support asymmetric traffic services in TDD-CDMA system. In chapter 4, we investigate how to effectively apply antenna beamforming techniques from a system perspective to suppress the cross-slot interference. In chapter 5, we propose a novel link-proportional dynamic channel assignment scheme with the assistance of directional antennas. In chapter 6,

we consider a high efficient time and space resource allocation algorithm to integrate the dynamic channel assignment and the smart antenna techniques. In chapter 7, we present a new hierarchical cellular system with an underlaid TDD/CDMA microcell and overlaying FDD/CDMA macrocells. By jointly applying the proposed antenna arrays at the cell site and a new power ratio adjustment technique, we demonstrate that the full capacity of the TDD/CDMA mircocell can be obtained without degrading the performance of FDD/CDMA marcocells. Chapter 8 provides the remarks of this project and the suggestions for future work.

CHAPTER 2

Background

The wireless networks that we analyze in this thesis are introduced as follows.

2.1 Introduction to the CDMA system

The third-generation mobile radio system Universal Terrestrial Radio Access (UTRA) provides low to high data rate service, whose air interface adopted the code division multiple access (CDMA) technique to allow users transmitting in the same time. To supply both voice and data services in the CDMA system, two operating mode are applied, namely frequency division duplex (FDD) and time division duplex (TDD). Figure 2.1 illustrates the difference of frequency allocation between FDD and TDD methods. One can find that the FDD method needs a pair of frequency band for both uplink and downlink transmission, while the TDD method only need a frequency band but switch the transmission direction in time. We briefly summarize the important characteristics of the FDD-CDMA and TDD-CDMA systems in Table 2.1 as follows.

The physical frame length is similar to that of the FDD-CDMA mode, which is 10ms and divided into 15 timeslots each of 2560 chips, i.e., the duration of timeslot is 666 μs. Figure 2.2 shows the frame structure, note that the number of code channels within one time slot depends on the channel conditions. In TDD-CDMA mode, each time slot can be utilized for uplink or downlink transmission alternatively.

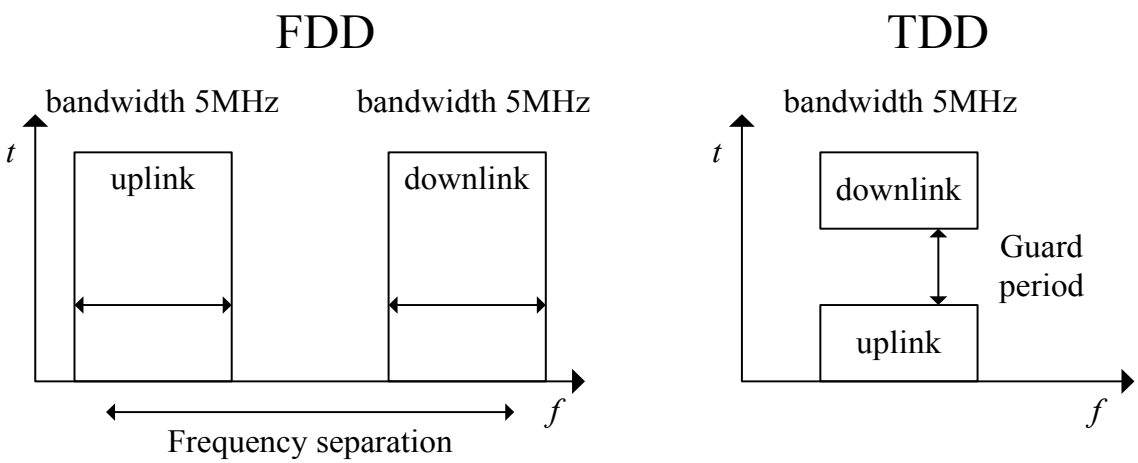

Figure 2.1: Spectrum utilization of FDD and TDD modes

Table 2.1: Comparison of UTRA FDD and TDD physical key parameters.

	UTRA TDD	UTRA FDD
Multiple access method	CDMA(inherent FDMA)	CDMA(inherent FDMA)
Duplex method	TDD (suitable for asymmetric services, e.g., web browsing.)	FDD (suitable for symmetric services, e.g., voice.)
Channel spacing	5 MHz (nominal)	
Carrier chip rate	3.84 Mcps	
Timeslot structure	15 slots/frame	
Frame length	10 ms	
Multirate concept	Multicode, multislot and orthogonal variable spreading factor (OVSF)	Multicode and OVSF
Modulation	QPSK	
Detection	Coherent, based on midamble	Coherent, based on pilot symbols
Intra-frequency handover	Hard handover	Soft handover
Inter-frequency handover	Hard handover	
Channel allocation	DCA supported	No DCA required
Intra-cell interference cancellation	Support for joint detection	Support for advanced receivers at base station

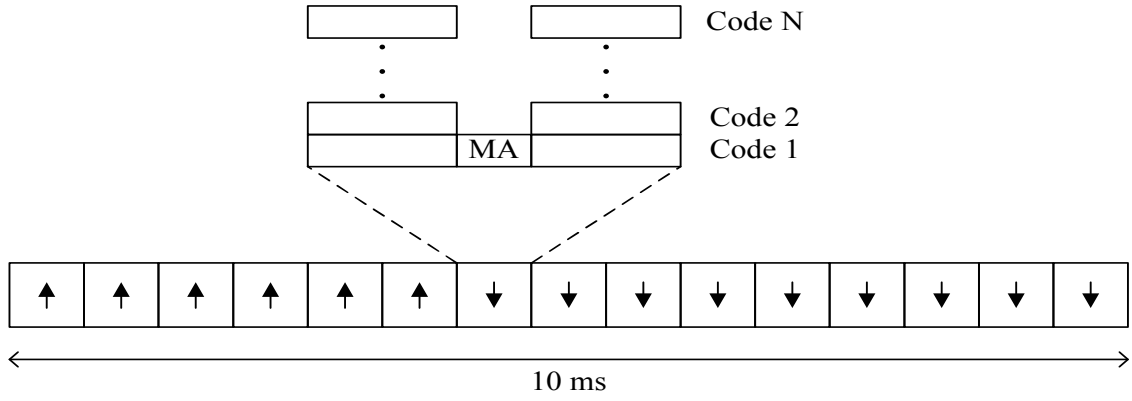

Figure 2.2: Frame structure of UTRA TDD (MA=midamble)

However, when altering the transmission direction, a guard period is needed to avoid the corruption of transmission by counting the propagation delay (as shown in Fig. 2.1). There some particular characteristics of the TDD-CDMA system listed below.

- Asymmetric uplink/downlink bandwidth allocation: In TDD mode, time slots are divided into uplink and downlink transmissions, thus it is possible to move capacity from uplink to downlink, or vice versa. By changing the duplex switching point to achieve the bandwidth requirement from users, the spectrum can be utilllized more efficiently. Nevertheless, two individual frequency band are assigned for uplink and downlinlk transmissions in FDD mode, when usrs demand the asymmetric services

- Intercell interference between uplink and downlink: Since uplink and downlink transmission share the same spectrum, the opposite transmission direction from neighboring cells can interfere with each other. Compare to the FDD-CDMA mode, this intercell interference is completely avoided by the frequency separation (as shown in Fig. 2.1). Therefore, a well designed code/time slot assignment scheme is needed to minimize this kind of intercell interference.

- Synchronization between base stations: However, not only the opposite transmission direction causes the intercell interference, but the asynchronous frame between base stations also. To avoid this interference, base stations should synchronize to each other at frame level.

- Reciprocal channel: The fast fading depends on the frequency, therefore, the channel condition is the same in uplink and downlink transmissions of the TDD mode. Based on the receiver signal, the transiver can estimate the channel condition and utilize this information in power control or adaptive modulation and coding schemes.

From above observations, we know that to minimize the intercell interference becomes an important issue in using TDD-CDMA system to deliver the asymmetric services.

CHAPTER 3

Interference Analysis and Resource Allocation for TDD-CDMA Systems to Support Asymmetric Services by Using Directional Antennas

This chapter explores the advantages of using directional antennas in time division duplex (TDD) code division multiple access (CDMA) systems to support asymmetric traffic services. In the TDD-CDMA system, the transmission for asymmetric traffic from neighboring cells may cause the cross-slot interference, which can seriously degrade system capacity. To avoid the cross-slot interference for TDD-CDMA systems, many current resource allocation algorithms typically require a global control on the transmission direction (either downlink or uplink) in each time slot. Apparently, this requirement substantially constrains the flexibility of TDD-CDMA systems to deliver asymmetric traffic services in a more practical situation where every cell may have different uplink and downlink bandwidth requirements.

We analyze the interference of the TDD-CDMA system with a trisector cellular architecture, where three directional antennas are employed at each base station. We find that the directivity of directional antennas can provide an additional degree of freedom for allocating radio resource. Taking advantage of this property, we introduce

the concept of *virtual cell*, defined as the same converge area of a cell but is composed of three sectors from the three adjacent base stations. Furthermore, we propose a new virtual cell-based distributed code/time slot allocation algorithm to enable a TDD-CDMA system to provide asymmetric services with *different* rates of asymmetry in *every* cell coverage area. We demonstrate that the proposed algorithm does not only offer more flexibility in handling non-uniform traffic patterns, but maintain good radio link performance and call blocking performance.

3.1 Introduction

Code division multiple access (CDMA) systems comprise of two operation modes, namely frequency division duplex (FDD) and time division duplex (TDD). In FDD-CDMA systems, a pair of frequency bands are used for uplink and downlink transmissions. In TDD-CDMA systems, the uplink and downlink transmissions are multiplexed into time slots on the same frequency band. The key advantage of the TDD-CDMA system is its capability of flexibly adjusting uplink and downlink bandwidth by allocating different numbers of time slots [2]. Thus, compared to the FDD-CDMA system, the TDD-CDMA system is more suitable for applications with asymmetric traffic, such as Internet browsing, file transfer, etc.

However, the transmission of asymmetric traffic from adjacent cells in the TDD-CDMA system may cause the *cross-slot interference*, which will seriously degrade system capacity. In TDD-CDMA systems, we usually define the switching point as the boundary between uplink time slots and downlink time slots within a transmission frame. If two neighboring cells have different switching points due to distinct uplink-to-downlink traffic ratios, then there may exist some time slots that are used for downlink transmissions in one cell, but for uplink transmissions in the other cell. In this chapter, we call the interference due to the opposite-direction transmissions

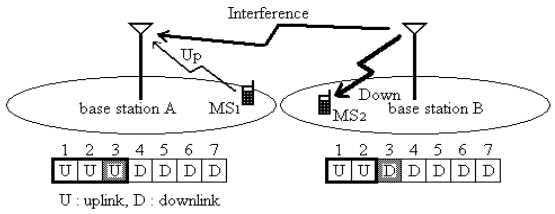

Figure 3.1: An example of cross-slot interference. In this example, during slot 3, base station B causes the cross-slot interference to MS1's transmission.

between two neighboring cells the *cross-slot interference*. Figure 3.1 illustrates a typical example of the cross-slot interference in the TDD-CDMA system. In this example, time slot 3 is used for the uplink transmission by base station A, while also being used for the downlink transmission by base station B. Note that the transmission power of a base station is much higher than that of a mobile terminal. This may interfere the reception quality of base station A. As a consequence, it is usually suggested that the *same* time slot be used for the *same* transmission direction for two neighboring cells, unless one of them is willing to leave the slot unused. Apparently, this approach may waste slot resources because neighboring cells do not necessarily have the same traffic patterns. Consequently, this requirement significantly limits the key advantages of the TDD system to support asymmetric traffic services.

In the literature, interference analysis for TDD-CDMA systems has been reported in [25–27]. In [25], the uplink interference, including the mobile-to- base and the base-to-base interference, was evaluated for the TDD-CDMA system with asymmetric traffic. It was concluded that the base-to-base interference (or called the cross-slot interference in this chapter) will significantly decrease system capacity. In [26], the authors concluded that the cross-slot interference will occur if frames are not synchronized between adjacent cells. The authors in [26] suggested using an additional antenna protection between adjacent base stations or careful network plan-

ning to reduce the base-to-base cross-slot interference. In [27], antenna beamforming techniques were suggested to suppress the cross-slot interference for the TDD-CDMA system.

To minimize the cross-slot interference in the TDD-CDMA system, many code/time slot allocation schemes have been proposed, such as [3,8,10,28,29] . In [10], the authors proposed a time slot allocation scheme that can maximize radio resource utilization subject to the constraint of having a global switching point in a multiple cell environment. In [3], the authors concluded that a TDD-CDMA system using different switching points for different cells would outperform a system using the same switching point for all cells, but it was mentioned that finding the optimal switching points is a difficult task in a multi-cell environment. In [28], an interference-resolving algorithm was proposed to allow users who are close to their serving base stations to utilize opposite transmission directions in the same slot. In [8,29], dynamic code/time slot allocation methods were suggested to minimize the cross-slot interference. However, the aforementioned works all assume that the TDD-CDMA system employs omni-directional antennas.

This chapter includes two major contributions. First, we develop an analytical framework to evaluate the interference problem of the TDD-CDMA system characterized by directional antennas and asymmetric traffics. To our knowledge, in the context of sectorized cellular structures, the interference issues in TDD-CDMA systems with asymmetric traffic have not been fully addressed in the literature. Second, we develop a resource allocation algorithm as applied to the "virtual cell" for a TDD-CDMA system. In [17], the concept of *virtual cell* was introduced, where a virtual cell consists of three neighboring sectors from three neighboring cells (e.g. sector S_1 of cell A, sector S_2 of cell C, and S_3 of cell D in Fig. 3.11). The similar concept was also proposed in [18] to reduce interference in FDD-CDMA systems. However, in the context of the TDD-CDMA system with asymmetric services, a resource allocation algorithm

to explore the advantage of direction separation in the trisector cellular architecture has not been found in the literature. In this chapter, we extend the work in [17,18] to develop such a resource allocation algorithm to resolve the cross-slot interference for the TDD-CDMA system. The basic idea of the proposed algorithm can be described in two folds. On the one hand, by employing simple sector antennas at base stations (as shown in Figure 3.11), we restrict the cross-slot interference within a cell coverage area. Applying the developed interference analysis framework, we will show that the interference between virtual cells can be suppressed due to the directivity of directional antennas. On the other hand, the cross-slot interference within a virtual cell can be resolved by a simple time slot allocation method. Hence, with trisector cellular architecture, the switching points of neighboring virtual cells can differ arbitrarily. In brief, taking advantage of this additional orthogonality from the direction separation of sector antennas, we propose a virtual cell-based interference-resolving algorithm to support asymmetric traffic services in TDD-CDMA systems.

The rest of this chapter is organized as follows. In Section 3.2, we analyze the uplink interference of the TDD-CDMA system with directional antennas and asymmetric services. Section 3.3 discusses the downlink interference analysis. Numerical results are provided in Section 3.4. In Section 3.5, we describe the concept of virtual cells and present a code/time slot assignment algorithm for the sectorized TDD-CDMA system. By exploring the directionality of sectored antennas, the proposed algorithm just needs to avoid the cross-slot interference within local areas, thereby enabling the provision of flexible asymmetric traffic services. Simulation results are all provided in Section 3.6. Finally, conclusions are given in Section 3.7.

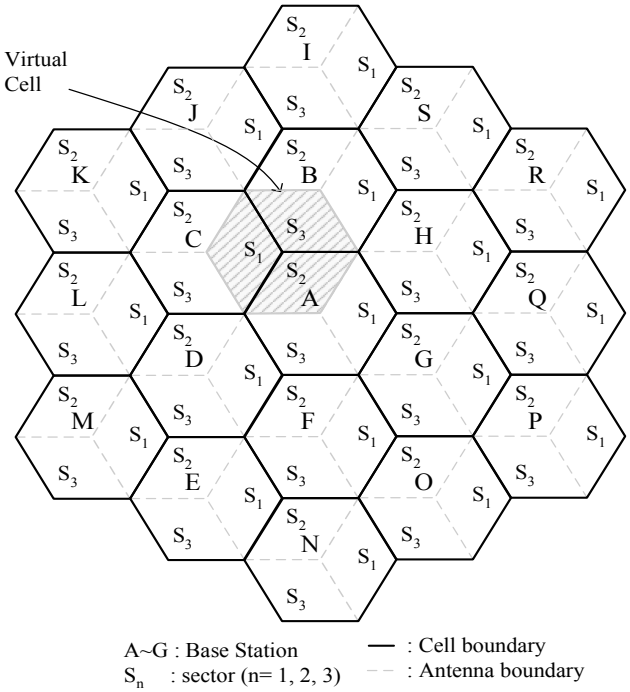

Figure 3.2: A trisector cellular system.

3.2 Uplink Interference Analysis for Base Stations

Figure 3.3 shows the uplink interference scenario of the TDD-CDMA system. Without loss of generality, take sector S_{13} of cell 1 as an example. There are four kinds of entities that will cause the uplink interference:

- the mobile stations in the same sector S_{13}, denoted as $I^{(u)}_{intra\_ms}$;
- the mobile stations in the neighboring two sectors S_{11} and S_{12}, denoted as $I^{(u)}_{intra\_ms\_v}$;
- the mobile stations in the neighboring cells O_2 and O_3, denoted as $I^{(u)}_{inter\_ms}$;
- the base-to-base cross-slot interference from the six directional antennas in O_2 and O_3, denoted as $I^{(u)}_{inter\_bs}$.

3.2.1 Intracell Interference

Assume that N mobile stations are uniformly distributed in each cell. Let p_{ms} be the received power at a base station after power control. Then the interference from the mobile stations of the same sector (i.e., sector S_{13}) can be expressed as follows

$$I^{(u)}_{intra\_ms} = \sum_{i=2}^{N/3} v_i p_{ms} \ , \tag{3.1}$$

where v_i is the activity factor for user i.

Secondly, the interference from the mobile stations of sectors S_{11} and S_{12} within the same cell can be written as

$$I^{(u)}_{intra\_ms\_v} = v\rho \ p_{ms} \sum_{\chi\in\{11,12\}} \int\int_{S_\chi} \frac{G_{13}(d_s,\theta_s)10^{\frac{\xi_s}{10}}}{G_\chi(d_s,\theta_s)10^{\frac{\xi_s}{10}}} \psi(G_{13}(d_s,\theta_s)10^{\frac{\xi_s}{10}}, G_\chi(d_s,\theta_s)10^{\frac{\xi_s}{10}})\, dxdy, \tag{3.2}$$

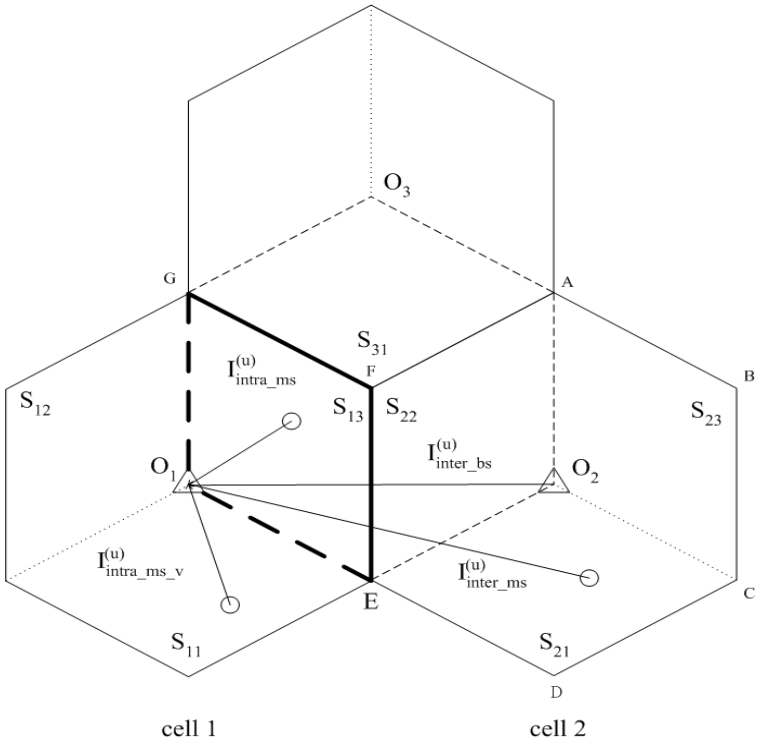

Figure 3.3: Uplink interference scenario in the TDD-CDMA system.

where $G_{13}(d_s, \theta_s)$ is the product of propagation loss and antenna gain for a user with a distance d_s and an angle θ_s to sector S_{13}, and ξ_s is the shadowing component, characterized by a Gaussian random variable with zero mean and standard deviation of σ_s dB. For example, if we consider the path loss model in [30] then,

$$G_{13}(d_s, \theta_s) = \frac{h_b^2 h_m^2 G_b(\theta_s) G_m(\theta_m)}{d_s^4}, \tag{3.3}$$

where h_b and h_m represent the antenna heights of base station and mobile terminal, respectively. Denote $G_b(\theta)$ and $G_m(\theta)$ the antenna gain betweens a base station and a mobile with the incident angle θ. Note that mobile terminals still use omni-directional antennas (i.e., $G_m(\theta) = 1,\ 0 < \theta \leq 360$). For ease of analysis, we set $h_b = 1$ and $h_m = 1$, and normalize the cell radius r_c to unity. Then the mobile stations density in each cell is $\rho = \frac{\sqrt{3}N}{6} \left(\frac{\text{mobiles}}{\text{unit area}}\right)$. Let α and β be the path loss from two base stations to a mobile terminal. The function $\psi(\alpha, \beta)$ can be used to indicate whether $\alpha \leq \beta$ or not, i.e.,

$$\psi(\alpha, \beta) = \begin{cases} 1, & \text{if } \alpha \leq \beta \\ 0, & \text{otherwise.} \end{cases} \tag{3.4}$$

For example in (3.2), if $G_{12}(d_s, \theta_s) 10^{\frac{\xi_s}{10}}$ is larger than $G_{13}(d_s, \theta_s) 10^{\frac{\xi_s}{10}}$, then the mobile terminal is served by sector S_{12}; otherwise it will be served by sector S_{13}. Note that in (3.2), $G_{13}(d_s, \theta_s) 10^{\frac{\xi_s}{10}}$ represents the link gain in sector S_{13} and $G_\chi(d_s, \theta_s) 10^{\frac{\xi_s}{10}}$ denotes the compensation factor for the link attenuation during power control in sector S_χ, where $\chi \in \{11, 12\}$. Here we adopt the same approach as in [31] to take average over v and ξ_s in (3.2). Accordingly, we obtain

$$E\left(I_{intra\_ms\_v}^{(u)}\right) = \rho\ p_{ms} E(v) \sum_{\chi \in \{11,12\}} \int\int_{S_\chi} \frac{G_{13}(d_s, \theta_s)}{G_\chi(d_s, \theta_s)}\, dxdy\ . \tag{3.5}$$

3.2.2 Intercell Interference

Let $I_{inter\_ms}^{(u)}$ represent the interference from the mobile stations of cell 2. Then, $I_{inter\_ms}^{(u)}$ can be written as[1]

$$I_{inter\_ms}^{(u)} = v\rho\ p_{ms} \sum_{\chi\in\{21,22,23\}} \int\int_{S_\chi} \frac{G_{13}(d_n,\theta_n)10^{\frac{\xi_n}{10}}}{G_\chi(d_s,\theta_s)10^{\frac{\xi_s}{10}}} \psi(G_{13}(d_n,\theta_n)10^{\frac{\xi_n}{10}}, G_\chi(d_s,\theta_s)10^{\frac{\xi_s}{10}})\, dxdy, \tag{3.6}$$

where d_n and θ_n are the distance and the angle of the interfering mobile from cell 2; d_s and θ_s are the distance and the angle to the serving sectors from cell 2's standpoint; ξ_s and ξ_n are Gaussian random variables with zero mean and standard deviation of σ_s and σ_n, respectively. Note that $(\xi_n - \xi_s)$ in (3.6) is another Gaussian distributed random variable with zero mean and a standard deviation of $\sqrt{\sigma_n^2+\sigma_s^2}$. Defining $\eta = \frac{\ln 10}{10}$ and taking the expected value of (3.6) with respect to v, ξ_n, and ξ_s, we obtain

$$E\left(I_{inter\_ms}^{(u)}\right) = \rho\ p_{ms} E(v) e^{\eta^2(\sigma_n^2+\sigma_s^2)/2}$$
$$\cdot \sum_{\chi\in\{21,22,23\}} \int\int_{S_\chi} \frac{G_{13}(d_n,\theta_n)}{G_\chi(d_s,\theta_s)} \left[1 - Q\left(\frac{\ln\left(\frac{G_\chi(d_s,\theta_s)}{G_{13}(d_n,\theta_n)}\right)}{\eta\sqrt{\sigma_n^2+\sigma_s^2}} - \eta\sqrt{\sigma_n^2+\sigma_s^2}\right)\right] dxdy, \tag{3.7}$$

where $Q(x) = \frac{1}{\sqrt{2\pi}}\int_x^\infty e^{-t^2/2}dt$.

[1]Hereafter, the subscript s and n denote the variables associated with the serving cell and the neighboring cell, respectively. For example, ξ_n is the shadowing component of the neighboring cell, and ξ_s is the shadowing component of the serving cell.

3.2.3 Base-to-Base Cross-Slot Interference

The base-to-base interference $I^{(u)}_{inter\_bs}$ can be expressed as

$$I^{(u)}_{inter\_bs} = v\rho\ p_{bs} G_{13}(\theta_3) \sum_{\chi\in\{21,22,23\}} \int\int_{S_\chi} \frac{G_\chi(2r_c,\theta_\chi)10^{\frac{\xi_{bs}}{10}}}{G_\chi(d_s,\theta_s)10^{\frac{\xi_s}{10}}} \psi(G_{13}(d_n,\theta_n)10^{\frac{\xi_n}{10}}, G_\chi(d_s,\theta_s)10^{\frac{\xi_s}{10}})\, dxdy, \tag{3.8}$$

where p_{bs} is the received power at the mobile terminal after power control, $G_{13}(\theta_3)$ is the receiver antenna gain, $2r_c$ is the separation distance between two neighboring base stations, θ_χ is the angle of transmit antenna from cell 2 to sector S_{13}. Note that referring to Fig. 3.4, for serving a user in sectors S_{21}, S_{22}, S_{23}, θ_χ is equal to $\angle DO_2O_1$, $\angle FO_2O_1$, $\angle BO_2O_1$, respectively. Furthermore, θ_3 in (3.8) is equal to $\angle FO_1O_2$. In (3.8) ξ_{bs} is the shadowing component between the two base stations with zero mean and standard deviation of σ_{bs}. Note that σ_{bs} is usually smaller than σ_n and σ_s because σ_{bs} is the shadowing component in the transmission path between two base stations. Taking average of (3.8) over v, ξ_n, ξ_s, and ξ_{bs}, we get

$$E\left(I^{(u)}_{inter\_bs}\right) = \rho\ p_{bs} E(v) e^{\eta^2(\sigma_s^2+\sigma_{bs}^2)/2} G_{13}(\theta_3) \sum_{\chi\in\{21,22,23\}} \int\int_{S_\chi} \frac{G_\chi(2r_c,\theta_\chi)}{G_\chi(d_s,\theta_s)} h\left(\frac{G_\chi(d_s,\theta_s)}{G_{13}(d_n,\theta_n)}\right) dxdy, \tag{3.9}$$

where

$$h\left(\frac{G_\chi(d_s,\theta_s)}{G_{13}(d_n,\theta_n)}\right) = \int_{-\infty}^{\infty} \frac{e^{-t^2}}{\sqrt{\pi}} Q\left(\sigma_s\eta + \frac{\sqrt{2}\sigma_n t - 10\log_{10}\left(\frac{G_\chi(d_s,\theta_s)}{G_{13}(d_n,\theta_n)}\right)}{\sigma_s}\right) dt. \tag{3.10}$$

To facilitate the computation of the numerical results in (3.9), we can apply the Hermite polynomial method of [32]. The Hermite approximation method can transfer an integration into a summation, i.e.,

$$\int_{-\infty}^{\infty} f(t)\exp(-t^2)\, dt = \sum_{i=1}^{k} w_i f(t_i) + R_k\ , \tag{3.11}$$

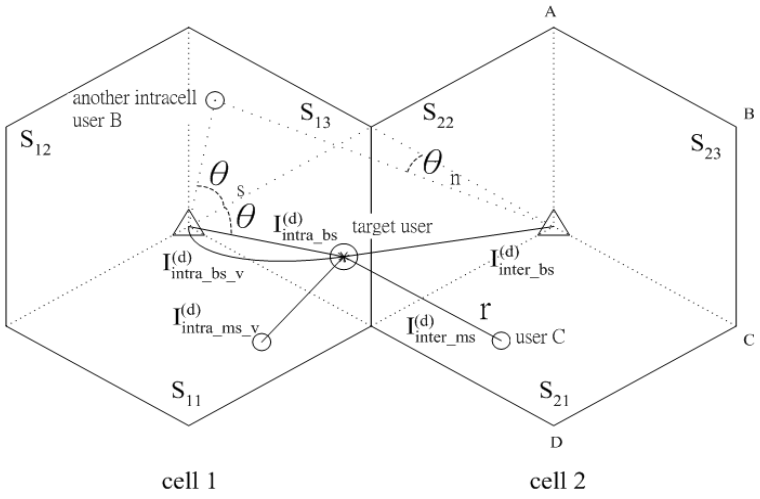

Figure 3.4: Downlink interference scenario in the TDD-CDMA system.

where t_i and w_i are pre-determined roots and weighting factors defined in [32]. Hence, we can simplify the computation of $h(\cdot)$ in (3.9) by applying (3.11) with

$$f(t) = \frac{1}{\sqrt{\pi}} Q\left(\sigma_s \eta + \frac{\sqrt{2}\sigma_n t - 10\log_{10}\left(\frac{G_\chi(d_s,\theta_s)}{G_{13}(d_n,\theta_n)}\right)}{\sigma_s} \right). \tag{3.12}$$

3.3 Downlink Interference Analysis for Mobile Terminals

Now we analyze the downlink interference as shown in Fig. 3.4. We focus on user A served by sector S_{13} of cell 1. There are five kinds of interference sources for user A:

- the interfering signals $I^{(d)}_{intra\_bs}$ from the same antenna S_{13}, but targeted at different users other than user A;
- the interfering signals $I^{(d)}_{intra\_bs\_v}$ from the neighboring antennas S_{11} and S_{12};

- the interfering signals $I^{(d)}_{inter\_bs}$ from the three directional antennas in O_2;
- the interfering signals $I^{(d)}_{intra\_ms\_v}$ from the mobile stations in the neighboring sectors S_{11} and S_{12};
- the interfering signals $I^{(d)}_{inter\_ms}$ from the mobile stations in the neighboring cell O_2.

3.3.1 Intracell Interference

The Same Sector Case

For the same antenna of the serving base station, we express $I^{(d)}_{intra\_bs}$ as

$$I^{(d)}_{intra\_bs} = v\rho\ p_{bs}\Phi_{_{S_{13}}} \int\int_{S_{13}} \frac{G_{13}(d,\theta)10^{\frac{\xi_i}{10}}}{G_{13}(d_s,\theta_s)10^{\frac{\xi_s}{10}}} \psi(G_{22}(d_n,\theta_n)10^{\frac{\xi_n}{10}}, G_{13}(d_s,\theta_s)10^{\frac{\xi_s}{10}})\ dxdy, \tag{3.13}$$

where $\Phi_{_{S_{13}}}$ is the orthogonality factor between the codes used in the same sector, $0 \leq \Phi_{_{S_{13}}} \leq 1$. In (3.13), as shown in Fig. 3.4, d and θ represent the distance and the angle of the target mobile terminal A to the base station; d_s and d_n represent the distance from another intracell user B to the serving cell and that to the neighboring cell, respectively; ξ_i is the shadowing component between the base station and the interfered mobile terminal A, which is characterized by a Gaussian random variable with zero mean and a standard deviation of σ_i. Taking average over v, ξ_n, ξ_s, and ξ_i, we can obtain

$$E\left(I^{(d)}_{intra\_bs}\right) = \rho\ p_{ms}E(v)e^{\eta^2(\sigma_s^2+\sigma_i^2)/2} \int\int_{S_\chi} \Phi_{_{S_{13}}} \frac{G_{13}(d,\theta)}{G_{13}(d_s,\theta_s)} h\left(\frac{G_{13}(d_s,\theta_s)}{G_{22}(d_n,\theta_n)}\right)\ dxdy, \tag{3.14}$$

where $h\left(\cdot\right)$ is the same as in (3.10).

The Neighboring Sector Case

The interference $I^{(d)}_{intra\_bs\_v}$ from the neighboring sectors' antennas of the serving cell can be expressed as

$$I^{(d)}_{intra\_bs\_v} = v\rho\ p_{bs} \sum_{\chi\in\{11,12\}} \int\int_{S_\chi} \frac{G_\chi(d,\theta)10^{\frac{\xi_i}{10}}}{G_\chi(d_s,\theta_s)10^{\frac{\xi_s}{10}}} \Phi_{S_\chi S_{13}} \psi(G_{13}(d_n,\theta_n)10^{\frac{\xi_n}{10}}, G_\chi(d_s,\theta_s)10^{\frac{\xi_s}{10}})\, dxdy\ , \tag{3.15}$$

where $\Phi_{S_\chi S_{13}}$ is the orthogonality factor between the codes in sectors S_χ and S_{13}. Noteworthily, by taking advantage of the separation of sector antennas, the orthogonality factor $\Phi_{S_\chi S_{13}} < 1$ in most sector antenna cases, while in the omni-directional antenna case $\Phi_{S_\chi S_{13}} = 1$. By taking average with respect to v, ξ_n, ξ_s, and ξ_i, we get

$$E\left(I^{(d)}_{intra\_bs\_v}\right) = \rho\ p_{bs} E(v) e^{\eta^2(\sigma_s^2+\sigma_i^2)/2} \sum_{\chi\in\{11,12\}} \int\int_{S_\chi} \frac{G_\chi(d,\theta)}{G_\chi(d_s,\theta_s)} \Phi_{S_\chi S_{13}} h\left(\frac{G_\chi(d_s,\theta_s)}{G_{13}(d_n,\theta_n)}\right) dxdy. \tag{3.16}$$

3.3.2 Intercell Interference

The downlink interference from the neighboring base station, $I^{(d)}_{inter\_bs}$, can be written as

$$I^{(d)}_{inter\_bs} = v\rho\ p_{bs} \sum_{\chi\in\{21,22,23\}} \int\int_{S_\chi} \frac{G_\chi(d,\theta)10^{\frac{\xi_i}{10}}}{G_\chi(d_s,\theta_s)10^{\frac{\xi_s}{10}}} \Phi_{S_\chi S_{13}} \psi(G_{13}(d_n,\theta_n)10^{\frac{\xi_n}{10}}, G_\chi(d_s,\theta_s)10^{\frac{\xi_s}{10}})\, dxdy. \tag{3.17}$$

Because of the protection from the directivity of sector antennas, $\Phi_{S_{21}S_{13}}$ and $\Phi_{S_{23}S_{13}}$ can be any values less than one as in (3.15). However, $\Phi_{S_{22}S_{13}}$ should be chosen as small as possible due to the lack of antenna separation. By taking average with

respect to v, ξ_n, ξ_s, and ξ_i, we obtain

$$E\left(I^{(d)}_{inter\_bs}\right) = \rho\ p_{bs}E(v)e^{\eta^2(\sigma_s^2+\sigma_i^2)/2} \sum_{\chi\in\{21,22,23\}} \int\int_{S_\chi} \frac{G_\chi(d,\theta)}{G_\chi(d_s,\theta_s)}\Phi_{S_\chi S_{13}} h\left(\frac{G_\chi(d_s,\theta_s)}{G_{13}(d_n,\theta_n)}\right) dxdy, \tag{3.18}$$

where $h(\cdot)$ is the same as (3.10).

3.3.3 Mobile-to-Mobile Cross-Slot Interference

The Same Cell Case

For the downlink interference $I^{(d)}_{intra\_ms\_v}$ from the mobile stations of the neighboring sector, because the omnidirectional antenna is used for mobile terminals, we ignore the antenna gain and express $I^{(d)}_{intra\_ms\_v}$ as

$$I^{(d)}_{intra\_ms\_v} = v\rho\ p_{ms} \sum_{\chi\in\{11,12\}} \int\int_{S_\chi} \frac{(r^{-4})\,10^{\frac{\xi_{ms}}{10}}}{G_\chi(d_s,\theta_s)10^{\frac{\xi_s}{10}}}\psi(G_{13}(d_s,\theta_x)10^{\frac{\xi_s}{10}}, G_\chi(d_s,\theta_s)10^{\frac{\xi_s}{10}})\,dxdy, \tag{3.19}$$

where r is the distance between the mobile terminal C in cell 2 and the interfered mobile B in cell 1, and ξ_{ms} is the shadowing component between the two mobile terminals. Taking average over v, ξ_s, and ξ_{ms}, we obtain

$$E\left(I^{(d)}_{intra\_ms\_v}\right) = \rho\ p_{ms}E(v)e^{\eta^2(\sigma_s^2+\sigma_{ms}^2)/2} \cdot \sum_{\chi\in\{11,12\}} \int\int_{S_\chi} \frac{(r^{-4})}{G_\chi(d_s,\theta_s)}\,dxdy. \tag{3.20}$$

The Other Cell Case

We can express the cross-slot interference from mobile stations of the other cells, $I^{(d)}_{inter\_ms}$, as

$$I^{(d)}_{inter\_ms} = v\rho\ p_{ms} \sum_{\chi\in\{21,22,23\}} \int\int_{S_\chi} \frac{(r^{-4})\,10^{\frac{\xi_{ms}}{10}}}{G_\chi(d_s,\theta_s)10^{\frac{\xi_s}{10}}}\psi(G_{13}(d_n,\theta_n)10^{\frac{\xi_n}{10}}, G_\chi(d_s,\theta_s)10^{\frac{\xi_s}{10}})\,dxdy. \tag{3.21}$$

Taking average over v, ξ_n, ξ_s, and ξ_{ms}, we obtain

$$E\left(I^{(d)}_{inter\_ms}\right) = \rho\ p_{ms} E(v) e^{\eta^2(\sigma_s^2+\sigma_{ms}^2)/2} \sum_{\chi\in\{21,22,23\}} \int\int_{S_\chi} \frac{(r^{-4})}{G_\chi(d_s,\theta_s)} h\left(\frac{G_\chi(d_s,\theta_s)}{G_{13}(d_n,\theta_n)}\right) dxdy. \tag{3.22}$$

Note that the computation of (3.14), (3.18), and (3.22) can be simplified by using the Hermite polynomial approach introduced in (3.11).

3.4 Effect of Directional Antenna

3.4.1 Uplink Interference

In this section, we present numerical results based on the interference analysis in Sections 3.2 and 3.3. Consider the interference scenario as shown in Fig. 3.3. Let the centers of cell 1 and cell 2 be located at $(0, 0)$ and $(2\text{ km}, 0)$, respectively, where cell radius r_c equal to 1 km. According to (3.7) and (3.9), we calculate the intercell interference of the TDD-CDMA system with omni-directional and directional base station antennas. In our simulation, we consider three different shadowing components: $\sigma_s = 9$ dB, $\sigma_n = 8$ dB, and $\sigma_{bs} = 3$ dB, where σ_s and σ_n are the standard deviations of the shadowing component between a mobile and a serving base station, and that between a mobile and the neighboring interfering base station, respectively; and σ_{bs} is that between two base stations.

Figure 3.5 shows the uplink base-to-base cross-slot interference $I^{(u)}_{inter\_bs}$ for the TDD-CDMA system with directional antennas. In the figure, points A, B, C, and D stand for the corners of cell 2 in Fig. 3.3. According to (3.9), we calculate the base-to-base interference when a mobile of cell 2 moves to different locations within the cell. The values in the z-axis represent the base-to-base interference normalized to p_{bs}, where $p_{bs} = -97$ dBm is the downlink received power at a mobile terminal

after power control. We find that if that user is located at points B, C, or D of cell 2, the base-to-base interference from cell 2 to cell 1 is reduced due to the separation of sector antennas. When the base station of cell 2 serves a particular mobile being located at point A, the base-to-base cross-slot interference will be amplified due to the directional antenna gain. Hence, using directional antennas in a trisector cellular system can restrict the strong base-to-base interference into a hexagon area labeled with A-O_2-E-O_1-G-O_3 as shown in Fig. 3.3. Consequently, the base-to-base cross-slot interference can be possibly avoided by just coordinating the switching points of downlink and uplink bandwidth ratio in only three sectors for the TDD-CDMA with the trisector cellular system.

For comparison, Fig. 3.6 shows the base-to-base cross-slot interference of the TDD-CDMA system with omni-directional antennas employed at base stations. One can find that cell 1 can very likely receive severe base-to-base cross-slot interference from cell 2 when a mobile terminal of cell 2 is located at the cell boundary, e.g., points A, B, C, and D of cell 2. Thus, unlike the trisector TDD-CDMA cellular system, the base-to-base cross-slot interference in the omni-directional cellular system will influence all the surrounding cells. Therefore, it is necessary to globally control the switching points in every cell.

Figure 3.7 shows the mobile-to-base interference $I^{(u)}_{inter\_ms}$ of (3.6) for the TDD-CDMA system with directional antennas. The values in the z-axis represent the mobile-to-base interference normalized to p_{ms}, where $p_{ms} = -112$ dBm is the uplink received power at the base station after power control. One can find that the shorter the distance to the serving base station, the less the interference to the neighboring cell. This is because at a further distance, such as point B, the mobile terminal needs to transmit higher power to compensate path loss and shadowing. Besides, because the mobile terminal still uses omni-directional antenna, the mobile-to-base interference in a system with omni-directional antennas is similar to the system with

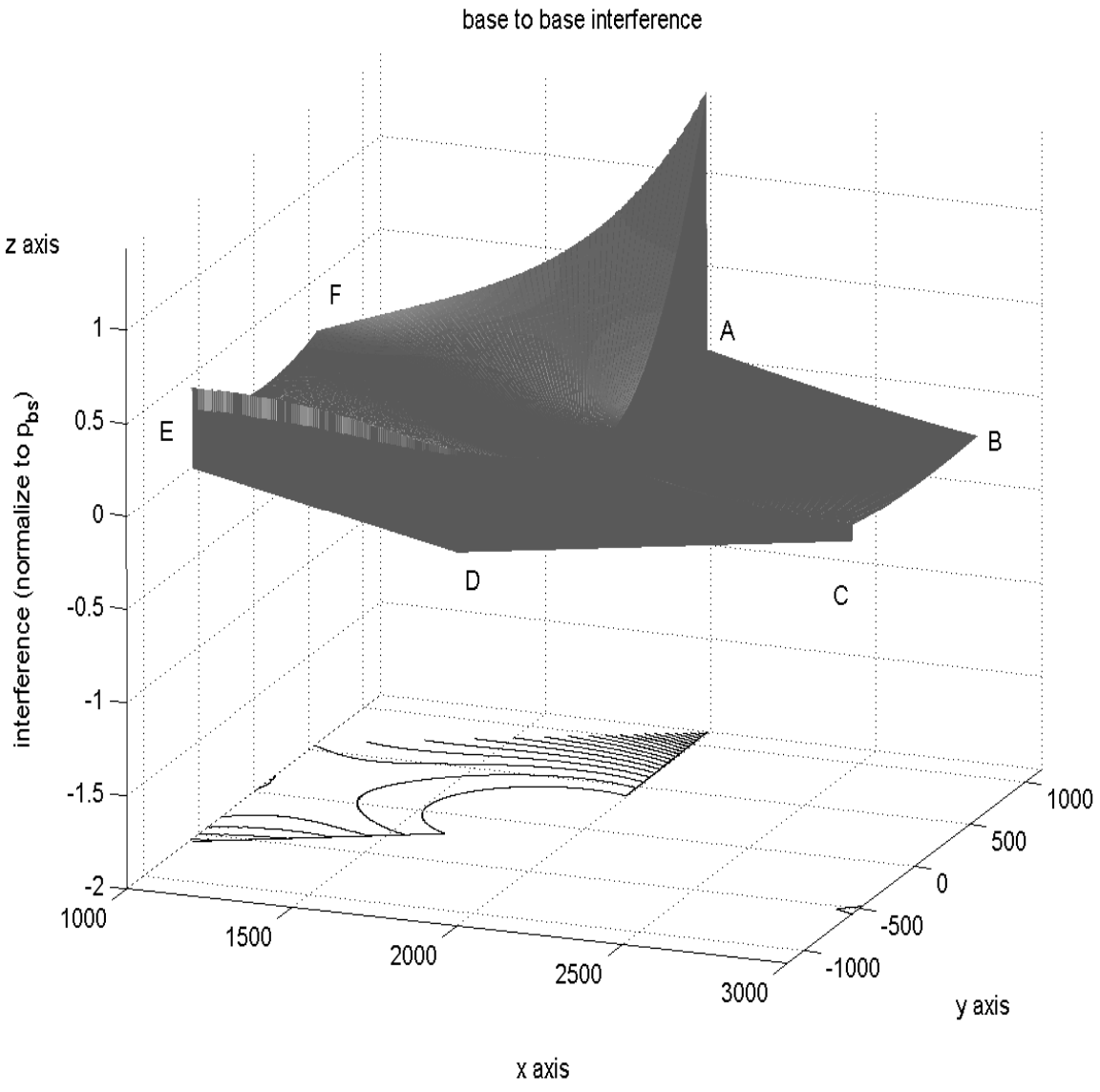

Figure 3.5: Uplink base-to-base interference from cell 2 to cell 1 with directional antenna, where p_{bs} is the downlink received power at a mobile in sector S_{13}, and points A, B, C, and D represent the corners of cell 2 in Fig. 3.3.

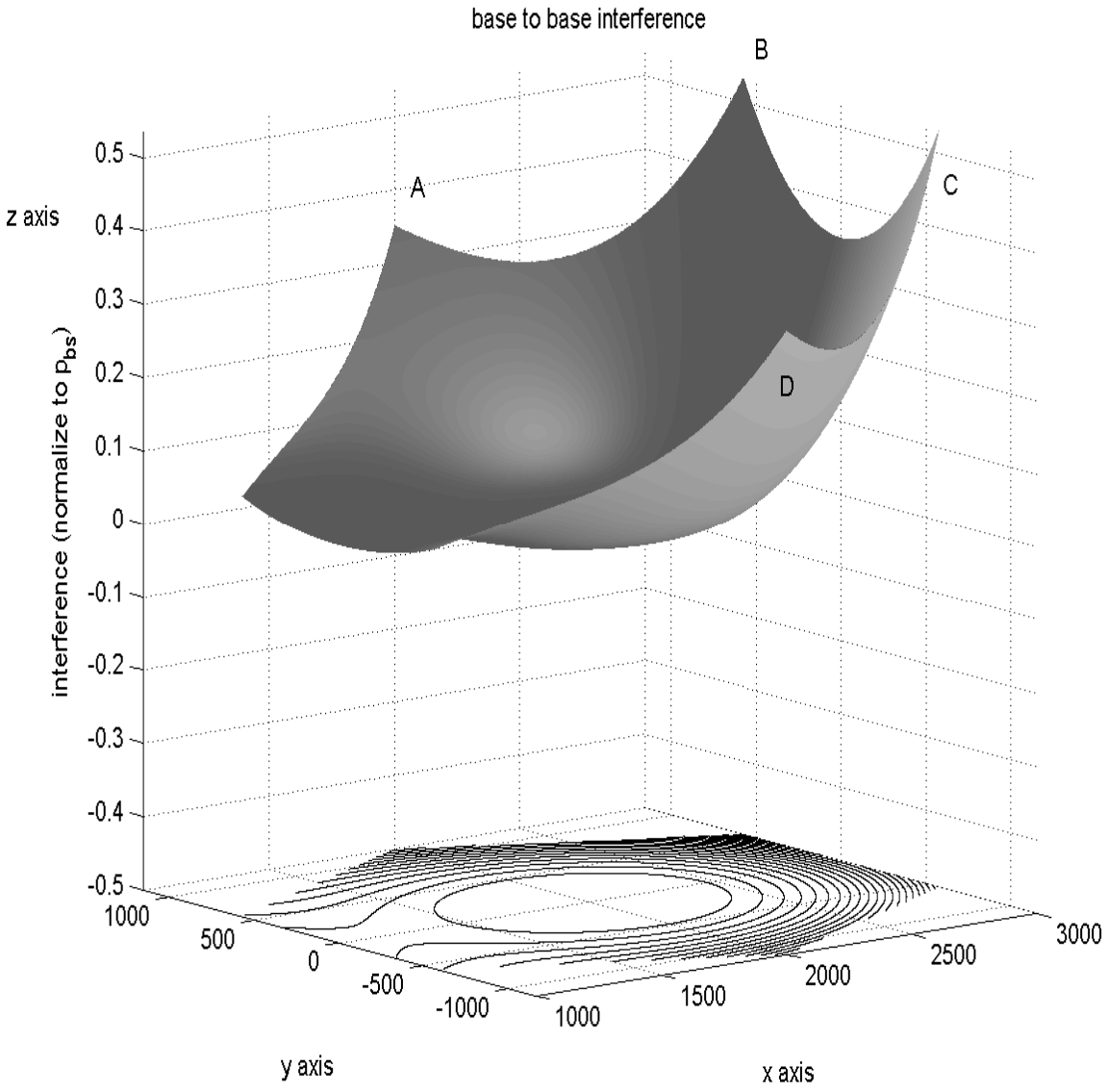

Figure 3.6: Uplink base-to-base interference from cell 2 to cell 1 with omni-directional antenna, where p_{bs} is the downlink received power at a mobile in sector S_{13}, and points A, B, C, and D represent the corners of cell 2 in Fig. 3.3.

directional antennas.

3.4.2 Downlink Interference

Now, we investigate the performance differences between the trisector TDD-CDMA cellular system and the omni-directional cellular system in terms of downlink interference. We consider the interference scenario as shown in Fig. 3.4. Let the mobile be located at (0.4 km, 0) of cell 1. We evaluate the received intercell interference of the TDD-CDMA system for the cases with omni-directional antennas and directional antennas according to (3.18) and (3.22). Denote σ_{ms} and σ_i as the standard deviation of shadowing component from the observed mobile to a nearby mobile and that to a base station, respectively. In our analysis, we adopt $\sigma_{ms} = 10$ dB and $\sigma_i = 8.5$ dB.

By evaluating (3.18), Figure 3.8 shows the base-to-mobile interference in the TDD-CDMA system with directional antennas. In the figure, points A, B, C, and D represent the corners of sectors S_{22}, S_{23}, and S_{21} in Fig. 3.4. One can see that only sector S_{22} of cell 2 will cause serious interference to cell 1, while the other sectors of cell 2 will not yield strong interference. This result indicates that in the trisector cellular system we should set the same downlink and uplink bandwidth ratio in sector S_{22} of cell 2 and sector S_{13} of cell 1. We define an area with three adjacent diamond-shaped sectors belonging to three different base stations as a *virtual cell*, which will be discussed in Section 3.5.

Figure 3.9 shows the base-to-mobile interference $I^{(d)}_{inter\_bs}$ in a system employing the omni-directional base station antenna. As shown in the figure, when the neighboring base station is serving a mobile station at a longer distance, the signal from the base station will cause very strong interference to the downlink reception quality at the target mobile station. For example, consider point B at cell 2. Unlike the small interference in the directional antennas case (i.e., 0.2 p_{bs}), the interference $I^{(d)}_{inter\_bs}$ to

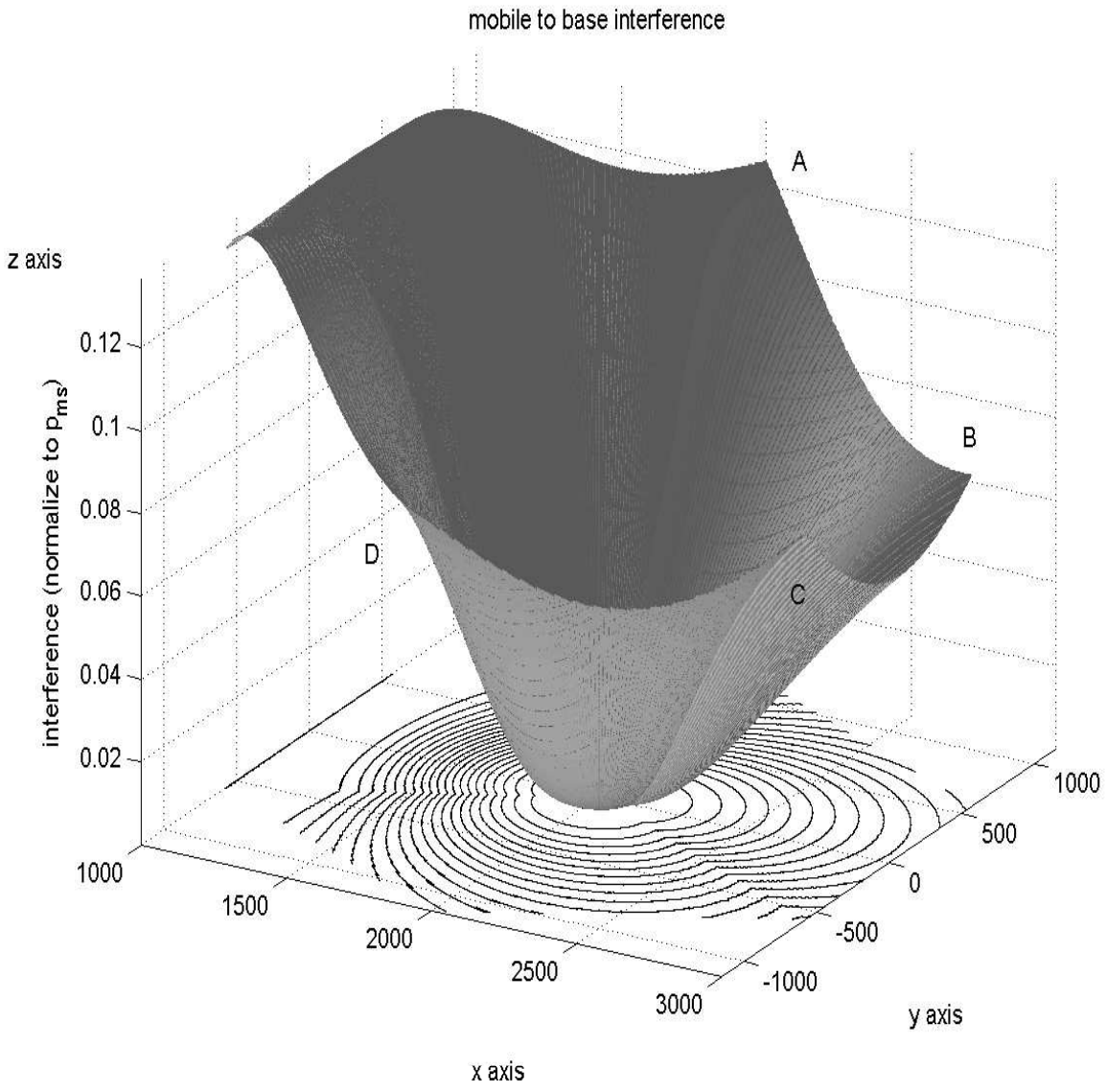

Figure 3.7: Uplink mobile-to-base interference from cell 2 to cell 1 with trisector directional antenna, where p_{bs} is the downlink received power at a mobile in sector S_{13}, and points A, B, C, and D represent the corners of cell 2 in Fig. 3.3.

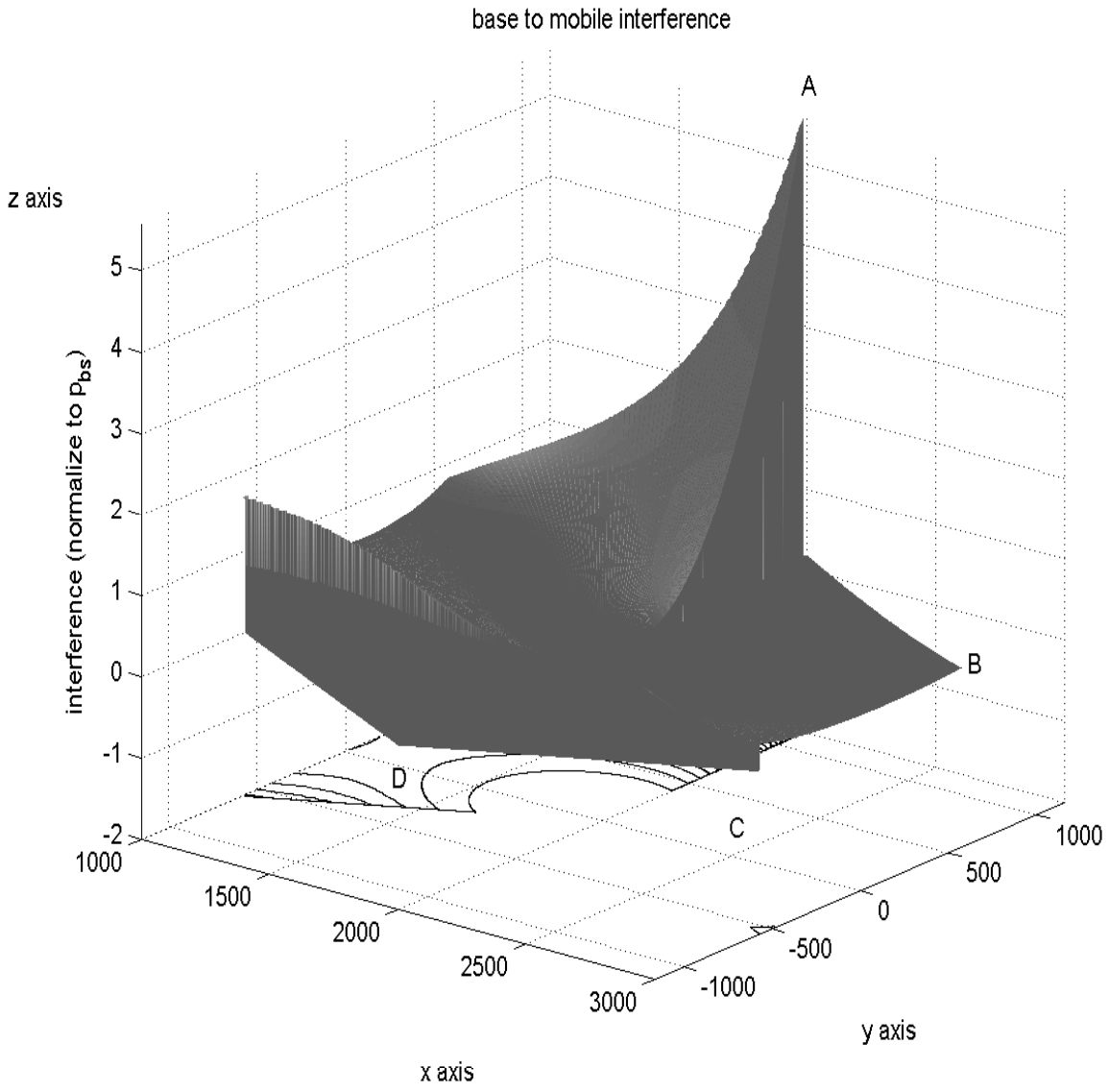

Figure 3.8: Downlink base-to-mobile interference from cell 2 to cell 1 with directional antenna, where p_{bs} is the downlink received power at a mobile in sector S_{13}, and points A, B, C, and D represent the corners of cell 2 in Fig. 3.4.

mobiles in cell 1 is 6.8 p_{bs}.

By evaluating (3.22), Fig. 3.10 shows the mobile-to-mobile cross-slot interference $I^{(d)}_{inter\_ms}$ from cell 2 in the TDD-CDMA system with directional antennas. If the transmission directions of two neighboring cells are opposite during a particular time slot, only the mobile station closer to the cell boundary of cell 2 will cause stronger cross-slot interference to a nearby mobile in cell 1. For the omni-directional cellular system, we obtain a similar result of mobile-to-mobile cross-slot interference, which is not shown here. We find that the cross-slot interference level in the omni-directional case is slightly larger than that in the directional antenna case because the transmission power from a mobile station in the omni-directional cellular system is greater than that in the trisector cellular system due to the smaller antenna gain.

3.4.3 Verification

To verify our analysis, the left part of Table I illustrates the uplink interference obtained from both analysis and simulation. By evaluating (3.7) and (3.9) according to the Hermite polynomial approach, we find that the estimated interference of the TDD-CDMA system is close to simulation results. Noteworthily, the base-to-base interference (i.e., $I^{(u)}_{inter\_bs}$) is higher than the interference from mobile terminals $I^{(u)}_{inter\_ms}$ because the transmission power of a base station is higher than that of a mobile station, i.e. $p_{bs} > p_{ms}$.

In the Table 3.4.3, we show the analytical and simulation results for downlink interference. The analysis results are obtained from (3.18) and (3.22). One can see that the cross-slot interference $I^{(d)}_{inter\_ms}$ can be quite significant as the interfering mobile terminals are close to the cell boundary although p_{bs} is 15 dB larger than p_{ms}. Thus, we are motivated to design a resource allocation scheme to coordinate the switching points within a virtual cell, i.e., an area with the three adjacent sectors

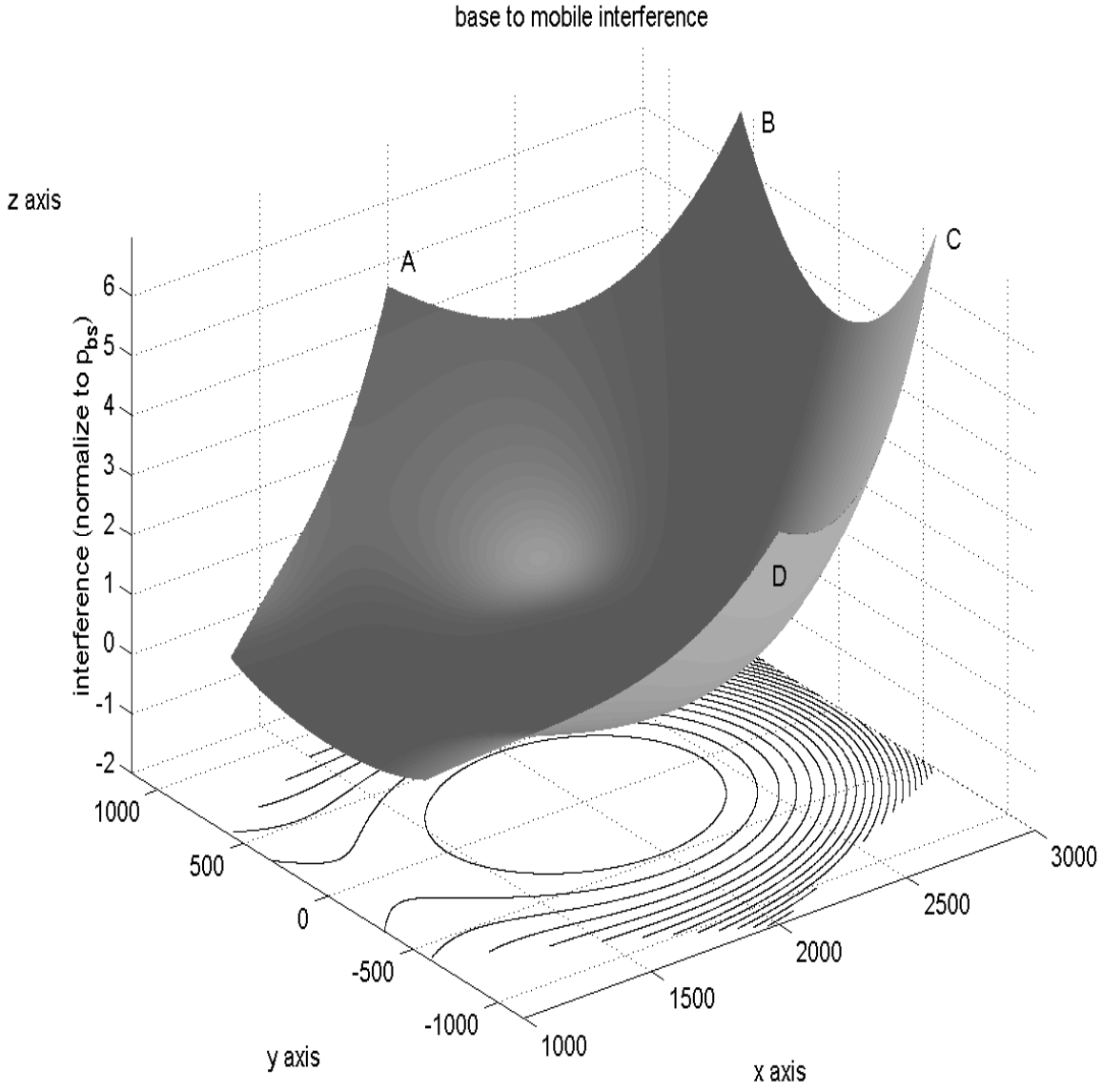

Figure 3.9: Downlink base-to-mobile interference from cell 2 to cell 1 with omni-directional antenna, where p_{bs} is the downlink received power at a mobile in sector S_{13}, and points A, B, C, and D represent the corners of cell 2 in Fig. 3.4.

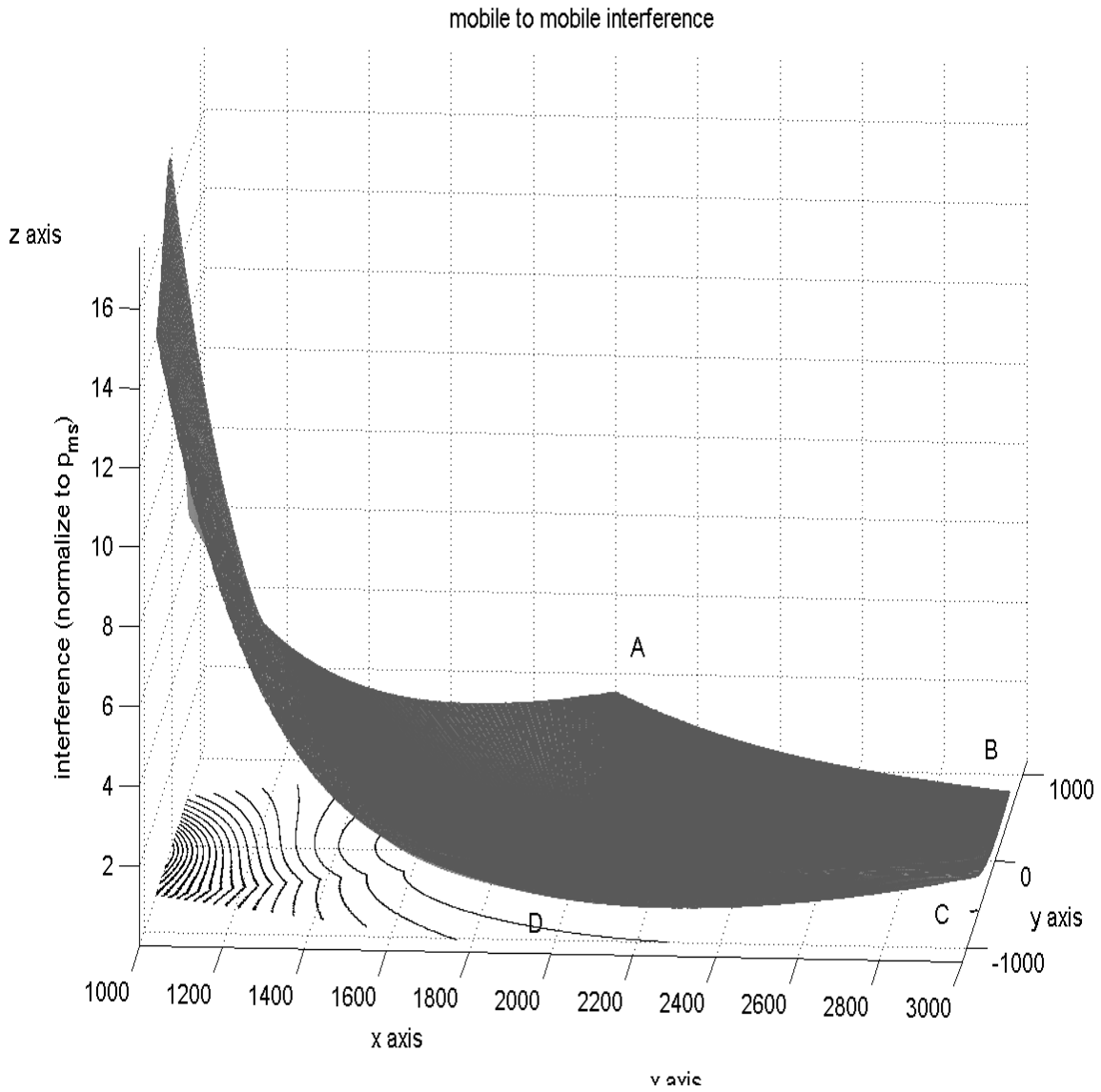

Figure 3.10: Downlink mobile-to-mobile interference from cell 2 to cell 1 with directional antenna, where p_{bs} is the downlink received power at a mobile in sector S_{13}, and points A, B, C, and D represent the corners of cell 2 in Fig. 3.4.

belonging to three different base stations. By doing so, we can avoid the mobile-to-mobile cross-slot interference for the TDD-CDMA system.

From the above observations, we find that the problem of setting switching point can be simplified from the complicated global control in the whole system to the simpler local control in only three sectors within a virtual cell. In the next section, we will present a code/time slot allocation scheme for the TDD-CDMA system to explore this advantage inherently in directional antenna.

Table 3.1: Comparison of Analysis and Simulation for Uplink and Downlink Interference.

Uplink			Downlink		
$I^{(u)}_{inter\_ms}$	Simulation	7.0999 (p_{ms})	$I^{(d)}_{inter\_ms}$	Simulation	158.1143 (p_{ms})
	Analysis	6.9223 (p_{ms})		Analysis	148.7765 (p_{ms})
	Difference	2.5652%		Difference	6.2764%
$I^{(u)}_{inter\_bs}$	Simulation	7.6744 (p_{bs})	$I^{(d)}_{inter\_bs}$	Simulation	30.5988 (p_{bs})
	Analysis	7.4540 (p_{bs})		Analysis	28.9837 (p_{bs})
	Difference	2.9571%		Difference	5.5726%

3.5 Virtual Cell-Based Code/Time Resource Allocation Algorithm

3.5.1 Concept of Virtual Cell

In the previous section, we find that with directional antennas employed at base stations, it is possible to relax the limitation of forcing neighboring cells to have the same uplink and downlink transmission directions required in the system with omni-directional antennas. Consider the trisector cellular system as shown in Figure 3.11,

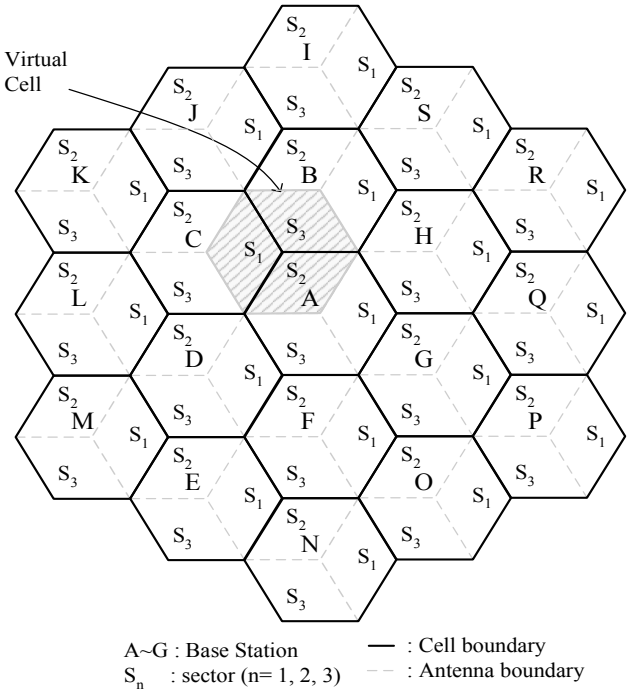

Figure 3.11: A trisector cellular system.

the uplink transmission of a user terminal at sector $\mathbf{S_2}$ of cell **A** will no longer be influenced by sector $\mathbf{S_2}$ of cells **B**, **C**, **D**, and **H**. This is because the location of cell **A** is behind the back lobe of cells B, C, D, and H. For the uplink transmission of the same user terminal, the interference from cells **F** and **G** is also lighter than that in the case with omni-direction antenna because these interfering sources face the back lobe of sector $\mathbf{S_2}$ of cell **A**. Hence, we find that the interference including the cross-slot interference in the tri-sector cellular architecture can be restricted in an area composing of three adjacent diamond-shaped sectors each of which belongs to three different cells. We call such an area in the trisector cellular system the virtual cell. The shaped area in figure 3.11 shows an example of a virtual cell, which is composed of sector $\mathbf{S_3}$ of cell **C**, sector $\mathbf{S_2}$ of cell **D**, and sector $\mathbf{S_1}$ of cell **F**.

3.5.2 Code/Time Slot Assignment Scheme

The main purpose of proposed *virtual cell*-based code/time slot assignment scheme is to set the same switching point in the three sectors of each virtual cell, while neighboring virtual cells can have different setting on their switching point. The switching point is used to divide the time frame into two groups for uplink and downlink transmissions. It also can be treated as the uplink-to-downlink ratio of a time frame. Specifically, the uplink slot assignment begins from the beginning of the frame until the switching point, and downlink slot assignment begins from the end of the frame to the switching point. Each virtual cell can support the same number of users as a regular cell in the system with omni-directional antennas, and the radio resources are shared within the three sectors in a virtual cell. Thus, to apply the virtual cell-based code/time slot assignment scheme in the TDD/CDMA system, we consider the traffic load in every diamond-shaped sector rather than a hexagon-shaped cell.

Figure 3.12 shows one probable scenario, where U_i, and D_i denotes the required uplink/downlink code/time slots of sector i in the uplink and those in the downlink, respectively. We define $L(SP)$ as the function of unsatisfied traffic requirements, and SP is the switching point, which is an integer over the interval [0,8]. For exmple, if we set SP equal to 0, $L(0)$ will equal to $U_1 + U_2 + U_3 = 10$ due to no uplink slot is allocated. On the contrary, if we set SP equal to 8, $L(8)$ will equal to $D_1+D_2+D_3 = 9$. Thus, we may find the minimum unsatisfied requirements by substituting all possible switching point setting into $L(\cdot)$. However, if $Max(U_1, U_2, U_3)+Max(D_1, D_2, D_3) < 8$, all integers over the interval $[Max(U_1, U_2, U_3), 8 - Max(D_1, D_2, D_3)]$ minimize the unsatisfied requirement.

After switching points among each virtual cell is set, the uplink slot assignment begins from the beginning of the frame until the switching point, and downlink slot

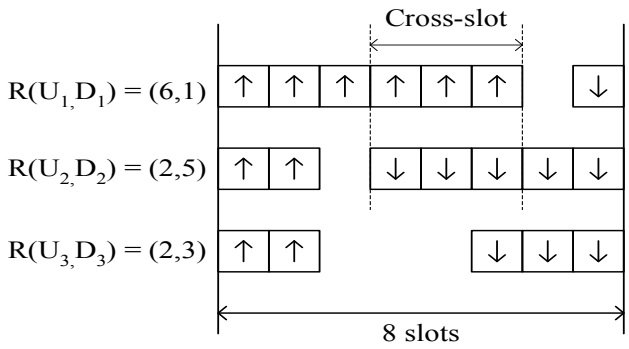

Figure 3.12: An example for setting the switching point among the virtual cell.

assignment begins from the end of the frame to the switching point. When there is a new mobile arrival, the system will allocate multi-codes within one time slot, or in the next time slot if necessary. If the remaining available code/time slots is not enough, this request from the mobile will be blocked. As shown in Fig. 3.13, we assume that a frame contains 8 time slots during each of which 4 orthogonal codes can be assigned to a user. In this example, mobile A requests two uplink time slots and five downlink time slots. Then we assign two codes in the first time slot for the uplink transmission and five codes in the last two time slots for the downlink transmission. When mobile B arrives and requests three uplink slots and four downlink slots, the remaining two codes in the first time slot and the one code in the second time slot are allocated for uplink transmissions. The remaining three codes in the seventh time slot and one code in the sixth time slot are allocated for downlink transmissions.

3.6 Simulation Results

Based on the proposed code/time slot assignment scheme, we simulate the signal-to-interference ratio (S/I) and call blocking performance in a TDD-CDMA system with

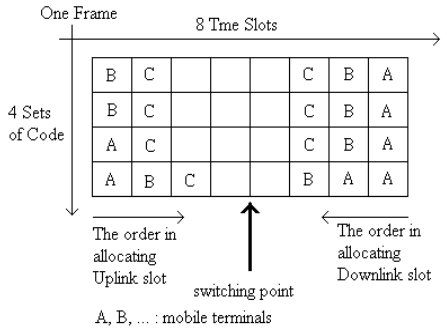

Figure 3.13: The scheme of time slot allocation.

19 cells as shown in Fig. 3.11. To demonstrate the advantage of using directional antennas in TDD-CDMA system, four kinds of slot assignment schemes are compared:

- Scheme I: the global control on the switching point setting in the TDD-CDMA system with omni-directional antennas;
- Scheme II: the distributed control on the switching point setting in the TDD-CDMA system with omni-directional antennas, where every cell has different switching point setting;
- Scheme III: the proposed virtual cell-based slot allocation algorithm in the trisector TDD-CDMA cellular system;
- Scheme IV: the sector-by-sector based switching point setting in the trisector TDD-CDMA cellular system.

In our simulation, we evaluate both the bit energy to the interference density ratio E_b/I_0 and call blocking performances in the TDD-CDMA system with directional antennas and those with omni-directional antennas, where $E_b/I_{0_{(dB)}} = S/I_{(dB)} + PG_{(dB)}$. Here we consider a processing gain $PG = 10$ dB. Assume that

the up/downlink bandwidth requirements in each sector are different as shown in Table 3.6. Let each cell have the same number of codes and time slots, i.e., a frame containing 8 time slots and 9 sets of orthogonal codes. Furthermore, we assume that every virtual cell is allowed to manage its own radio resource, To eliminate the boundary effect in simulation, we also adopt the wrap-around technique in a 19-cell environment.

Figure 3.14 compares the uplink E_b/I_0 performance of the four aforementioned slot assignment schemes. In the figure, there are two groups of curves. The curves in the right part are the E_b/I_0 performance for a system with directional antennas, and the left part is that for a system with omni-directional antennas. It is obvious that both Schemes III and IV with directional antennas outperform Schemes I and II with omni-directional antennas. Focusing on the curves of Schemes III and IV, we find that the E_b/I_0 performance of Scheme III is slightly better than Scheme IV. This is because the intercell interference is smaller in Scheme III. Though in Scheme IV the intercell interference can also be restricted in a small area, if the switching point settings of the three neighboring sectors in a virtual cell are different, the cross-slot interference among the three sectors can still degrade the 90^{th} percentile of E_b/I_0 performance by 1.5 dB compared to Scheme III. Because of the same reason, the E_b/I_0 performance of Scheme I (i.e., the omni-directional antenna case with the global control on the switching point setting) is better than Scheme II (i.e., the omni-directional antenna case with local setting). Thus, in the system with omni-directional antennas, it may be necessary to set the same switching point in all cells to avoid cross-slot interference.

Figure 3.15 compares the downlink E_b/I_0 performances of the aforementioned four time slot allocation schemes. In the figure, one can see that the E_b/I_0 performances of Schemes III and IV (the curves in the right part) outperform Schemes I and II. For example, the 90^{th} percentiles of E_b/I_0 for Schemes III and IV are 5 and 1.5 dB, respectively, while the 90^{th} percentiles of E_b/I_0 for Schemes I and II are -9

Table 3.2: Uplink and downlink traffic requirement in each sector of Fig. 3.11.

	Sector 1		Sector 2		Sector 3	
Cell	Required UL Slot	Required DL Slot	Required UL Slot	Required DL Slot	Required UL Slot	Required DL Slot
A	2	5	2	6	2	4
B	2	5	2	3	2	6
C	5	2	2	5	3	3
D	2	4	2	2	3	4
E	5	3	2	4	3	2
F	2	5	3	5	2	5
G	2	4	2	6	2	5
H	4	2	2	5	2	3
I	2	4	2	4	2	5
J	3	3	2	3	2	2
K	3	4	4	3	4	2
L	5	2	2	5	2	4
M	3	5	2	4	2	5
N	2	5	2	4	2	5
O	2	3	2	4	2	4
P	2	5	3	3	4	3
Q	5	2	3	4	4	3
R	4	2	5	2	2	5
S	2	4	3	5	2	4

and -10 dB. The performance improvements of Schemes III and IV over Schemes I and II are explained as follows. The major cross-slot interfering signals are from all the surrounding six cells in Schemes I and II, while there are only three sectors within a virtual cell causing cross-slot interference in Schemes III and IV. Besides, one can see that the E_b/I_0 performance of the two omni-directional cases are very close. This is because in Schemes I and II most interfering signals during downlink transmissions are from base stations and their interference scenarios are similar.

Figure 3.16 shows the call blocking performance of the four different allocation schemes. We can see that the proposed Scheme III has the same call blocking performance as the omni-directional antenna case, i.e. Scheme II. Recall that Scheme III aggregates all the codes/time slots of the three sectors in a virtual cell and then assigns these time slot/codes to the covered mobile terminals, while Scheme II assigns codes/time slots to mobile terminals in a cell with omni-directional antenna. Since a virtual cell has the same coverage area and the same number of codes/time slots as an omni-cell, the call blocking probability of the two schemes perform closely. However, Scheme II has poor radio link performance as shown in Figs. 3.14 and 3.15. In Scheme I, an optimal switching point setting is required for the global uplink/downlink bandwidth ratio among all the cells within the entire system. If adopting a global uplink/downlink bandwidth ratio as in Scheme I, each cell may sacrifice its actual traffic requirement, thereby causing higher call blocking than Schemes II and III. The blocking rate of Scheme IV is very high due to the decrease of trunking efficiency. Observing from Figs. 3.14, 3.15, and 3.16, we can conclude that the proposed virtual cell-based resource allocation in TDD-CDMA systems with trisector cellular architecture can have the best E_b/I_0 performance, while maintaining good blocking rate performance.

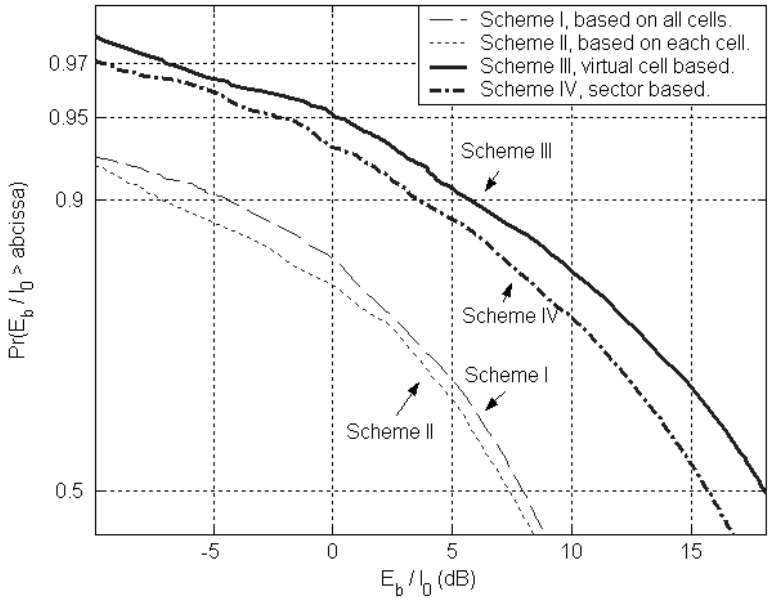

Figure 3.14: Uplink E_b/I_0 performance of slot allocation schemes in both omni-directional and trisector cellular system, where Scheme I is the global setting in omni case, Scheme II is the local setting in omni case, Scheme III is the proposed virtual cell-based case, and Scheme IV is the sector based setting in directional case.

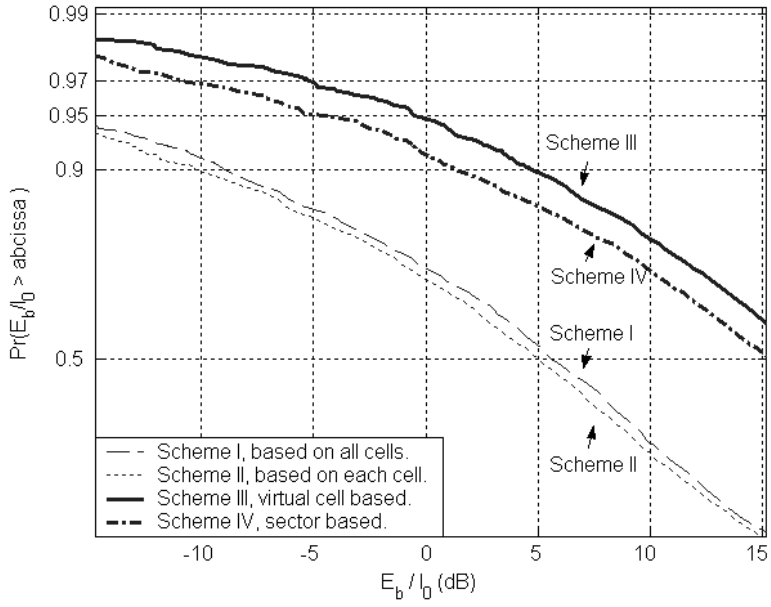

Figure 3.15: Downlink E_b/I_0 performance of slot allocation schemes in both omni-directional and trisector cellular system, where Scheme I is the global setting in omni case, Scheme II is the local setting in omni case, Scheme III is the proposed virtual cell-based case, and Scheme IV is the sector based setting in directional case.

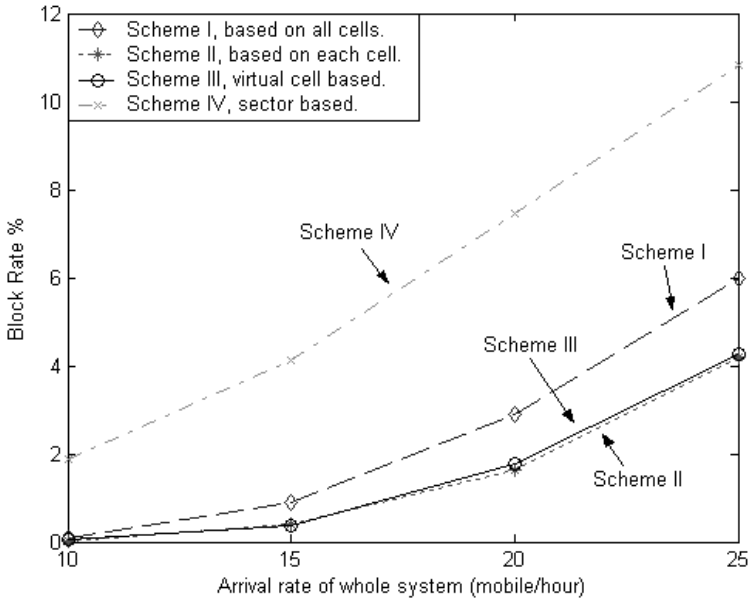

Figure 3.16: The blocking rate comparison of TDD-CDMA system between four different setting, where Scheme I is the global setting in omni case, Scheme II is the local setting in omni case, Scheme III is the proposed virtual cell-based case, and Scheme IV is the sector based setting in directional case.

CHAPTER 4

Suppressing Opposite Direction Interference in TDD/CDMA Systems with Asymmetric Traffic by Antenna Beamforming

One of the key advantages for the TDD system is the capability to deliver asymmetric traffic services by allocating different numbers of uplink and downlink time slots. However, in a TDD/CDMA system, asymmetric traffic may result in severe *opposite direction interference* because *downlink* transmitted signals from neighboring base stations may interfere with the *uplink* received signals of the home cell. In this chapter, we investigate the effect of four antenna beamforming schemes from the perspective of suppressing the opposite direction interference. We compare the uplink bit energy-to-interference density ratio of a traditional beam-steering technique (Scheme I) with that of the minimum variance distortionless response (MVDR) beamformer (Scheme II). Furthermore, Scheme III applies the conventional beam-steering technique for both downlink transmissions and the uplink reception. In Scheme IV we implement beam-steering for downlink transmissions, while adopting the MVDR beamformer to process the uplink signals received at base stations. Our numerical results indicate that Scheme IV outperforms all the other three schemes, which can ef-

fectively suppress the strong opposite direction interference in TDD/CDMA systems. While keeping low implementation costs in mind, employing the simpler Scheme III in a sectorized cellular system can also allow every cell to provide different rates of asymmetric traffic services.

4.1 Introduction

In future wireless Internet services, the traffic volume in the downlink direction is expected to be much higher than that in the uplink direction. The time division duplex (TDD) system can support asymmetric traffic services in an unpaired frequency band by allocating different numbers of time slots in the uplink and downlink [2, 17, 33]. However, in the TDD/CDMA system, because uplink and downlink transmissions share the same frequency band in every cell, additional interference can occur when a base station receives uplink signals in the time slots that are also used for downlink transmissions in other cells. Figure 4.1 illustrates a typical interference scenario in the TDD/CDMA system. Assume that cells A and B in the figure have different rates of traffic asymmetry and allocate time slots independently according to their own traffic requirements. During a particular time slot t_o, one can find that the uplink received signals at cell A may suffer strong interference from the downlink transmitted signals of the neighboring cell B. In this chapter, we call this kind of base stations to base stations interference the *opposite direction interference* because the desired signal is in the *uplink* direction, while the interference is from the *downlink* direction.

On the other hand, in time slot t_s of Fig. 4.1, the uplink transmissions from the users in cell B will interfere with the uplink signals of cell A. We call this kind of mobile stations to base stations interference the *same direction interference*. The same direction interference also occurs in FDD/CDMA systems. Many previous works, such as [31, 34], have analyzed the impact of the same direction interference. Thanks

to power control mechanisms and other techniques, the impact of the same direction interference can be effectively managed in FDD/CDMA systems. However, the opposite direction interference, which is unique in TDD/CDMA systems, is substantially different from the same direction interference. First, it is difficult to coordinate many base stations throughout the entire service area to perform downlink power control simultaneously. Moreover, since the transmitter power of a base station is much higher than that of a mobile station, the opposite direction interference introduced by the neighboring base stations will severely degrade the quality of uplink signals transmitted from a mobile station [3, 8, 25].

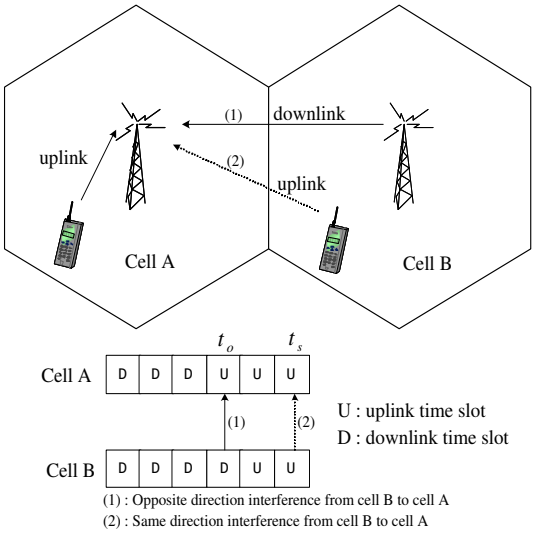

Figure 4.1: Opposite direction interference in the TDD/CDMA system.

In this chapter, we focus on the uplink performance of TDD/CDMA systems. Traditionally, to avoid the opposite direction interference in TDD/CDMA systems, we usually use different frequency carriers among adjacent cells. Obviously, this approach sacrifices frequency reuse efficiency. To use the same frequency carriers in every TDD/CDMA cell, one possible solution to avoid the opposite direction interference is to restrict all the neighboring cells to adopting the same slot allocation pattern [4],

i.e., all the assignments for either uplink or downlink transmissions in every time slot are the same. However, this approach implies that all cells will be forced to adopt the same rate of traffic asymmetry in the entire system, which is obviously not a very practical restriction. The key to relax this restriction is to overcome the opposite direction interference in the TDD/CDMA system.

In the literature, there are two research directions to avoid the opposite direction interference. The first research direction is from the perspective of channel assignment techniques, such as [3, 33]. In [33], Haas and McLaughlin proposed a dynamic channel assignment algorithm to reduce the occurrence of the opposite direction interference due to asymmetric traffic. However, the authors in [3] concluded that it may be difficult to achieve the optimal time slot allocation in an environment with multiple TDD/CDMA cells. Another research direction to alleviate the impact of the opposite direction interference in TDD/CDMA systems is to apply advanced antenna techniques [14–17]. The authors in [17] and those in [14] proposed to adopt sector antennas combined with time slot allocation methods to suppress the opposite direction interference for the TDD/CDMA system and for the TDD/TDMA system, respectively. In [15], Choi and Murch suggested to employ a pre-rake transmitter to improve the downlink performance of the TDD/CDMA system and apply spatial diversity to improve the uplink performance. In [16], a joint space-time detection technique was presented to improve the uplink performance of the TD-SCDMA system.

Compared with other categories of smart antenna technology, beamforming is known for its capability of suppressing strong interference [19, 20]. In addition, beamforming can easily exploit the reciprocity of TDD channels to leverage the benefit of joint downlink and uplink beamforming. Thus, beamforming is a promising technology in resolving the opposite direction interference of TDD/CDMA systems. The application of beamforming technique in FDD/CDMA systems has been studied

extensively [21–23]. To our knowledge, in the context of the TDD/CDMA system with consideration of asymmetric traffic, the performance improvements by adopting antenna beamforming techniques have not been studied fully in the literature yet. The goal of this chapter is, from a system perspective of the TDD/CDMA cellular network, to investigate how to effectively apply antenna beamforming techniques to suppress the opposite direction interference. To this end, we evaluate two types of antenna beamformers: the conventional beam-steering technique and the minimum variance distortionless response (MVDR) beamformer. We will derive the received bit energy-to-interference density ratio [1] of TDD/CDMA signals in the presence of opposite direction interference, and evaluate how these two antenna beamforming techniques can improve the performance.

In addition, we exploit the channel reciprocity of TDD systems and propose to incorporate downlink transmitting beamforming at base stations. Although downlink transmitting beamforming can significantly enhance the downlink capacity of a cellular system [23, 24], it is still a challenging task to implement the optimal downlink beamforming solution. Specifically, the optimal downlink beamforming solution requires sophisticated calculations for the beamformer weights of all users and the transmission power levels of all base stations in the entire network [23, 24]. In order to get the insight of how to leverage the synergy of combining transmitting and receiving beamforming, we adopt a simpler downlink beam-steering technique in this work. We believe that the concept of simultaneously using transmitting and receiving beamformers is new in the TDD/CDMA system because the synergy of combining the downlink transmitting and uplink receiving beamforming has not been fully investigated from a system perspective, i.e., from the angle of suppressing the opposite

[1] The bit energy-to-interference density ratio could be more accurately expressed as the bit energy-to-interference-plus-noise density ratio. For ease of presentation, we shall use the former term throughput the chapter.

direction interference.

In summary, the ultimate goal of this work is to examine if every cell in the TDD/CDMA system is allowed to provide asymmetric traffic services with greater flexibility, but without suffering the opposite direction interference. It is noteworthy that in this chapter we assume that the rates of traffic asymmetry of all cells are different from each other. We will investigate the effect of the following four antenna beamforming schemes:

- Scheme I: the uplink receiving beam-steering method is employed at base stations;
- Scheme II: the uplink receiving MVDR beamformer is employed at base stations;
- Scheme III: the beam-steering method is jointly applied in both the downlink transmission and uplink reception at all base stations;
- Scheme IV: the downlink transmitting beam-steering and the uplink receiving MVDR beamformer are jointly employed at all base stations.

The rest of this chapter is organized as follows. In Section 4.2, we formulate and analyze the issue of the opposite direction interference in the TDD/CDMA cellular system. In Section 4.3, we derive the uplink bit energy-to-interference density ratio for Schemes I and II. In Section 4.4, we extend our analysis to incorporate downlink transmitting beamforming (Schemes III and IV). Section 4.5 shows the numerical results of the four aforementioned beamforming schemes. In Section 4.6, we provide our concluding remarks.

4.2 System Model

In this chapter, we consider a TDD/CDMA cellular system with seven cells as shown in Fig. 7.1, where the home cell is indexed with $k = 0$ and six adjacent cells are

labelled with 1 to 6. Assume that cell 0 in the center is in the uplink mode during a particular time slot t_o. Let $\mathcal{B}_{od}$ and $\mathcal{B}_{sd}$ denote the set of the neighboring cells during time slot t_o operating in the downlink mode and those operating in the uplink mode, respectively. Figure 7.1 illustrates an example with $\mathcal{B}_{od} = \{2, 4, 6\}$ and $\mathcal{B}_{sd} = \{1, 3, 5\}$. In this example, downlink transmissions of cells 2, 4, and 6 will cause the opposite direction interference (i.e., the base stations to base stations interference) to the uplink receiving signals of cell 0, while cells 1, 3, and 5 result in the same direction interference (i.e., the mobile stations to base stations interference).

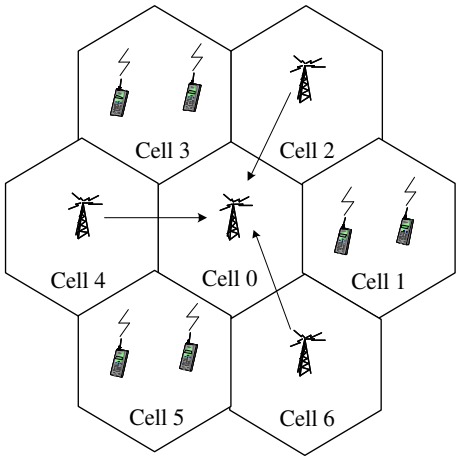

Figure 4.2: An example to illustrate the interference scenario in the TDD/CDMA system, where $\mathcal{B}_{od} = \{2, 4, 6\}$ represents the set of the neighboring cells generating the opposite direction interference and $\mathcal{B}_{sd} = \{1, 3, 5\}$ represents the cells generating the same direction interference.

In our model, we consider propagation loss and log-normal distributed shadowing. Then the link gain $G(r, \alpha)$ between the transmitter and receiver is described as

$$G(r, \alpha) = \kappa_0 r^{-m} 10^{\alpha/10} \ , \tag{4.1}$$

where r is the propagation distance, κ_0 is a constant, m is the path loss exponent and

α is a normal distributed random variable with zero mean and standard deviation of σ dB. Let P_T be the total transmit power of a base station, and d_k the distance from cell k ($k \in \mathcal{B}_{od}$) to the home cell. Then the total opposite direction interference introduced by the adjacent cells is equal to

$$I_{od} = \sum_{k \in \mathcal{B}_{od}} P_T G(d_k, \alpha_k) \ . \tag{4.2}$$

Assume that uplink power control is ideally executed so that the received signal power of each mobile user is maintained at a constant level P_r at base stations. Then the same direction interference introduced by mobile i_k of $\mathcal{B}_{sd}$ ($k \in \mathcal{B}_{sd}$) is equal to

$$\begin{aligned} I_{i_k} &= P_r G(r_0, \alpha_0)/G(r_{i_k}, \alpha_{i_k}) \\ &= P_r \left(\frac{r_{i_k}}{r_0}\right)^m 10^{(\alpha_0 - \alpha_{i_k})/10} \ , \end{aligned} \tag{4.3}$$

where r_0 and r_{i_k} are the distance from mobile i_k of $\mathcal{B}_{sd}$ to cell 0 and that to cell k ($k \in \mathcal{B}_{sd}$), respectively. For ease of notation, let

$$\beta_{i_k} = \left(\frac{r_{i_k}}{r_0}\right)^m 10^{(\alpha_0 - \alpha_{i_k})/10}. \tag{4.4}$$

Note that the term $\alpha_0 - \alpha_{i_k}$ in (4.4) can be represented by another normal distributed random variable with a modified standard deviation [34]. Let N_k denote the number of mobile users in cell k ($k \in \mathcal{B}_{sd}$) that are in their uplink transmission cycles during a particular time slot t_o. Then from (4.3) and (4.4), the total same direction interference introduced by adjacent cells can be expressed by

$$\begin{aligned} I_{sd} &= \sum_{k \in \mathcal{B}_{sd}} \sum_{i_k=1}^{N_k} I_{i_k} \\ &= \sum_{k \in \mathcal{B}_{sd}} \sum_{i_k=1}^{N_k} P_r \beta_{i_k} \ . \end{aligned} \tag{4.5}$$

In addition to the opposite direction and the same direction interfering signals, there still exists the intracell interference in the TDD/CDMA system, denoted as I_{ic}. Since power control is assumed to be ideal, the received signal power of all users in a cell will be maintained at a constant level P_r. Thus, I_{ic} can be expressed as

$$I_{ic} = P_r(N_0 - 1) \ , \tag{4.6}$$

where N_0 is the number of mobile users in the home cell that are transmitting uplink signals in time slot t_o. Thus, based on the definitions of I_{od}, I_{sd}, and I_{ic} corresponding to (4.2), (4.5) and (4.6), respectively, the uplink received bit energy-to-interference density ratio γ_i for a target mobile i in the home cell can be written as

$$\gamma_i = \frac{LP_r}{I_{od} + I_{sd} + I_{ic} + \eta} \ , \tag{4.7}$$

where L is the processing gain and η is the white thermal noise power. In the next section, we will further derive the expression of γ_i with consideration of the effect of antenna beamforming.

4.3 Interference Analysis with Beamforming

In this section, we investigate how antenna beamforming can improve the performance of TDD/CDMA systems. We consider the conventional beam-steering method and the minimum variance distortionless response (MVDR) beamformer. The reasons why these two beamformers are studied in this chapter are explained as follows. From the viewpoint of implementation, the beam-steering technique is the most economical and practical solution because of its simplicity. In [22], the authors demonstrated that remarkable capacity gain can be achieved for FDD/CDMA systems by using this kind of beamformer. In this chapter, the beam-steering technique is evaluated to provide the baseline performance for comparison. As for the MVDR beamformer, it is well

known for its capability of suppressing strong interference [35]. In [36], it is shown that the MVDR criterion can lead to the optimal solution in the sense of maximizing the output signal to interference plus noise ratio. Thus, in our chapter, the MVDR beamformer is evaluated to give a performance upper bound for the TDD/CDMA system with antenna beamforming techniques.

4.3.1 Generic Interference Analysis

To begin with, we first derive the expression of the received bit energy-to-interference density ratio with a generic antenna beamformer. Assume an M-element uniform circular array (UCA) is employed at a base station. The array manifold vector (or steering vector) of an UCA is written as [35]

$$\mathbf{a}(\theta,\phi) = \frac{1}{\sqrt{M}} \begin{bmatrix} e^{j2\pi l/\lambda \sin\phi\cos\theta} \\ e^{j2\pi l/\lambda \sin\phi\cos(\theta-2\pi/M)} \\ \vdots \\ e^{j2\pi l/\lambda \sin\phi\cos(\theta-2\pi(M-1)/M)} \end{bmatrix} , \tag{4.8}$$

where l is the radius of the circular antenna array, λ the wavelength, θ the azimuth angle, and ϕ the vertical angle. The factor $1/\sqrt{M}$ in (4.8) is a normalization factor such that $\mathbf{a}^H\mathbf{a} = 1$, where $[\cdot]^H$ denotes the complex transpose conjugate. In this chapter, we assume that l is equal to half the wavelength and the vertical angle ϕ is equal to $\pi/2$.

Let $\mathbf{x}(t) = [x_1(t), x_2(t), \cdots, x_M(t)]^T$ be the received signal vector at an M-element antenna array. Then $\mathbf{x}(t)$ can be written as

$$\mathbf{x}(t) = \mathbf{x}_i(t) + \mathbf{x}_{od}(t) + \mathbf{x}_{sd}(t) + \mathbf{x}_{ic}(t) + \mathbf{n}(t) \ , \tag{4.9}$$

where $\mathbf{x}_i(t)$ is the desired signal for user i, $\mathbf{x}_{od}(t)$ is the opposite direction interference, $\mathbf{x}_{sd}(t)$ is the same direction interference, $\mathbf{x}_{ic}(t)$ is the intracell interference and $\mathbf{n}(t)$ is

the white noise. Specifically, $\mathbf{x}_{od}(t)$ in (4.9) is given by

$$\mathbf{x}_{od}(t) = \sum_{k \in \mathcal{B}_{od}} \sqrt{P_T G(d_k, \alpha_k)} \mathbf{b}_k \ , \tag{4.10}$$

where $\mathbf{b}_k$ is the array manifold vector for the signals arriving from cell k ($k \in \mathcal{B}_{od}$). Meanwhile, $\mathbf{x}_{sd}(t)$, $\mathbf{x}_{ic}(t)$ and $\mathbf{x}_i(t)$ can be respectively expressed as

$$\mathbf{x}_{sd}(t) = \sum_{k \in \mathcal{B}_{sd}} \sum_{i_k=1}^{N_k} \sqrt{P_r \beta_{i_k}} u_{i_k} \left(\left\lfloor \frac{t - \tau_{i_k}}{T} \right\rfloor \right) c_{i_k}(t - \tau_{i_k}) \mathbf{a}_{i_k} \ , \tag{4.11}$$

$$\mathbf{x}_{ic}(t) = \sum_{i_0 \neq i}^{N_0} \sqrt{P_r} u_{i_0} \left(\left\lfloor \frac{t - \tau_{i_0}}{T} \right\rfloor \right) c_{i_0}(t - \tau_{i_0}) \mathbf{a}_{i_0} \ , \tag{4.12}$$

and

$$\mathbf{x}_i(t) = \sqrt{P_r} u_i \left(\left\lfloor \frac{t - \tau_i}{T} \right\rfloor \right) c_i(t - \tau_i) \mathbf{a}_i \ . \tag{4.13}$$

In (4.11)–(4.13), $\mathbf{a}_{i_k}$ is the array manifold vector for the signals arriving from mobile i_k of cell k; $u_{i_k}(\cdot)$ is the bit waveform with a period T; τ_{i_k} is the propagation delay; $c_{i_k}(\cdot)$ is the spreading code; P_r and β_{i_k} are already defined in (4.3) and (4.4).

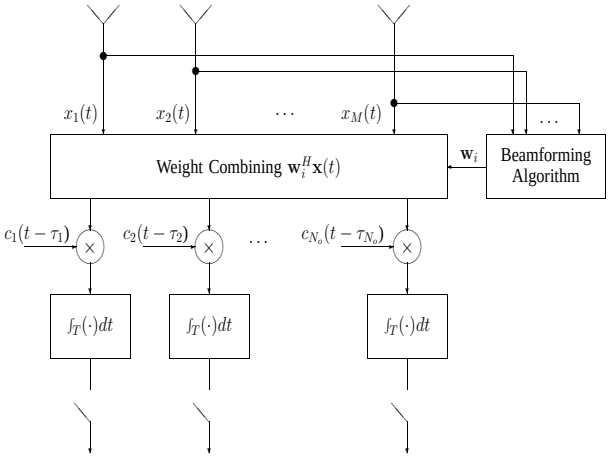

Figure 4.3: A receiver block diagram with antenna beamformers.

Figure 4.3 shows the receiver block diagram of an antenna beamformer. In Fig. 4.3 the received signal $\mathbf{x}(t)$ for a target user i ($i = 1, \cdots, N_0$) is first combined with

the beamformer weights $\mathbf{w}_i$. After weight combining, the output signal $\mathbf{w}_i^H \mathbf{x}(t)$ is connected to the despreader with processing gain L. Assume that the code sequences of different users are mutually uncorrelated. Then the opposite direction interference I_{od} in (4.2), the same direction interference I_{sd} in (4.5) and the intracell interference I_{ic} in (4.6) become

$$I_{od} = \sum_{k \in \mathcal{B}_{od}} P_T G(d_k, \alpha_k) \|\mathbf{w}_i^H \mathbf{b}_k\|^2 \ , \tag{4.14}$$

$$I_{sd} = \sum_{k \in \mathcal{B}_{sd}} \sum_{i_k=1}^{N_k} P_r \beta_{i_k} \|\mathbf{w}_i^H \mathbf{a}_{i_k}\|^2 \ , \tag{4.15}$$

and

$$I_{ic} = \sum_{i_0 \neq i}^{N_0} P_r \|\mathbf{w}_i^H \mathbf{a}_{i_0}\|^2 \ , \tag{4.16}$$

respectively.

By substituting (4.14), (4.15) and (4.16) into (4.7), the bit energy-to-interference density ratio of mobile i with antenna beamforming becomes

$$\begin{aligned} \gamma_i \ = \ & LP_r \left\{ \sum_{k \in \mathcal{B}_{od}} P_T G(d_k, \alpha_k) \|\mathbf{w}_i^H \mathbf{b}_k\|^2 + \sum_{k \in \mathcal{B}_{sd}} \sum_{i_k=1}^{N_k} P_r \right. \\ & \left. \cdot \beta_{i_k} \|\mathbf{w}_i^H \mathbf{a}_{i_k}\|^2 + \sum_{i_0 \neq i}^{N_0} P_r \|\mathbf{w}_i^H \mathbf{a}_{i_0}\|^2 + \eta \right\}^{-1} \ . \end{aligned} \tag{4.17}$$

Next we will investigate the effect of two specific beamformer algorithms, i.e., the beam-steering method and the MVDR beamformer.

4.3.2 Conventional Beam-Steering Technique (Scheme I)

Scheme I adopts the conventional beam-steering algorithm. According to the beam-steering method, we know that the beamformer weight $\mathbf{w}_{bs}$ for user i is equal to its array manifold vector [35], i.e.,

$$\mathbf{w}_{bs} = \mathbf{a}_i \ , \tag{4.18}$$

where $\mathbf{a}_i$ is defined in (4.8). As a result, the bit energy-to-interference density ratio after applying beam-steering (denoted as γ_{bs}) becomes

$$\gamma_{bs} = LP_r \left\{ \sum_{k\in\mathcal{B}_{od}} P_T G(d_k,\alpha_k)\|\mathbf{a}_i^H\mathbf{b}_k\|^2 + \sum_{k\in\mathcal{B}_{sd}}\sum_{i_k=1}^{N_k} P_r \cdot\beta_{i_k}\|\mathbf{a}_i^H\mathbf{a}_{i_k}\|^2 + \sum_{i_0\neq i}^{N_0} P_r\|\mathbf{a}_i^H\mathbf{a}_{i_0}\|^2 + \eta \right\}^{-1} . \quad (4.19)$$

The effect of utilizing the conventional beam-steering technique (Scheme I) is equivalent to steering a beam of signals concentrating at the desired direction. By controlling the direction of the receiving beam to track the position of the target mobile station, the beam-steering technique can reduce the effective interference thanks to a lesser number of interferers falling within the angle of the established receiving beam. Assume that the interfering mobiles are uniformly distributed in a cell and W is the effective beamwidth in radian formed by the beam-steering technique. Then the terms $\|\mathbf{a}_i^H\mathbf{b}_k\|^2$ and $\|\mathbf{a}_i^H\mathbf{a}_{i_k}\|^2$ in (4.19) can be approximated by a Bernoulli random variable with a successful probability $W/2\pi$. Because the opposite direction interference I_{od} and the same direction interference I_{sd} are reduced by the factors $\|\mathbf{a}_i^H\mathbf{b}_k\|^2$ and $\|\mathbf{a}_i^H\mathbf{a}_{i_k}\|^2$, respectively, the received γ_{bs} can be improved.

It has been demonstrated that the beam-steering method can significantly improve the performance of FDD/CDMA systems [22]. However, we conjecture that this kind of beam-steering technique may not be good enough to suppress the opposite direction interference in the TDD/CDMA system. Take Fig. 4.4 as an example. Figures 4.4-(a) and 4.4-(b) illustrate a beam pattern formed by the beam-steering technique from the viewpoints of the whole system and the antenna beam pattern, respectively. In these two figures, a triangle-shaped target mobile is located in the center cell. Cells 2, 4, and 6 surround the center cell and generate the opposite direction interference. From Fig. 4.4-(b), one can see that the conventional beamformer

can establish a narrow beam pattern directing toward the target mobile at the angle of 150^0. However, this beamformer can only reduce the impact of the opposite direction interference by smaller antenna gains ranged from 10 dB, 5.6 dB, and 16 dB at the angles of 60^0 and 180^0 and 300^0, respectively. Therefore, the beam pattern of Scheme I may not be good enough to resolve the opposite direction interference issue for TDD/CDMA systems. This is because the beam-steering technique only directs the main beam towards the desired mobile instead of suppressing the opposite direction interference from the side lobe. Based on this observation, in the TDD/CDMA system we prefer the MVDR beamformer to the beam-steering technique.

4.3.3 MVDR Beamformer (Scheme II)

It is well known that the MVDR beamformer can direct the main receiving beam toward the desired user, while cancelling the strong interference simultaneously. Therefore, we expect that the MVDR beamformer is more suitable to resolve the issue of the opposite direction interference in the TDD/CDMA system compared with the conventional beam-steering technique. In the following, we will incorporate the effect of the MVDR beamformer into the analysis of the uplink received signals in the TDD/CDMA system.

The goal of the MVDR criteria is to minimize the output power, while maintaining signal strength equal to one in the desired direction. That is, the MVDR beamformer will determine the weight factor $\mathbf{w}_{mv}$ of the combining scheme according to the following criteria:

$$\begin{aligned} &\mathbf{w}_{mv} = \arg\min_{\mathbf{w}_i} E\{\|\mathbf{w}_i^H \mathbf{x}\|^2\} \\ &\text{s.t.} \quad \mathbf{w}_i^H \mathbf{a}_i = 1 \ . \end{aligned} \tag{4.20}$$

In (4.20) the term $E\{\|\mathbf{w}_i^H\mathbf{x}\|^2\}$ can be expressed as

$$E\{\|\mathbf{w}_i^H\mathbf{x}\|^2\} = \mathbf{w}_i^H\Phi_x\mathbf{w}_i \ , \tag{4.21}$$

where Φ_x is the sampled covariance matrix of the received signal $\mathbf{x}(t)$, i.e., $\Phi_x = E\{\mathbf{x}(t)\mathbf{x}(t)^H\}$. Referring to (4.9), Φ_x can be written as

$$\Phi_x = P_r\mathbf{a}_i\mathbf{a}_i^H + \Phi_{od} + \Phi_{sd} + \Phi_{ic} + \eta\mathbf{I} \tag{4.22}$$

where

$$\Phi_{od} = \sum_{k\in\mathcal{B}_{od}} P_T G(d_k,\alpha_k)\mathbf{b}_k\mathbf{b}_k^H \ , \tag{4.23}$$

$$\Phi_{sd} = \sum_{k\in\mathcal{B}_{sd}}\sum_{i_k=1}^{N_k} P_r\beta_{i_k}\mathbf{a}_{i_k}\mathbf{a}_{i_k}^H \ , \tag{4.24}$$

and

$$\Phi_{ic} = \sum_{i_0\neq i}^{N_0} P_r\mathbf{a}_{i_0}\mathbf{a}_{i_0}^H \ . \tag{4.25}$$

Here Φ_{od}, Φ_{sd}, and Φ_{ic} denote the signal covariance matrices of the opposite direction interference, the same direction interference, and the intracell interference, respectively.

Applying the Lagrange multiplier approach, one can obtain the MVDR beamformer weight $\mathbf{w}_{mv}$ as follows [35]

$$\mathbf{w}_{mv} = \frac{\Phi_x^{-1}\mathbf{a}_i}{\mathbf{a}_i^H\Phi_x^{-1}\mathbf{a}_i} \ . \tag{4.26}$$

According to [35], the total output power after the MVDR beamforming is equal to

$$E\{\|\mathbf{w}_{mv}^H\mathbf{x}\|^2\} = (\mathbf{a}_i^H\Phi_x^{-1}\mathbf{a}_i)^{-1} \ . \tag{4.27}$$

Then similar to the derivation of (4.19), we can first substitute the weight $\mathbf{w}_{mv}$ of (4.26) into (4.17) and then refer to (27) to obtain the bit energy-to-interference density ratio γ_{mv} with the MVDR beamformer (Scheme II) as follows:

$$\gamma_{mv} = \frac{LP_r}{(\mathbf{a}_i^H\Phi_x^{-1}\mathbf{a}_i)^{-1} - P_r} \ . \tag{4.28}$$

Comparing (4.22) and (4.28), we can further simplify γ_{mv} as

$$\gamma_{mv} = L(\mathbf{a}_i^H \Phi_i^{-1} \mathbf{a}_i) \ , \tag{4.29}$$

where

$$\Phi_i = (\Phi_{od} + \Phi_{sd} + \Phi_{ic} + \eta \mathbf{I})/P_r \ . \tag{4.30}$$

In (4.30), Φ_i represents the normalized covariance matrix of the received interference plus noise signals.

Since it is not easy to further derive the closed-form expression for γ_{mv}, we will evaluate γ_{mv} numerically to demonstrate the advantage of using the MVDR beamformer in TDD/CDMA systems later in Section 4.5. Now we use Fig. 4.5 to explain intuitively why the MVDR beamformer outperforms the beam-steering technique in TDD/CDMA systems. Figures 4.5-(a) and 4.5-(b) show a beam pattern of the MVDR beamformer with the same scenario as Fig. 4.4. Compared to Fig. 4.4, one can observe that the MVDR beamformer not only directs the beam towards the target mobile at the angle of 150^o, but also nullifies the opposite direction interference at the arrival angles of 60^o, 180^o, and 300^o. Note that to obtain the weights of the MVDR beamformer, it only requires the knowledge of the direction of arrival (DOA) from the target mobile. In our work, we assume that the information of DOA of the target mobile is available, which can be obtained by the DOA estimation algorithms such as in [21] and [37].

The superiority of MVDR beamforming in suppressing strong interference requires that the signal and interference are uncorrelated. In the multipath environment, the correlation between the desired signal and its multipath arrivals (regarded as interference) may seriously degrade the output signal-to-interference ratio performance. Several techniques to desensitize the correlation of the signal and interference in the received covariance matrix can be found in [37]. Fortunately, in the CDMA system, the delayed arrivals of the desired signal can be resolved by temporal filter-

ing of Rake receivers. Thus, using a two-dimensional spatial-temporal architecture with each branch for an individual delayed path, the MVDR algorithm can still work well and even capture more energy of the desired signal in the multipath environment [19, 38, 39].

4.4 Downlink Beamforming

In this section, we discuss how to improve the performance of the TDD/CDMA system further by exploiting the synergy of adopting both the downlink transmitting and uplink receiving beamforming simultaneously. Note that in TDD systems, due to channel reciprocity between the downlink and uplink, downlink beamforming can be easily implemented by taking advantage of the estimated parameters from uplink signals. The benefits of incorporating downlink transmitting beamforming can be illustrated by an example shown in Fig. 4.6. In the figure, the beam pattern of the center cell is for the uplink reception, while the beam patterns of the neighboring cells are for the downlink transmission. Assume that a simple downlink beam-steering technique has been adopted at the base stations of cells 2, 4 and 6. Obviously, the impacts of the opposite direction interference signals from cells 2, 4, and 6 are alleviated because of weaker power radiating toward the direction of the home cell.

4.4.1 Joint Downlink and Uplink Beam-Steering (Scheme III)

Now we evaluate the effect of Scheme III, where the beam-steering method is adopted for both the downlink transmission and uplink reception at base stations. With down-

link transmitting beamforming, the opposite direction interference $\tilde{\mathbf{x}}_{od}(t)$ [2] introduced by the neighboring cells can be modified from (4.10). That is,

$$\tilde{\mathbf{x}}_{od}(t) = \sum_{k\in\mathcal{B}_{od}} \sum_{i_k=1}^{\tilde{N}_k} \sqrt{p_{i_k} G(d_k, \alpha_k)} \|\tilde{\mathbf{w}}_{i_k}^H \tilde{\mathbf{b}}_k\| \; u_{i_k}\left(\left\lfloor \frac{t-\tau_{i_k}}{T} \right\rfloor\right) c_{i_k}(t-\tau_{i_k}) \mathbf{b}_k \ , \tag{4.31}$$

where $\tilde{\mathbf{b}}_k$ is the array manifold vector of the signal transmitting from cell k ($k \in \mathcal{B}_{od}$), $\tilde{\mathbf{w}}_{i_k}$ is the downlink beamformer weight of mobile i_k, $\tilde{N}_k$ is the number of mobile users in the downlink cycle, and p_{i_k} is the transmission power allocated to the mobile i_k from a base station. Then, the opposite direction interference I_{od} at the output of the receive beamformer can be modified from (4.14) as follows:

$$\tilde{I}_{od} = \sum_{k\in\mathcal{B}_{od}} \sum_{i_k=1}^{\tilde{N}_k} p_{i_k} G(d_k, \alpha_k) \|\tilde{\mathbf{w}}_{i_k}^H \tilde{\mathbf{b}}_k\|^2 \|\mathbf{w}_i^H \mathbf{b}_k\|^2 \ . \tag{4.32}$$

Note that $P_T = \sum_{i_k=1}^{\tilde{N}_k} p_{i_k}$ is the total transmitter power of a base station. Comparing (4.32) with (4.14), one can observe that after incorporating downlink transmitting beamforming, the effective radiation power that causes the opposite direction interference from cell k ($k \in \mathcal{B}_{od}$) can be reduced from P_T to a smaller value

$$\tilde{P}_T = \sum_{i_k=1}^{\tilde{N}_k} p_{i_k} \|\tilde{\mathbf{w}}_{i_k}^H \tilde{\mathbf{b}}_k\|^2 \ . \tag{4.33}$$

From (4.18), we know that the downlink beamformer weight for mobile i_k of cell k ($k \in \mathcal{B}_{od}$) is given by

$$\tilde{\mathbf{w}}_{i_k} = \tilde{\mathbf{a}}_{i_k} \ , \tag{4.34}$$

where $\tilde{\mathbf{a}}_{i_k}$ is the array manifold vector of the signal transmitting from cell k to its serving mobile i_k ($k \in \mathcal{B}_{od}$). Due to the reciprocity of TDD channels, $\tilde{\mathbf{a}}_{i_k}$ can be

[2] We add a word about notations. When $\tilde{[\cdot]}$ is used as superscripts, they denote the case when downlink beam-steering is applied.

approximated by modifying $\mathbf{a}_{i_k}$ which is already obtained in the uplink beamforming. Replacing P_T of (4.19) with the effective radiated power $\tilde{P}_T$ of (4.33), we can obtain the bit energy-to-interference density ratio $\tilde{\gamma}_{bs}$ of Scheme III as follows:

$$\tilde{\gamma}_{bs} = LP_r \left\{ \sum_{k\in\mathcal{B}_{od}} \sum_{i_k=1}^{\tilde{N}_k} p_{i_k} G(d_k,\alpha_k) \|\tilde{\mathbf{a}}_{i_k}^H \tilde{\mathbf{b}}_k\|^2 \|\mathbf{a}_i^H \mathbf{b}_k\|^2 + \right.$$
$$\left. \sum_{k\in\mathcal{B}_{sd}} \sum_{i_k=1}^{N_k} P_r \beta_{i_k} \|\mathbf{a}_i^H \mathbf{a}_{i_k}\|^2 + \sum_{i_0\neq i}^{N_0} P_r \|\mathbf{a}_i^H \mathbf{a}_{i_0}\|^2 + \eta \right\}^{-1} . \quad (4.35)$$

4.4.2 Joint Downlink Beam-Steering and Uplink MVDR Beamformer (Scheme IV)

In the following, we derive the bit energy-to-interference density ratio $\tilde{\gamma}_{mv}$ for Scheme IV. In Scheme IV, a base station transmits downlink signals through the beam-steering process, while in the uplink reception the MVDR beamformer is applied. Let $\tilde{\Phi}_{od}$ represent the signal covariance matrix of the opposite direction interference. Then $\tilde{\Phi}_{od}$ can be obtained by replacing P_T of (4.23) with $\tilde{P}_T$ of (4.33). That is,

$$\tilde{\Phi}_{od} = \sum_{k\in\mathcal{B}_{od}} \sum_{i_k=1}^{\tilde{N}_k} p_{i_k} G(d_k,\alpha_k) \|\tilde{\mathbf{w}}_{i_k}^H \tilde{\mathbf{b}}_k\|^2 \mathbf{b}_k \mathbf{b}_k^H \ . \quad (4.36)$$

Substituting (4.36) into (4.30), we can obtain the normalized covariance matrix $\tilde{\Phi}_i$ of the total interference plus noise as follows:

$$\tilde{\Phi}_i = (\tilde{\Phi}_{od} + \Phi_{sd} + \Phi_{ic} + \eta\mathbf{I})/P_r \ . \quad (4.37)$$

Finally replacing Φ_i of (4.29) with $\tilde{\Phi}_i$ of (4.37), we can obtain $\tilde{\gamma}_{mv}$ for Scheme IV as follows:

$$\tilde{\gamma}_{mv} = L(\mathbf{a}_i^H \tilde{\Phi}_i^{-1} \mathbf{a}_i) \ . \quad (4.38)$$

Note that in both Schemes III and IV, the conventional beam-steering technique is used for downlink transmitting beamforming. One may wonder why the MVDR beamforming is not applied in the downlink transmitting beamforming. We will discuss this issue in the following. Unlike the uplink receiving beamformer, which does not impose any negative impacts on other users, the downlink transmitting beamformer may possibly exacerbate the downlink performance of other users. For example, consider the receiving MVDR beam pattern of Fig. 4.5, where the main beam is directing to the desired user at the angle of 150^o and three nulls at the angles of 60^o, 180^o, and 300^o. It is noteworthy that compared to the conventional beam-steering technique, the uplink MVDR beamformer place the nulls at the directions of interfering sources at the cost of increasing the magnitude of side lobes. Thus, because of higher amplitude in the side lobes, the downlink MVDR transmitting beamforming may cause strong interference to other mobiles, e.g., the mobile at the angle of 93^o in Fig. 4.5. From this observation, we believe that it is not feasible to apply the weight obtained in the uplink MVDR beamforming straightforwardly for downlink transmitting beamforming. To determine the optimal weights of downlink transmitting beamforming is a complicated issue [23, 24] and beyond the scope of this chapter. Here, we only consider the suboptimal beam-steering technique for downlink beamforming. In the next section, we will show that even with this kind of simple downlink beam-steering technique, the performance of the TDD/CDMA system can be significantly improved.

4.5 Numerical Results

This section demonstrates the performance results of the aforementioned four different beamforming techniques. We consider a TDD/CDMA multicellular system, where all cells provide asymmetric traffic services based on their own traffic requirements.

Through simulation, we evaluate the bit energy-to-interference density ratio γ for Schemes I, II, III and IV according to (4.19), (4.29), (4.35) and (4.38), respectively. The number of active users in every cell is set to 20 during one time slot, i.e. $N_k = \tilde{N}_k = 20$. In all simulations, we assume mobiles are uniformly distributed and the other system parameters used in simulation are listed in Table 4.1.

4.5.1 Performance of Uplink Beamforming

Figure 4.7 compares the uplink performance of Schemes I and II. In Scheme I beam-steering is applied to suppress the opposite direction interference, while Scheme II adopts the MVDR beamformer. We define the reliability function p as the complementary cumulative distribution function of γ, i.e., $p = 1 - \text{Prob}\{\gamma \leq \gamma_{th}\}$, where γ_{th} is the required bit energy-to-interference density ratio. In the figure, curves (a)$\sim$(d) show the performances of the MVDR beamformer with different number of antenna elements, whereas curve (e) shows the performance of the beam-steering technique. For comparison, the performance without using any beamforming technique is shown in curve (f). In this figure and hereafter, $B = |\mathcal{B}_{od}|$ denotes the number of surrounding cells generating the opposite direction interference. Let's focus on the case when $\gamma_{th} = 7$ dB and $p = 90\%$. From curves (a), (b) and (c), one can find that the uplink MVDR beamformer with antenna elements $M = 9, 7$ and 5 can have satisfactory performance. Because in our simulation scenario there are three neighboring cells generating the strong opposite direction interference, it is necessary to have at least four antenna elements in the MVDR beamformer to place enough nulls to suppress the three strong interfering signals. By contrast, from curve (e) one can see that even with nine antenna elements, Scheme I still cannot yield any feasible solution to overcome the opposite direction interference

Figure 4.8 compares the performances of Schemes I and II with different num-

bers of cells generating the opposite direction interference. With nine antenna elements ($M = 9$), curves (e)$\sim$(g) and curves (a)$\sim$(d) show the performances of Schemes I and II, respectively. Assume that the required reliability p is equal to 90%. We find that when we increase the number of neighboring cells generating the opposite direction interference from one to three, the 90th percentile of γ in Scheme II degrades 3 dB, whereas in Scheme I the 90th percentile of γ degrades 6 dB. Thus, we can conclude that as compared to the conventional beam-steering method, the MVDR beamformer is less sensitive to the increase of the number of cells generating the opposite direction interference.

4.5.2 Performance of Downlink Beamforming

Figure 4.9 demonstrates the performance improvements by adopting downlink transmitting beamforming. One can find that when the downlink transmitting beam-steering method is employed, both Schemes III and IV improve the performance of the TDD/CDMA system significantly as compared to Schemes I and II, respectively. Compared to Scheme II (curve (b)), Scheme IV can improve the 90th percentile of γ from 8.74 dB to 11.94 dB (curve (d)). Note that Scheme IV adopts both the downlink transmitting beam-steering and uplink receiving MVDR beamformers, while Scheme II only utilizes the MVDR beamformer in the uplink reception. For Scheme I the 90th percentile of γ is -0.76 dB (curve (a)), while for Scheme III the 90th percentile of γ is improved to 5.36 dB (curve (c)).

Figure 4.10 demonstrates the impacts of the four aforementioned beamforming techniques in TDD/CDMA systems against the increase of the number of cells generating the opposite direction interference. One can see that Scheme IV is least sensitive to the increase of the number of cells causing the opposite direction interference. Let's consider the case when the required γ_{th} is equal to 7 dB. One can observe that the

reliability function with Scheme IV is slightly degraded to 98% as B increases from zero to six. However, for Scheme III the reliability function is degraded to 84%. Note that Scheme II can also be an effective approach to suppress the opposite direction interference since its reliability is still higher than 90%.

4.5.3 Discussion

To determine which beamforming scheme should be used in TDD/CDMA systems is a complicated tradeoff issue between performance improvements and implementation costs. Scheme IV, using the uplink MVDR beamforming and downlink transmitting beam-steering, can effectively suppress the opposite direction interference, thereby providing greater flexibility in delivering asymmetric traffic services. In Scheme IV every TDD/CDMA cell can *independently* designate traffic patterns for either uplink modes or downlink modes in every time slot according to its own rate of traffic asymmetry. On the other hand, using a simpler beam-steering method in both the uplink reception and downlink transmission, Scheme III provides satisfactory performance only when the number of cells generating the opposite direction interference is not large. Thus, it is suggested to combine Scheme III with other sectorization or channel assignment techniques to reduce the number of cells generating the opposite direction interference.

Scheme II is another effective technique to reduce the impact of the opposite direction interference. Recall that Scheme II utilizes the MVDR beamforming only in the uplink. Note that the performance of Scheme II is better than Scheme III but worse than Scheme IV. As remarked earlier, the extra cost of implementing downlink transmitting beam-steering may not be very high. If so, Scheme IV will be a better choice than Scheme II provided that the MVDR beamformer has already been adopted in the uplink. As for Scheme I, it is shown that only using beam-steering in the uplink

can not provide acceptable performance.

Although in this chapter we concentrate on the uplink performance of TDD/CDMA systems, antenna beamforming can also be exploited to improve the downlink performance. For example, by taking advantage of the reciprocity of TDD channels, downlink transmitting beamforming from neighboring base stations can lower the effective interfering power to the mobile station in the home cell. Furthermore, when the mobile station is employed with a small number of array sizes [40, 41], the downlink performance can be further enhanced with the beamforming techniques similar to the Schemes III and IV.

Table 4.1: System Parameters

Processing gain	$L = 128$
COST-231 propagation model	$10\log(\kappa_0) = -128.1$, $m = 3.76$
Shadowing standard deviation	$\sigma = 8$ dB
Cell radius	$R = 1$ Km
Total transmit power of a base station	$P_T = 8$ W
Base station transmit power allocated for each mobile	$p_{i_k} = 0.4$ W
Thermal noise	$\eta = -112$ dBm
Power control level	$P_r/\eta = -1$ dB [5]

4.6 Conclusions

In this chapter, we have investigated the effects of beamforming techniques from the perspective of suppressing the opposite direction interference to improve the uplink performance of TDD/CDMA systems. We exploit the synergy of combining the downlink transmitting and uplink receiving beamforming to search a feasible scheme

to resolve the opposite direction interference from a network viewpoint. Based on our numerical results, we can draw the following conclusions:

- Schemes IV, which adopts the MVDR beamformer in the uplink and the beam-steering in the downlink, can effectively suppress the strong opposite direction interference of TDD/CDMA systems, thereby allowing every cell to provide asymmetric traffic services with different rates of traffic asymmetry.

- Scheme III, which adopts the beam-steering method in both the downlink transmission and uplink reception, can provide satisfactory performance when the number of cells generating the opposite direction interference is not large. When combined with other sectorization or channel assignment techniques, Scheme III can be a very effective mechanism to overcome the opposite direction interference in the TDD/CDMA system with lower implementation costs.

- If only the uplink beamforming is considered, the MVDR beamformer (Scheme II) instead of the conventional beamforming method (Scheme I) should be adopted since the conventional beam-steering can not effectively suppress the opposite direction interference.

While we have sketched some potential advantages of using antenna beamforming to enhance the downlink performance of TDD/CDMA systems in Section 4.5, it is still worth further investigating the downlink performance improvement in the future studies. In summary, this work has demonstrated the great potential of applying antenna beamforming techniques in the TDD/CDMA system. Even with the severe impact of the opposite direction interference, we find that there exists a feasible and economical beamforming mechanism (e.g. Scheme III suggested in the chapter), which can enable the TDD/CDMA system to deliver asymmetric traffic services within the entire service area with greater flexibility.

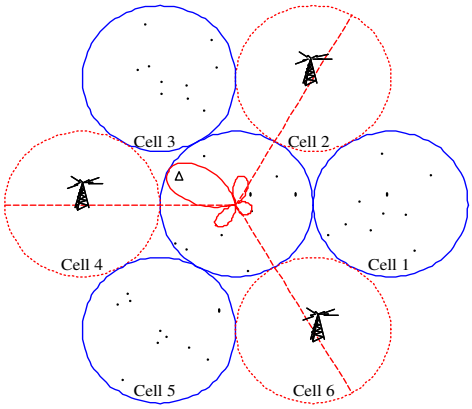

(a) : Beamforming with beam-steering technique

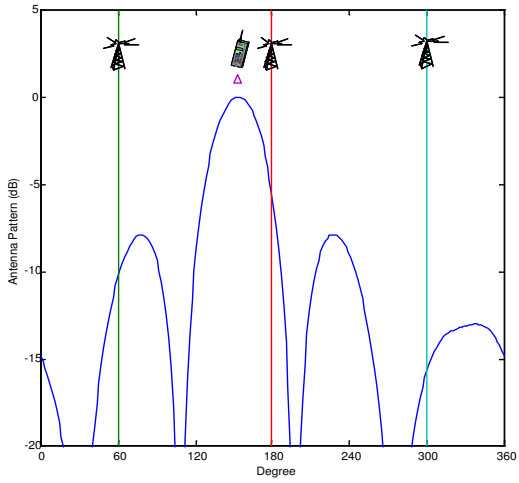

(b) : Antenna pattern with beam-steering technique

Figure 4.4: An illustrative example for a TDD/CDMA system with Scheme I, where the home cell employs beam-steering at the base station. In this example, there are three adjacent cells ($\mathcal{B}_{od} = \{2, 4, 6\}$) generating the opposite direction interference to the center cell.

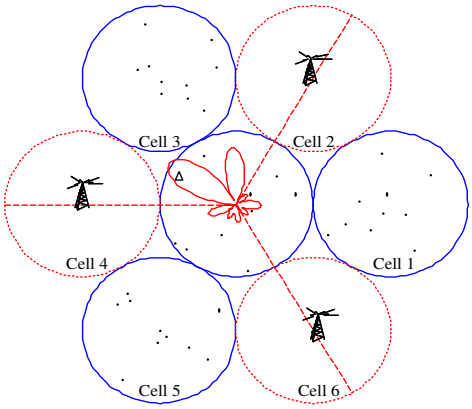

(a) : Beamforming with MVDR beamformer

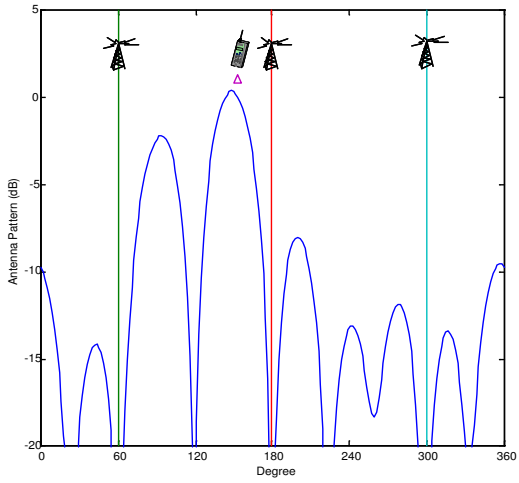

(b) : Antenna pattern with MVDR beamformer

Figure 4.5: An illustrative example for a TDD/CDMA system with Scheme II, where the home cell employs the MVDR beamformer at the base station. In this example, there are three adjacent cells ($\mathcal{B}_{od} = \{2, 4, 6\}$) generating the opposite direction interference.

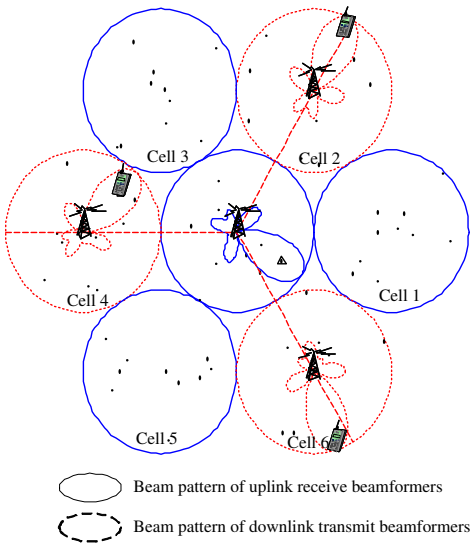

Figure 4.6: An illustrative example for a TDD/CDMA system with Scheme III, where the beam pattern in the center cell is for the uplink reception and those in the neighboring cells $\mathcal{B}_{od} = \{2, 4, 6\}$ are for the downlink transmission.

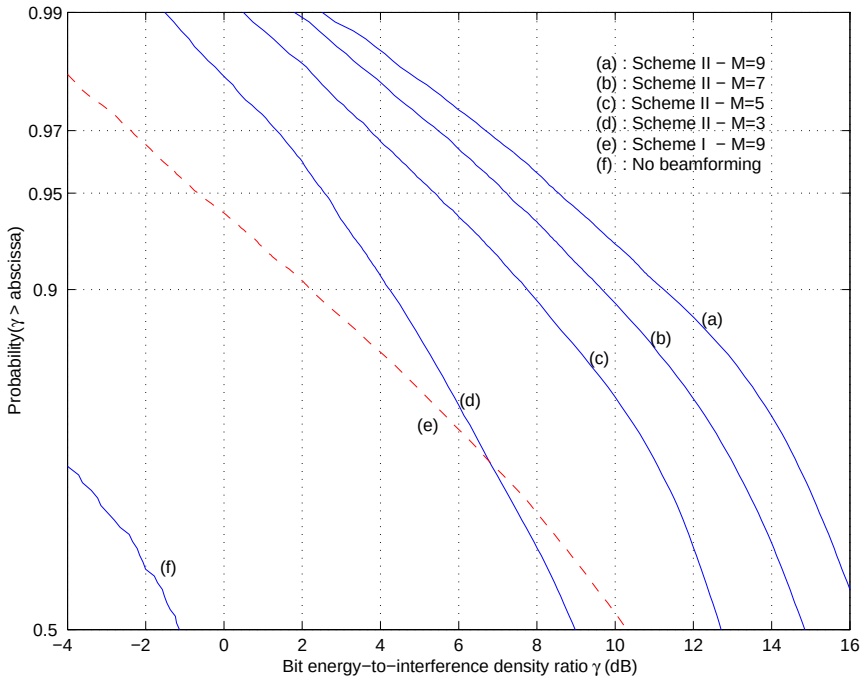

Figure 4.7: Uplink performance comparison of Schemes I and II with different numbers of antenna elements (denoted as M in the figure). Note that in this case the number of cells generating the opposite direction interference is equal to three.

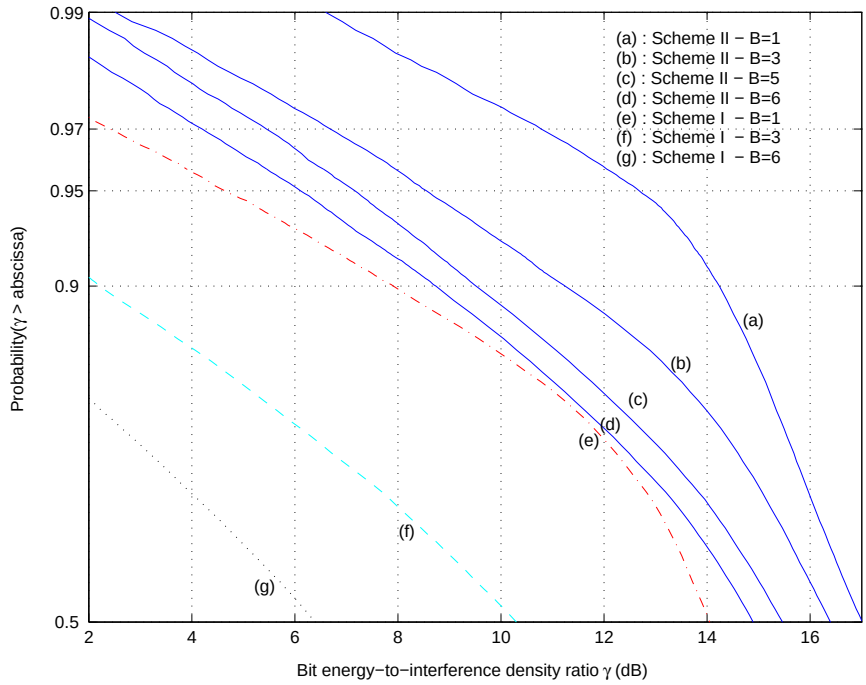

Figure 4.8: Uplink performance comparison of Schemes I and II with different numbers of cells generating the opposite direction interference (denoted as B in the figure). Note that in this case the number of antenna elements is equal to nine.

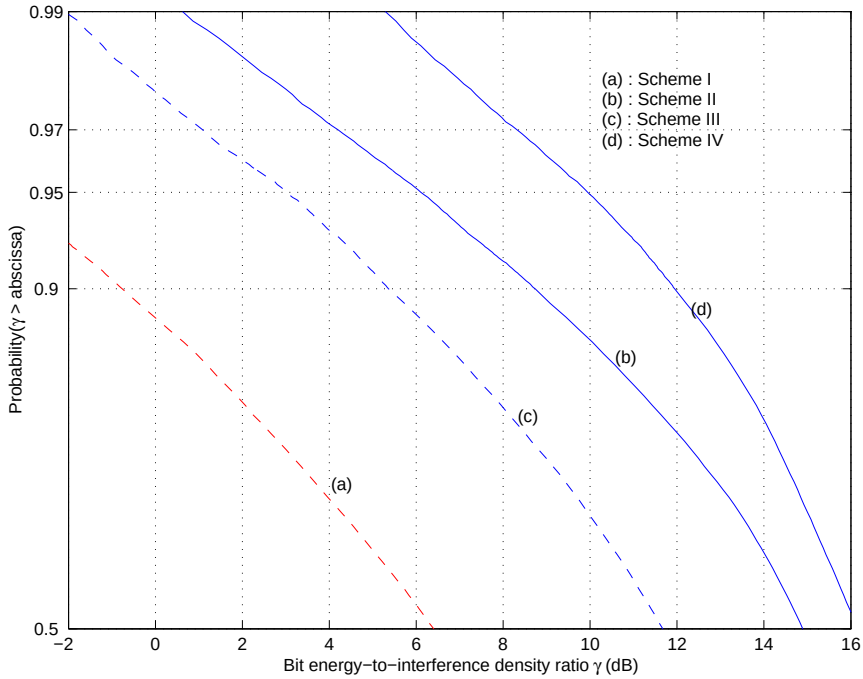

Figure 4.9: Performance improvements by implementing downlink transmitting beamformer in the surrounding base stations, where the number of cells generating the opposite direction interference equal to six and the number of antenna elements equal to nine.

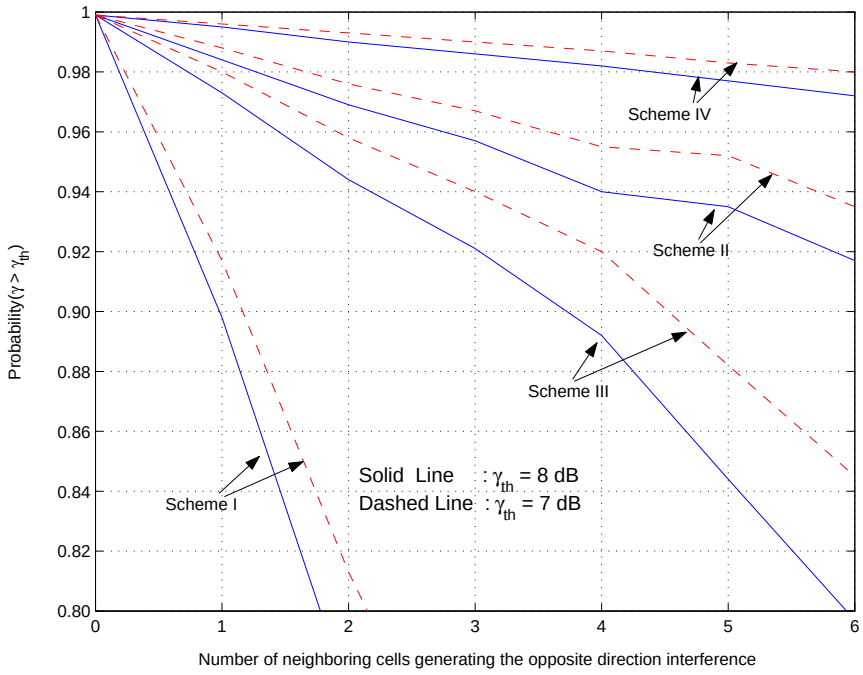

Figure 4.10: Performance comparison of four beamforming schemes with different numbers of cells generating the opposite direction interference, where an antenna array with nine elements is deployed at base stations.

CHAPTER 5

A Novel Link Proportional Dynamic Channel Assignment for a Virtual-cell Based TDD/CDMA System with Asymmetric Traffic

The increasing demands for the higher speed wireless internet applications impose many new challenges on spectrum and radio resource management in wireless networks. One of key challenges in supporting the wireless Internet services is to handle the traffic asymmetry between the uplink and the downlink. Time division duplex (TDD) is an efficient approach to resolve the traffic asymmetry issue, which can dynamically allocate the resource (time slots) to the uplink and the downlink. However, asymmetric traffic will cause the cross-slot co-channel interference, thereby seriously degrading the system performance. This chapter proposes a novel link-proportional dynamical channel assignment (LP-DCA) scheme combined with tri-sector directional antennas to alleviate the impact of cross-slot interference for the TDD code division multiple access (CDMA) systems. With the help of directional antennas, the tri-sector cellular system will form a virtual cell, which is composed of three sectors from three different base stations. We find that for this kind of cellular structure, the cross-slot interference is restricted within a virtual cell. Thus the proposed LP-DCA scheme can

concentrate on combating the cross-slot interference within a virtual cell by assigning time slots to the users according to their radio link quality. Our numerical results show that LP-DCA combined with tri-sector cellular structure can significantly reduce the cross-slot interference, thereby improving the outage and throughput performances for the TDD CDMA system under asymmetric traffic.

5.1 Introduction

The main objective of the future wireless communication systems is to support the high speed multi-media services [42]. These multi-media services, such as web browsing, video or audio playing, net meeting, and so on, are significantly different from the traditional voice service. An important feature of these services is asymmetric traffic requirement. That is, some services may require more radio resources in the downlink transmission, while some services may require more uplink radio resources [1]. Hence, an intelligent radio resource allocation to support asymmetric services becomes an important topic in the future wireless networks.

With unpaired frequency bandwidth, time division duplex (TDD) can support asymmetric traffic services efficiently with more flexibility than the frequency division duplex (FDD) systems becomes FDD systems usually use a pair of equal-bandwidth frequency bands for downlink and uplink transmissions [2–4]. However, in TDD-code division multiple access (CDMA) systems, because uplink and downlink transmissions share the same frequency band in every cell, the transmissions of asymmetric traffic from adjacent cells may cause heavy *cross-slot* interference [8, 9]. For example in Fig. 5.1, the frame is divided into 15 time slots, where the first slot is usually used for signaling, and the others are allocated for either the uplink or the downlink traffic channels [6, 7, 43]. Define the switching point as the boundary between uplink time slots and downlink time slots within a transmission frame. For two neighboring cells

having different switching points due to distinct uplink-to-downlink traffic ratios, downlink transmissions of some time slots in one cell will interfere uplink transmissions in other cells. Because the opposite-direction transmissions between two neighboring cells occurs when the uplink slots of one cell cross the switching point of other adjacent cells, we call it the cross-slot interference. Note that as shown in Fig. 5.1, there are two kinds of cross-slot interference: base-to-base cross-slot interference in the uplink and the mobile-to-mobile cross-slot interference in the downlink. Both types of cross-slot interference will degrade the system performance [8]. Therefore, it is usually suggested that the same time slot of two neighboring cells should be used for the same transmission direction, which leads to some time slot unused in some cells. Apparently, this approach will waste resources and lose the key advantages of the TDD systems in supporting asymmetric traffic services [3, 10].

Many related works regarding the issues of suppressing the cross-slot interference in the TDD/CDMA systems have been reported in the literature. In [44], the author applied a random time slot opposing algorithm to quantify the impact of cross-slot interference. In [11], an ordered slot assignment scheme was proposed to allocate downlink time slots in descending order from the left side of a frame and uplink time slots in descending order from the right side of a frame. This method can alleviate the cross-slot interference by reducing the probability of using the time slots with a higher opportunity experiencing the cross-slot interference. When the traffic load or the traffic asymmetry between the uplink and the downlink is high, the method in [11] may still have difficulty in overcoming the cross-slot interference. In [12], the authors proposed a region-based channel assignment, while allocating the clean time slots without cross-slot interference to the users in the outer region of a cell. The performance of this region-base time slot allocation will highly depend on the way of separating the inner and outer regions. In the time-varying radio channel, a proper boundary to separate the inner and the outer regions is usually very difficult. The

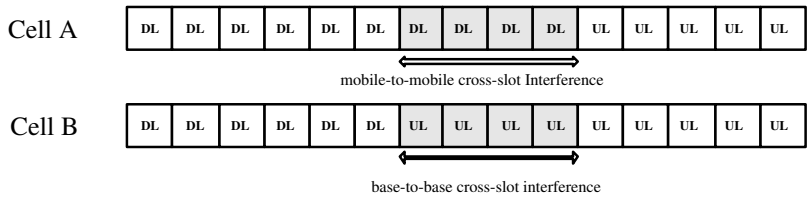

(a) TDD/CDMA frame structure

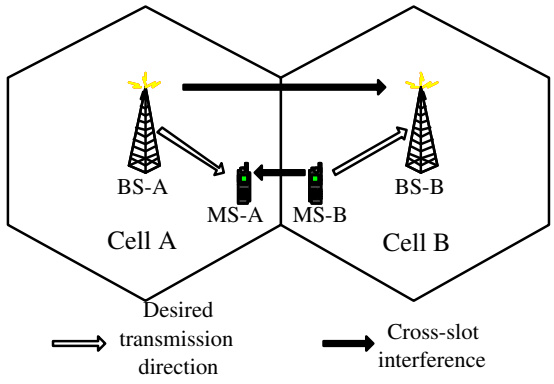

(b) cross-slot interference scenario

Figure 5.1: Frame structure and cross-slot interference in TDD/CDMA system.

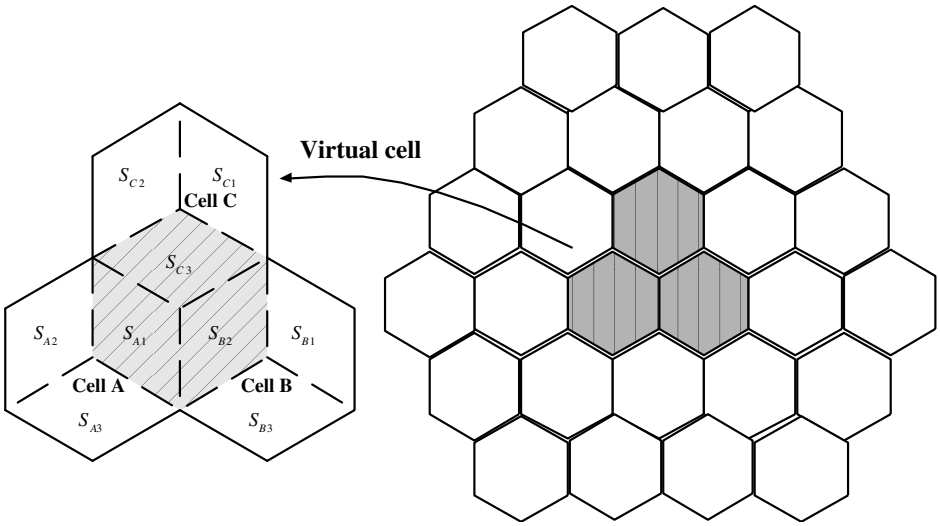

Figure 5.2: A trisector cellular system with the virtual cell.

authors in [27] applied the beamforming technique to eliminate the cross-slot interference in the reverse link, whereas the downlink mobile-to-mobile cross-slot interference has not been considered.

In this work, aiming to alleviate the cross-slot interference, we propose a link-proportional dynamic channel assignment scheme (LP-DCA) with sectorized antennas. With the assistant of directional antennas, we utilize the concept of virtual cell composed from three neighboring sectors with the same coverage area of a cell [17]. By taking the advantages of virtual cell, we propose a effective DCA algorithm to flexibly alleviate the co-channel interference, especially for the cross-slot interference. The key idea of LP-DCA scheme is to classify the cross-slot interference and allocate the radio resource according to the users' received signal quality. The total users of a sector are sorted based on their received signal strength. We partition these sorted users into some different groups and allocate the time slots with the consideration of alleviating the cross-clot interference. Specifically, the sector with the largest downlink traffic load will allocate both the downlink and uplink groups in a ascending order from the left side of available time slots. The sector with largest uplink traffic load will allocate both the downlink and uplink groups in a ascending order from the right side of the available time slots. The sector with similar uplink and downlink traffic load will allocate the downlink groups in ascending order from left side of the available time slots and uplink groups in ascending order from right side of the available time slots. By properly allocating users, we find that LP-DCA can efficiently alleviate the received inter-cell and intra-cell interference in the TDD/CDMA systems with multiple asymmetric traffic services.

The rest of this chapter is organized as follows. Section 5.2 describes the system model. In Section 5.3, we discuss the signal quality and capacity of the TDD/CDMA system with directional antennas. In Section 5.4, we describe our proposed LP-DCA scheme. Numerical results will be provided in Section 5.5. We give our conclusion

remarks in Section 5.6.

5.2 System Model

In this chapter, a radio resource unit (RU) is defined as the combination of spreading code, time slot, and frequency [42]. As [43], we consider a system with maximum 32 codes (RU) simultaneously in each time slot on a single frequency of 5 MHz bandwidth. Hence, there are 448 RU allocated to provide the services for users. Different users with different services may require difference amount of RU. Next, we will introduce the cellular system model, and the propagation model used in this chapter. We consider a TDD/CDMA hexagonal cellular system with directional antennas employed at the base station. Mobiles are assumed to be uniformly distributed over the cells.

5.2.1 Virtual Cell Concept

By taking the advantage of directional antennas, a *virtual cell* can be established [45]. Figure 5.3 illustrates a trisector cellular system with the virtual cell, where a virtual cell is defined as the same coverage area of a cell but is composed of three sectors from the three neighboring base stations. As shown in Fig. 5.3, sectors S_{A1}, S_{B2}, and S_{C3} forms a virtual cell. By employing simple sector antennas at base stations, it is clear that the inter-cell interference can be restricted within a virtual cell coverage area. The similar concept was also proposed in [18] to reduce interference in sectorized FDD/CDMA systems. The intra-cell interference between sectors of a cell can be ignored. Here we assume that the antenna gain is the same over the whole sector. Taking advantages of this additional orthogonality from the direction separation of sector antennas, we propose a virtual-cell based interference avoidance algorithm to

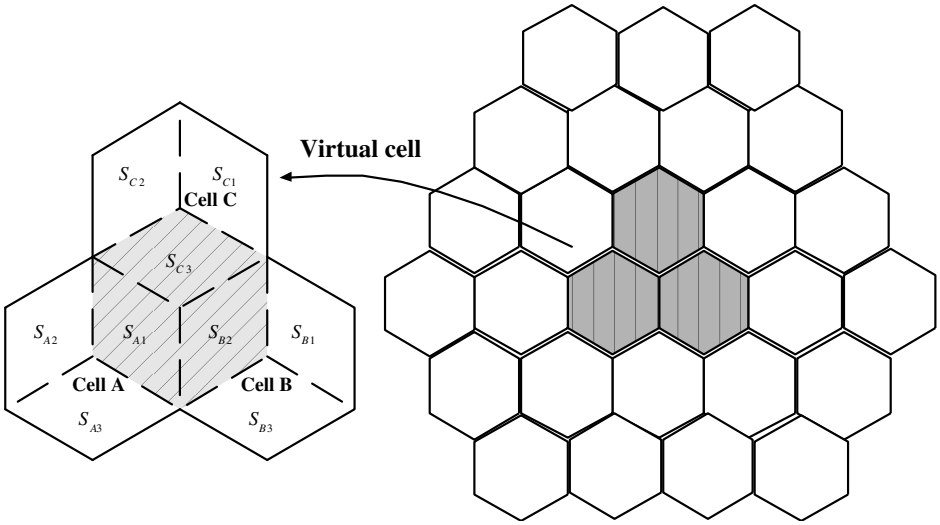

Figure 5.3: A trisector cellular system with the virtual cell.

support asymmetric traffic services in TDD/CDMA systems.

5.2.2 Propagation Model

In our propagation model, we consider propagation loss, lognormal distributed shadowing effect and the minimum link budget between two wireless entities (a mobile or a base station) i and j as $G_i(\gamma, \alpha)$ described as

$$G_{i,j} = G(r_{i,j}, \alpha_{i,j}) = \min\left(\frac{G_i G_j h_i^2 h_j^2}{d_{i,j}^4} \cdot 10^{\frac{\alpha_{i,j}}{10}}, MCL_{i \to j}\right) \tag{5.1}$$

where G_i and G_j are the antenna gain of communication entities i and j, h_i and h_j are the antenna height, $d_{i,j}$ is the distance between two communication connectors i and j, $\alpha_{i,j}$ is the log-normal shadowing component with a standard deviation of $\sigma_{i,j}$. Otherwise, we introduce minimum coupling loss (MCL) as the minimum distance loss including antenna gain measured between antenna connectors [46]. The value of σ and MCL are different with the distinct environment conditions. Here, we

set shadowing deviation between the mobile to its served base station $\sigma_s = 6$ dB, shadowing deviation between the mobile to the adjacent base station $\sigma_n = 8$ dB, shadowing deviation between the base station to the adjacent base station $\sigma_b = 3$ dB, shadowing deviation between mobile to mobile $\sigma_m = 10$ dB, MCL between base station and mobile equal to $10^{-5.3}$, and MCL between base station and mobile equal to 10^{-4} [47].

5.3 The Proposed Link-Proportional Dynamical Channel Scheme

Based on the virtual cell concept, we propose a novel efficient virtual-cell based dynamical channel assignment scheme. The objective of the proposed scheme is to minimize the overall system interference. With the advantage of directional antennas, we can easily get the desired information of some specific neighboring sectors and assume the slot synchronization between adjacent sectors is achievable. In our proposed scheme, the number of time slots allocated for the downlink or the uplink in a frame depends on the ratio between downlink traffic load to uplink traffic load of each cell. The proposed scheme can support diverse asymmetric services.

Assume that there exists N_s active users in sector s. Define $\mathcal{K}_s = \{1, 2, 3, \ldots, N_s\}$ as the index set of all active users. And $\pi : \mathcal{K}_s \rightarrow \mathcal{K}_s$ is the permutation of the index set with respect to the link gains of all connections in index set so that

$$\forall n,\ m \in \pi(\mathcal{K}_s) \text{ and } n < m, G_{h,\pi(n)} \leq G_{h,\pi(m)} \ .$$

where $G_{h,i}$ is the link gain from user i to his home serving base station defined in 6.1.

Algorithm: LP-DCA

Step 1: Traffic Load Information Updating

The sector s measures the aggregated request rates of the downlink and the uplink, denoted by $\overline{R}_s^{(d)}$ and $\overline{R}_s^{(u)}$, respectively. As long as the measured $\overline{R}_s^{(d)}$ and $\overline{R}_s^{(u)}$ of sector s are updated, these two values will be signaled to other two sectors in the same virtual cell.

Step 2: Time-slot Number Determination

The number of time slots for downlink and uplink, denoted by $T^{(d)}$ and $T^{(u)}$, can be obtained by $T^{(d)} = \text{round}\left(T \cdot \frac{\overline{R}_s^{(d)}}{\overline{R}_s^{(d)}+\overline{R}_s^{(u)}}\right)$ and $T^{(u)} = T - T^{(d)}$, where $T = T^{(d)} + T^{(u)}$ is the total number of time slots in each frame.

Step 3: User Grouping

Define $\Omega_{RU} = \sum_{k\in\mathcal{K}_s} RU_k$ the total requested radio units. For the downlink time slots, the users in $\mathcal{K}_s$ set can be partitioned into $T^{(d)}$ groups according to a *partition vector*, $\omega_d = \left\{\omega_{d,0}, \omega_{d,1}, \omega_{d,2}, \ldots, \omega_{d,T^{(d)}}\right\}$, which can be derived by

$$
\begin{aligned}
\omega_{d,0} &= 0. \\
\omega_{d,1} &= \arg\min_k \left\{ \sum_{m=1}^{\pi(k)} RU_m \,\middle|\, \sum_{m=1}^{\pi(k)} RU_m \geq \frac{\Omega_{RU}}{T^{(d)}} \cdot \frac{\overline{R}_s^{(d)}}{\overline{R}_s^{(d)} + \overline{R}_s^{(u)}} \right\}. \\
\omega_{d,x} &= \arg\min_k \left\{ \sum_{m=\omega_{d,(x-1)}+1}^{\pi(k)} RU_m \,\middle|\, \right. \\
&\qquad \left. \sum_{m=\omega_{d,(x-1)}+1}^{\pi(k)} RU_m \geq \frac{\Omega_{RU}}{T^{(d)}} \cdot \frac{\overline{R}_s^{(d)}}{\overline{R}_s^{(d)} + \overline{R}_s^{(u)}} \right\}, x = 2, \ldots, T^{(d)}. \qquad (5.2)
\end{aligned}
$$

Similarly, the user grouping for uplink time slot can be directly obtained by (5.2). We give an example about the distribution of users for each group in Fig. 5.4, when $T^{(d)}$ or $T^{(u)}$ equal to 5.

Step 4: Time Slot Allocation

The sector s determines the *time slot assignment order* in terms of the traffic load information from the other sectors. Three possible orders with corresponding status are shown in Fig. 5.5.

Status 1: The $\overline{R}_s^{(d)}$ is maximum among the virtual cell

The time slot x is allocated to the users in downlink group x, $\big(\pi(\omega_{d,(x-1)}+1),\ldots,\pi(\omega_{d,(x)})\big)$, where the allocation of time slot x is in the ascending order from slot 1 to $T^{(d)}$. For uplink, the time slot x is then allocated to the users in uplink group $(x-T^{(d)})$, $\big(\pi(\omega_{d,(x-T^{(d)}-1)}+1),\ldots,\pi(\omega_{d,(x-T^{(d)})})\big)$, where the allocation of time slot x is also in the ascending order from slot $(T^{(d)}+1)$ to time slot T.

Status 2: The $\overline{R}_s^{(u)}$ is maximum among the virtual cell

The time slot x is allocated to the users in downlink group $(T^{(d)}-x+1)$, where the allocation of time slot x is in the descending order from slot $T^{(d)}$ to 1. For uplink, the time slot x is then allocated to the users in uplink group $(T-x+1)$, where the allocation of time slot x is also in the descending order from slot T to $(T^{(d)}+1)$.

Status 3: Otherwise

The time slot x is allocated to the users in downlink group x, $\big(\pi(\omega_{d,(x-1)}+1),\ldots,\pi(\omega_{d,(x)})\big)$, where the allocation of time slot x is in the ascending order from slot 1 to $T^{(d)}$. For uplink, the time slot x is then allocated to the users in uplink group $(T-x+1)$, where the allocation of time slot x is also in the descending order from slot T to $(T^{(d)}+1)$.

The proposed scheme can alleviate the cross-slot interference as like region-based dynamic channel assignment. The users near the cell boundary are automatically allocated in the edge time slots of a frame in which the users have lower probability to be impacted by the cross-slot interference. The proposed algorithm is more

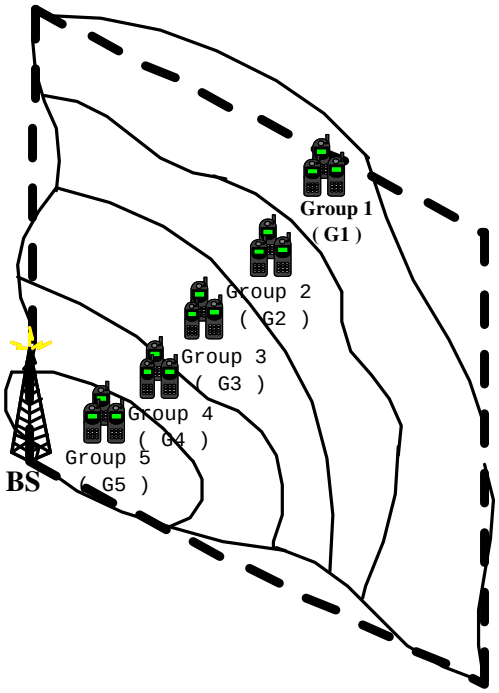

Figure 5.4: Example: Users' location distribution of each group in a sector.

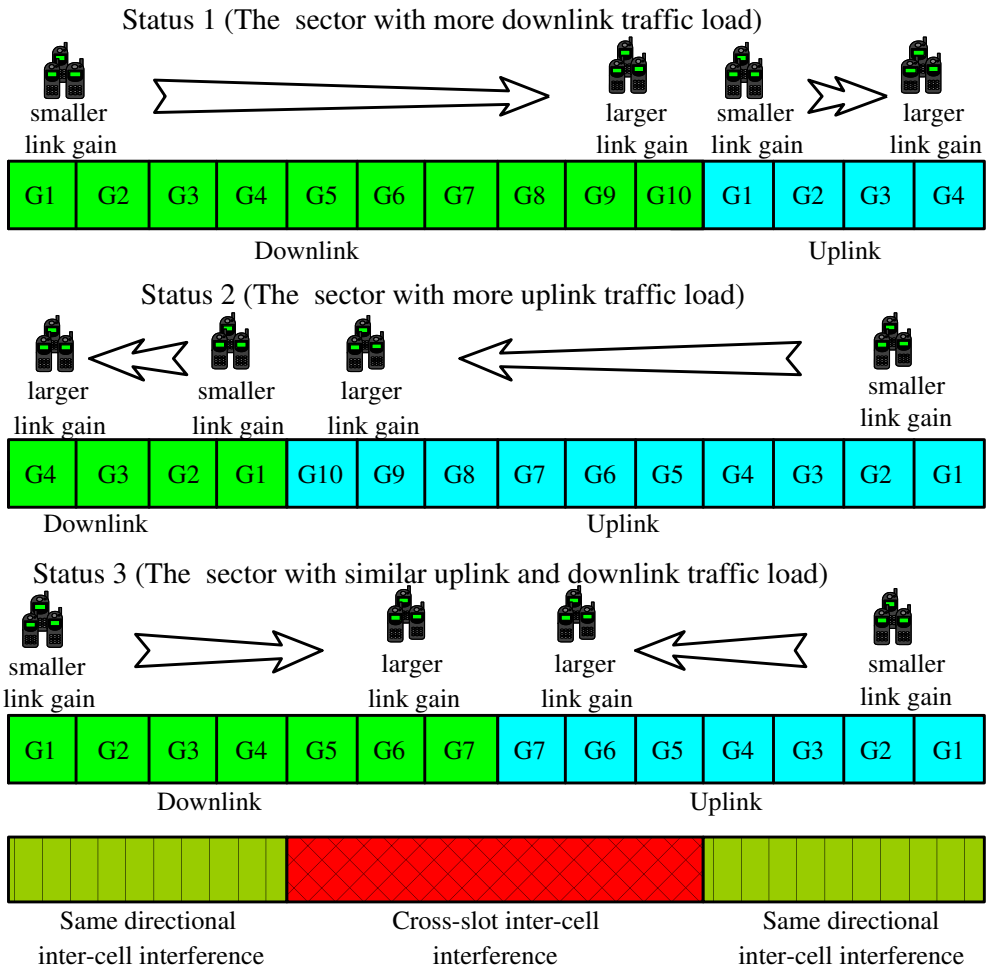

Figure 5.5: The proposed virtual-cell based LP-DCA.

flexible than region-based method which only defines a proper region radius threshold. Otherwise, the proposed scheme can reduce the near-far effect by allocating the users with similar received signal strength to the same time slot. Since the codes are not perfectly orthogonal due to the multipath fading, the proposed method can reduce the intra-cell interference resulted from the near far effect. Furthermore, the proposed method can reduce the same directional inter-cell interference [48]. This phenomenon can be seen when the group of higher link gain in one sector is allocated in the time slot in which the other group of lower link gain in the neighboring sector is allocated at the same time. It has been shown that this way can effectively increase the system performance.

5.4 Interference and Capacity Analysis

In this section, we will introduce the interference and capacity analysis method used in this work.

5.4.1 Uplink

Then the intra-cell interference for user i in the uplink transmission is defined as

$$I_{h,i}^{(u)} = \sum_{j=1, j\neq i}^{N_h} P_{m,j} \cdot G(d_{h,j}, \alpha_{h,j}) \tag{5.3}$$

where N_h is the total number of users in the home sector h, $P_{m,i}$ be the transmit power level of the target mobile i.

The received same directional inter-cell interference from the mobiles the neighboring sector in the uplink transmission can be denoted as

$$I_{m\rightarrow b,i}^{(u)} = \sum_{k\in B^{(u)}} \sum_{i_k=1}^{N_k} P_{m,i_k} \cdot G(d_{i_k,h}, \alpha_{i_k,h}) \tag{5.4}$$

where $B^{(u)}$ is the set of neighboring sectors in the uplink transmission, N_k is the number of users in the sector k.

If the adjacent sector k within the same virtual cell is in the downlink transmission, then the base-to-base cross-slot interference from sector k is

$$I^{(u)}_{b\to b,i} = \sum_{k\in B^{(d)}} G(d_{k,h}, \alpha_{k,h}) \sum_{i_k=1}^{N_k} P_{b,i_k} \tag{5.5}$$

where $B^{(d)}$ is the set of neighboring sectors in are downlink transmission, and P_{b,i_k} is the transmission power form the neighboring sector k to the mobile i_k. By taking the advantages of virtual cell, we can ignore the intra-cell inter-sector interference.

From (5.3), (5.4), and (5.5), we can obtain the bit energy-to-noise ratio for user i as follows

$$\left(\frac{E_b}{N_0}\right)_i = \frac{\frac{W}{R_i}\cdot P_r}{I^{(u)}_{h,i} + I^{(u)}_{m\to b,i} + I^{(u)}_{b\to b,i} + \eta} \tag{5.6}$$

where P_r is the received power level after power control, R_i is the transmission data rate of user i, and η is the white thermal noise power.

We define $\left(\frac{E_b}{N_0}\right)_t$ as the target bit energy-to-noise ratio. We can obtain the achievable data rate of user i as ζ_i, where

$$\zeta_i = \frac{W\cdot P_r}{\left(\frac{E_b}{N_0}\right)_t \cdot (I^{(u)}_{total,i} + \eta)} \tag{5.7}$$

where $I^{(u)}_{total,i} = I^{(u)}_{h,i} + I^{(u)}_{m\to b,i} + I^{(u)}_{b\to b,i}$, and then we can get the overall sector aggregate data rate as

$$C = \sum_{i=1}^{N_h} \zeta_i. \tag{5.8}$$

5.4.2 Downlink

Similarly as subsection 5.4.1, the intra-cell interference of the downlink user i can denoted as

$$I_{h,i}^{(d)} = (1-\rho) \cdot \sum_{j=1, j\neq i}^{N_h} P_{b,j} \cdot G(d_{h,i}, \alpha_{h,i}) \tag{5.9}$$

where ρ is the orthogonal factor between the codes utilized in the same sector.

The received same directional inter-cell interference from the neighboring sector k in the downlink transmission can be denoted as

$$I_{b\to m,i}^{(d)} = \sum_{k\in B^{(d)}} \sum_{i_k=1}^{N_k} P_{b,i_k} \cdot G(d_{k,i}, \alpha_{k,i}) \tag{5.10}$$

And the mobile-to-mobile cross-slot interference is denoted as

$$I_{m\to m,i}^{(d)} = \sum_{k\in B^{(u)}} \sum_{i_k=1}^{N_k} P_{b,i_k} \cdot G(d_{i_k,i}, \alpha_{i_k,i}) \tag{5.11}$$

Then we can get the bit energy-to-noise ration and aggregate data rate of the sector in the downlink as like the uplink case.

5.5 Numerical Results

In this section, we will investigate the location-dependent interference analysis, the capacity evaluation of the proposed link-proportional DCA scheme, and the blocking probability between the different dynamic channel assignment schemes. In subsection 5.5.1 and subsection 5.5.2, we analyze the impact of two different inter-cell interference to explain the proposed scheme design rule. In subsection 5.5.3 and subsection 5.5.4, we evaluate the system capacity corresponding to the different dynamic channel assignment scheme and the degree of traffic asymmetry. To further verify the advantage of the proposed link-proportional dynamic channel assignment scheme,

we design a multiple services environment with different kinds of asymmetric traffic services in subsection 5.5.4. We evaluate the system blocking probability when each dynamic channel assignment scheme experiences different kinds of traffic load and traffic asymmetry. These numerical results will demonstrate that the proposed link-proportional dynamic channel assignment scheme outperform the other dynamic channel assignment algorithms in most aspects.

5.5.1 Average Uplink Location-dependent Interference Analysis

In subsection 5.5.1 and subsection 5.5.2, we analyze the mean received interference associated with a specific range which will form a partial ring in the sector as shown in Fig. 5.6. We assume each user applies one RU and uniformly distributed in a specific area. In [45], the received interference is highly dependent on the location of the target user and the interfering sources. Here, we focus on the analysis of the impact of inter-cell interference according to the group of users' distributed range in the sector. We partition the sector into ten rings. Each ring has the equal and distinct distance range from the base station. Table 5.1 illustrates the system parameters used in this chapter.

Since the location of the receiver (base station) is fixed in the uplink, the received inter-cell interference will highly depend on the locations of the interfering users. We assume the number of users is the same in each analysis. In [45], we have derived the mean received cross-slot interference and same directional inter-cell interference mobile according to a served user of the neighboring sector MSn in a specific location, denoted by $Im^{(u)}_{b\to b}(r_s, \theta_s)$, and $Im^{(u)}_{m\to b}(r_s, \theta_s)$, respectively, where r_s and θ_s denote the distance and the angle of the user MSn according to its serving base station BSn. As an extension, we can obtain the mean cross-slot interference

Table 5.1: System Parameters .

Cell radius	R=500 m
Base station antenna hight	h_b = 15 m
Mobile antenna height	h_m =2 m
Target SINR	$\frac{E_b}{N_0}$ = 4 dB
Thermal noise	η = -112 dBm
Power control level	P_r/η = -1 dB
number of rings for analysis	N_r = 10
number of users per analysis	N = 16
k^{th} ring's distance range of the BS	$50(k-1) \sim 50k$(m)

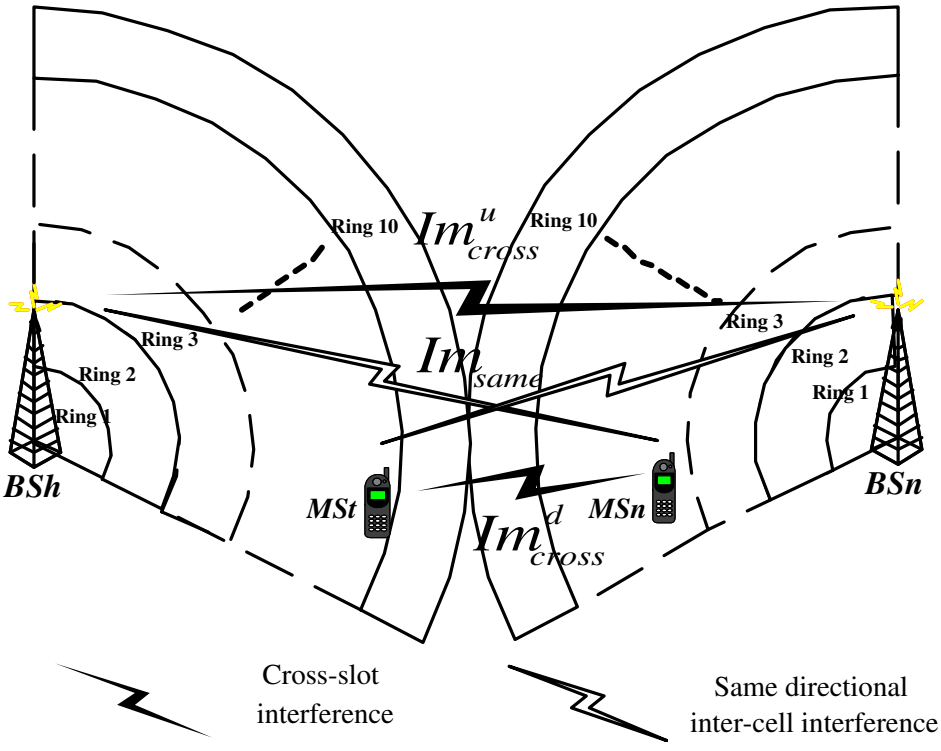

Figure 5.6: Ring separation inside a sector.

Table 5.2: Inter-cell Interference Analysis in uplink.

	Ring 6	Ring 7	Ring 8	Ring 9	Ring 10
$Ir_{b\to b}^{(u),k}$	8.4	16.2	28.6	47.1	73.3
$Ir_{m\to b}^{(u),k}$	0.32	0.79	1.82	3.5	5.7

from a specific k-th ring of the adjacent sectors in the uplink as

$$Ir_{b\to b}^{(u),k} = \frac{N}{A_{ring}^{k}} \cdot \int\int_{\substack{k^{th}{}_{ring} \\ inBsn}} Im_{b\to b}^{(u)}(r,\theta)\ drd\theta\ . \tag{5.12}$$

And the mean received inter-cell interference from the uplink mobiles within ring k of adjacent sector is obtained as

$$Ir_{m\to b}^{(u),k} = \frac{N}{A_{ring}^{k}} \cdot \int\int_{\substack{k^{th}{}_{ring} \\ inBsn}} Im_{m\to b}^{(u)}(r,\theta)\ drd\theta\ . \tag{5.13}$$

Table 5.2 illustrates the mean received inter-cell interference in the uplink while the users of neighboring sector are in the different rings. Because the received inter-cell interference from ring 1 to ring 5 is much smaller than the received inter-cell interference from ring 6 to ring 10 , we don't list them here. For ease of analysis, we normalize $Ir_{b\to b}^{(u),k}$ and $Ir_{m\to b}^{(u),k}$ to P_r.

5.5.2 Average Downlink Location-dependent Interference Analysis

In the downlink case, we show the mean received interference level of the specific users who locate inside a specific ring. We assume that the interfering users are uniformly distributed in the neighboring sectors. From [45], we can get the mean received cross-slot interference $Im_{m\to m}^{(d)}(r_s,\theta_s)$ and same directional inter-cell interference from adjacent sector $Im_{b\to m}^{(d)}(r_s,\theta_s)$ of the target user MSt, where r_s and θ_s are the distance and the angle of the target user MSt to its serving base station BS_h, respectively.

Table 5.3: Inter-cell Interference Analysis in downlink.

	Ring 6	Ring 7	Ring 8	Ring 9	Ring 10
$Ir_{m\to m}^{(d),k}$	0.034	0.115	0.4	1.83	28.9
$Ir_{b\to m}^{(d),k}$	0.3	0.65	1.14	1.9	2.9

Consequently, we can get the mean received cross-slot interference of all users in the ring k of neighboring sector as follows

$$Ir_{m\to m}^{(d),k} = \frac{N}{A_{ring}^{k}} \cdot \int \int_{\substack{k^{th}{}_{ring} \\ inBSh}} Im_{m\to m}^{(d)}(r,\theta)\ \ drd\theta\ \ . \tag{5.14}$$

where A_{ring}^{k} is the area of the ring. And the mean received the same directional inter-cell interference of all users in the k^{th} ring as

$$Ir_{b\to m}^{(d),k} = \frac{N}{A_{ring}^{k}} \cdot \int \int_{\substack{k^{th}{}_{ring} \\ inBSh}} Im_{b\to m}^{(d)}(r,\theta)\ \ drd\theta\ \ . \tag{5.15}$$

Table 5.3 illustrate the mean received inter-cell interference for the users located in the difference rings of the sector in the downlink.

From the above inter-cell interference analysis, it can be found that the cross-slot interference is much dominant in the outer ring of a sector in both the downlink and uplink cases. We must avoid to allocate to the users near the cell boundary with the time slots that will receive huge cross-slot interference. In the uplink case, because the transmission power of a base station and the antenna gain between base stations are quite high, the received cross-slot interference will be always larger than the same directional inter-cell interference. To alleviate the cross-slot interference in the uplink is an important design issue. In the downlink case, because the link gain between mobile and mobile is small, the received cross-slot interference will be serious just in some outer rings. Since the probability for two mobiles closed to each other in different base stations is small, the mobile-to-mobile cross-slot interference problem will be

less than base-to-base cross-slot interference in the uplink. To increase the system capacity effectively in the downlink, both the intra-cell interference and the inter-cell interference should be taken into consideration. The proposed link-proportional dynamical channel assignment is designed to alleviate both of the intra-cell and inter-cell interference, and then increase the system performance.

5.5.3 Uplink Capacity Analysis

In the analysis, single service is assumed and each user is with the same amount of RU requirement and the target bit energy-to-noise ratio. To evaluate the effects on capacity resulting from traffic asymmetry, we define a parameter Λ as the degree of the traffic asymmetry among three sectors in the virtual cell. First, We choose the sector with the most symmetric load between the downlink and the uplink as the referenced cell, denoted as IND

$$IND = \min_i \left\{ \left| T_i^{(d)} - T_i^{(u)} \right|, \text{ i} \in \text{the sectors in the virtual cell} \right\}; \tag{5.16}$$

where $T_i^{(d)}$ and $T_i^{(u)}$ are the number of time slots allocated in the downlink and the uplink for the sector i.

We set the degree of traffic asymmetry for the indicator Λ_{IND} to be zero and define the number of downlink time slots of the sector IND as a indication $T_{IND}^{(d)}$. Then we set the degree of traffic asymmetry for the sector i as

$$\Lambda_i = \| T_i^{(d)} - T_{IND}^{(d)} \| \tag{5.17}$$

With the definition of traffic asymmetric level, we design a system traffic condition to evaluate the system performance corresponding to different degrees of traffic asymmetry as shown in Table 5.4. Table 5.4 illustrates the setting of the traffic loads of the considered sectors. We define the traffic factor T_F to represent the total system

Table 5.4: Simulation Example of Cellular Traffic Load.

Sector A			Sector B			Sector C		
$T_A^{(d)}$	$T_A^{(u)}$	Λ_A	$T_B^{(d)}$	$T_B^{(u)}$	Λ_B	$T_C^{(d)}$	$T_C^{(u)}$	Λ_C
7	7	0	7	7	0	7	7	0
7	7	0	8	6	1	6	8	1
7	7	0	9	5	2	5	9	2
7	7	0	10	4	3	4	10	3
7	7	0	11	3	4	3	11	4

traffic load as

$$\text{Traffic Factor } (T_F) = \frac{\text{the utilized resource unit (RU)}}{\text{the total number of available resource unit (RU)}} \tag{5.18}$$

Table 5.5 lists the system parameters for the rest of numerical results. Figure 5.7 depicts the impact of base-to-base cross-slot interference with respect to the traffic asymmetry for different dynamic channel assignment schemes in the uplink. Is is shown that the proposed LP-DCA scheme has the better system performance than those of other methods. The proposed scheme is the most robust one to suppress with the base-to-base cross-slot interference.

Table 5.5: System Parameters for Simulation.

Traffic Factor	F_T=0.95
Orthogonal factor in downlink	F_{orth}=0.8
Radius factor for the inner-region (for region-based DCA)	R_{region} = 0.62

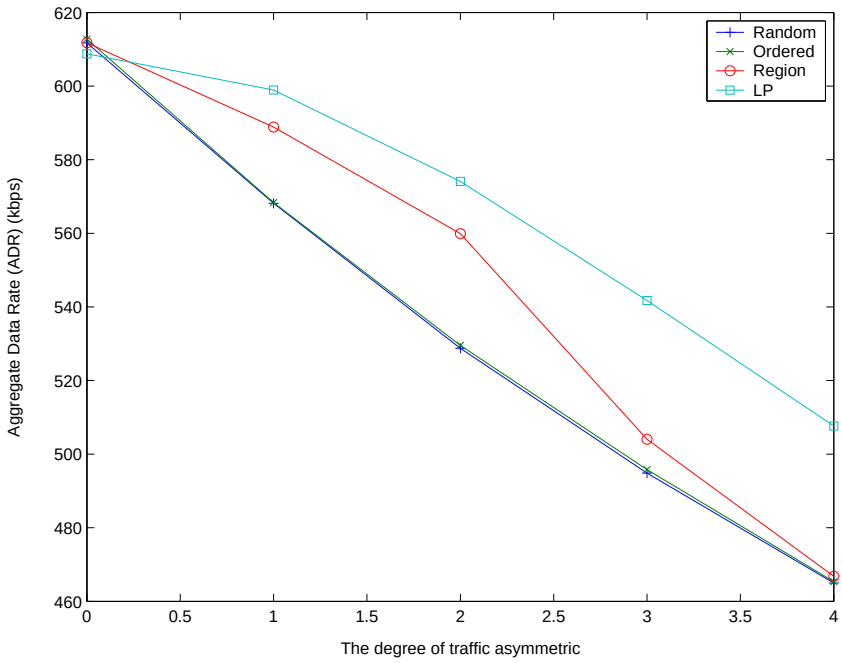

Figure 5.7: The impact of the base station to base station cross-slot interference to the different degree of asymmetric traffic in the uplink.

5.5.4 Downlink Capacity Analysis

Figure 5.8 illustrates the impact of the mobile-to-mobile cross-slot interference with respect to the traffic asymmetry for the different dynamic channel assignment schemes in the downlink. It can be found that the impact of the mobile-to-mobile cross-slot interference is not as severe as the base station to base station cross-slot interference. Since the degradation of the link gain is in several order of the distance between two mobiles, only few very closed mobiles may cause large interference. While the users are uniformly distributed, the probability that two mobiles approaches to each other in different sectors is quite small. However, the proposed scheme can still outperform the other algorithms due to the alleviation of near-far intra-cell interference and inter-cell interference from the downlink users in the neighboring sector. The LP-DCA scheme can reduce the impact of the cross-slot interference similar with the region-based method but is more flexible and efficient. It can expend less radio resource to compensate the near-far effect and the same directional inter-cell interference with a proper slot allocation mechanism. It can be also found that the radius factor of the region-based dynamic channel assignment algorithm should be adequate to the degree of traffic asymmetry. In this environment, region-based algorithm will have the higher performance when the degree of traffic asymmetry Λ between adjacent sectors equals to 2. The performance of the ordered dynamic channel assignment scheme is slightly better than that of random dynamic channel assignment scheme. When the traffic load is heavy, the ordered dynamic channel assignment scheme fails to combat with cross-slot interference and approaches the performance of random dynamic channel assignment scheme. To further demonstrate the performance of the proposed scheme, we adopt a multiple services scenario in the next section. Two important factors, users density of the sector and the traffic asymmetry, are considered in this scenario that will affect the performance of TDD/CDMA systems significantly.

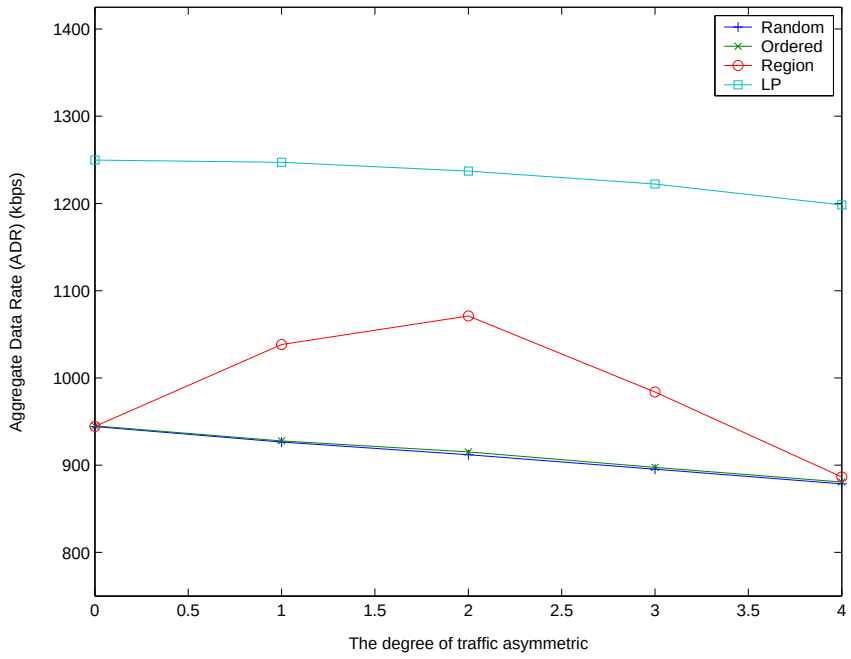

Figure 5.8: The impact of the mobile to mobile cross-slot interference to the different degree of asymmetric traffic in the downlink.

5.5.5 Multiple Services

In this subsection, we evaluate the performance of the system outage probability of the LP-DCA scheme compared with other dynamic channel assignment schemes in the multiple services environment. Each service class has its requirements of radio resource and the bit energy-to-noise ratio, and different traffic asymmetry of different service classes is imposed on the system. The performance of outage probability significantly impacts on the transmission quality of each service class. In TDD mode, cross-slot co-channel interference is a dominant factor to cause severe performance degradation. A well designed DCA scheme to address the different traffic asymmetry among the virtual cell will effectively improve the performance of system outage probability. Three different classes of service are assumed in the system and the setting of the parameters for these service classes are shown in Table 5.6. Service class 1 is the traditional voice service with balanced traffic load in the downlink and uplink. Service class 2 has the heavy traffic load in the downlink and called downlink enhancement data service. And Service class 3 has the heavy traffic load in the uplink and called uplink enhancement data service. The data service has the lower target $\frac{E_b}{N_0}$ than the voice service due to advanced error correction coding schemes. The system outage probability in the multiple service environment is defined by

$$P_{sys,o} = \sum_{\forall i} \sum_{k=1}^{3} Pr\left\{ \frac{E_b}{N_0} < \gamma_k \middle| \, i \in \text{ class } k \right\} \cdot \phi_k, \tag{5.19}$$

where γ_k is the bit energy-to-noise ratio requirement for class k, and $\phi_k = Pr\{i \in \text{ class } k\}$ is the traffic ratio of class k.

The performance of system outage probability is mainly affected by two factors: the distribution of the traffic asymmetry of all sectors in a virtual cell and the traffic load of each sector. To evaluate the performance of outage probability with respect to traffic asymmetry, a scenario is adopted to vary the traffic ratios ϕ_k to adjust the

Table 5.6: Multiple Services Parameters.

	Required Radio Resource in the Downlink	Required Radio Resource in the Uplink	Target $\frac{E_b}{N_0}$
Service Class 1	1 RU	1 RU	4 dB
Service Class 2	5 RU	1 RU	1 dB
Service Class 3	1 RU	5 RU	1 dB

Table 5.7: The Distribution of Traffic Load of three services in each sector.

	Sector A		Sector B		Sector C	
	ϕ_1	$\phi_2 : \phi_3$	ϕ_1	$\phi_2 : \phi_3$	ϕ_1	$\phi_2 : \phi_3$
Step 1	1/3	1 : 1	1/3	1 : 1	1/3	1 : 1
Step 2	1/3	1 : 1	1/3	3 : 2	1/3	2 : 3
Step 3	1/3	1 : 1	1/3	3 : 1	1/3	1 : 3
Step 4	1/3	1 : 1	1/3	9 : 1	1/3	1 : 9
Step 5	1/3	1 : 1	1/3	1 : 0	1/3	0 : 1

distribution of the traffic asymmetry with a fixed total number of users. In each sector, the number of voice users is fixed to be one-third ($\phi_1 = 1/3$) of the total number of users. Initially, the traffic ratios for downlink and uplink enhancement service, ϕ_2 and ϕ_3, are set to be $\phi_2 = \phi_3 = 1/3$, too. In the following steps, we gradually change some users in sector B from the downlink enhancement data service to the uplink enhancement data service for each time. Conversely, we gradually reduce some users in sector C from the uplink enhancement data service to the downlink enhancement data service at the same time. And the traffic ratios ϕ_2 and ϕ_3 of sector A are all fixed 1/3. Table 5.7 illustrates the traffic load condition in the following results.

Figure 5.9, 5.10, and 5.11 illustrate the system outage probability with respect to the traffic asymmetry with given total number of users by 60, 75, and 90. Here, the traffic asymmetry is defined as the difference of the traffic load in downlink between sector B and sector C that is set according to the above description. While the user density is light as shown in Fig. 5.9, the proper outage probabilities of each DCA schemes are below 6% in most traffic asymmetry condition. When the user density increases as shown in Fig. 5.10 and Fig. 5.11, the outage probabilities of LP-DCA are always the lowest one as the traffic asymmetry is increased, while the outage probabilities of random, ordered, and region-based DCA schemes are higher than that of LD-DCA by 5%, 4%, and 2.5% , respectively. It can be also found in Fig. 5.9, Fig. 5.10, and Fig. 5.11 that the increase of the additional outage probability of LP-DCA is limited below 6% as the traffic asymmetry is increased, while the increase of the additional outage probability of the random, ordered, and region-based DCA schemes are about 11.5%, 11%, and 9%, respectively. This is because that LP-DCA can minimize the total receive interference flexibly. The proposed LP-DCA scheme can attain the better system performance and alleviate the cross-slot interference due to the increasing traffic asymmetry. From the above numerical results, the proposed link-proportional DCA can be demonstrated to achieve the better system performance

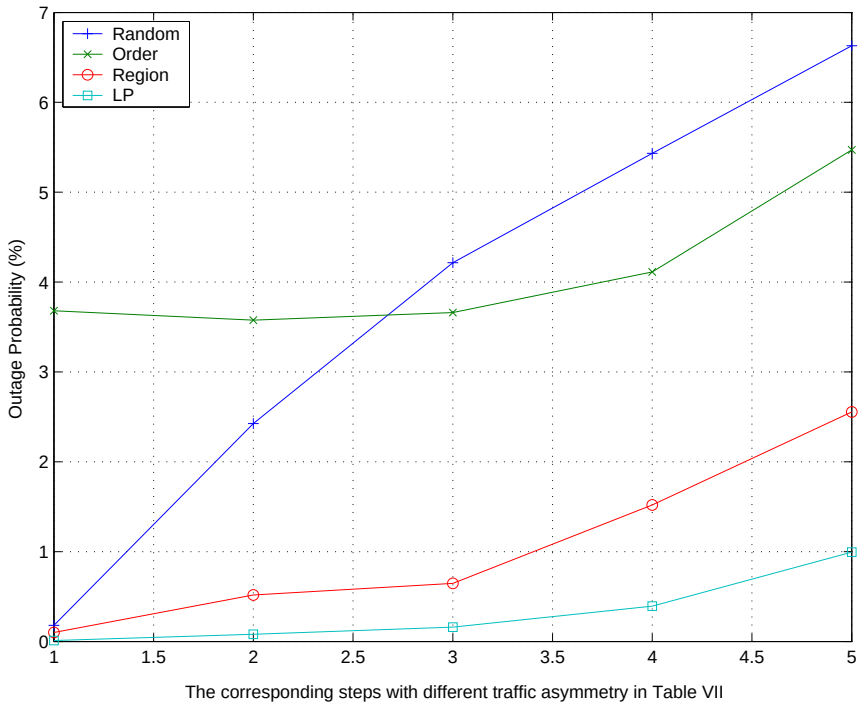

Figure 5.9: The Outage Probability corresponds to the different kinds of traffic asymmetry when there are 60 users in each sector.

and support asymmetric traffic services effectively.

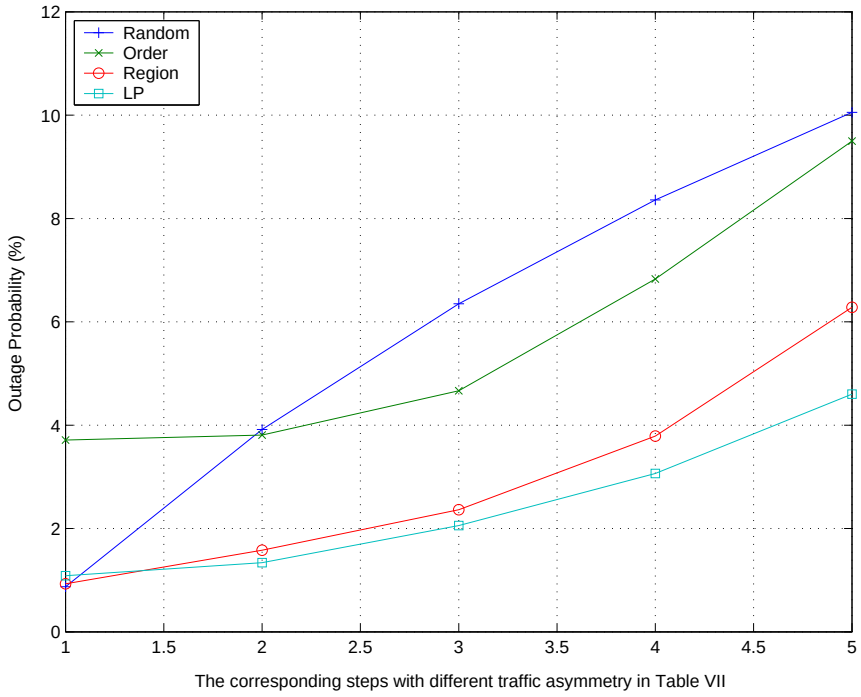

Figure 5.10: The Outage Probability corresponds to the different kinds of traffic asymmetry when there are 75 users in each sector.

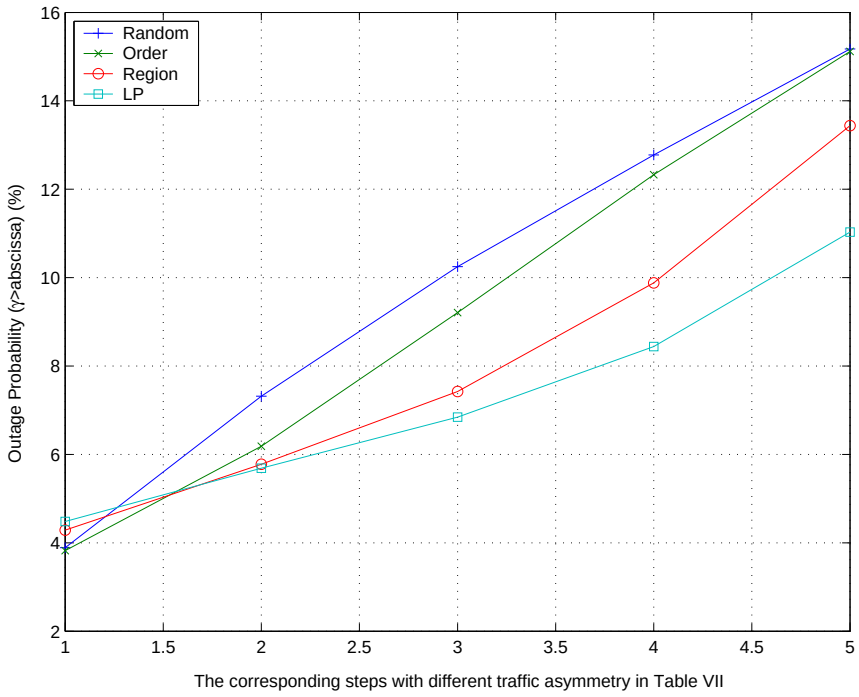

Figure 5.11: The Outage Probability corresponds to the different kinds of traffic asymmetry when there are 90 users in each sector.

CHAPTER 6

Joint Cross-Slot Interference-Based Dynamic Channel Assignment and Antenna Beamforming for the TDD/CDMA Systems with Asymmetric Traffic

As the requirement for the asymmetric data services is growing, the time division duplex/code division multiple access (TDD/CDMA) system has been considered as an important wireless network in the future. However, different asymmetric traffic loads among cells may cause heavy cross-slot interference, which can seriously degrade the system performance. To alleviate the impact of the cross-slot interference and improve the system performance, we propose a cross-slot interference-based dynamic channel assignment algorithm incorporated with antenna beamforming techniques. The proposed cross-slot interference-based DCA algorithm aims to reduce downlink cross-slot interference and distributedly assign downlink and uplink time slots to support asymmetric traffic services in each cell. The antenna beamforming techniques adopted here are mainly to avoid the impact of heavy uplink cross-slot interference. Our numerical results show that synergy of combining the cross-slot interference-

based DCA algorithm and antenna beamforming can effectively suppress the cross-slot interference in both downlink and uplink, thereby enabling a TDD/CDMA system to flexibly provide various asymmetric traffic loads in different cells and achieve high system performance.

6.1 Introduction

The increasing demands for high speed and high-quality asymmetric traffic services are the driving forces toward the rapid development of wireless communication technologies [49]. Code Division multiple access (CDMA) system is a promising radio access technique for the third-generation mobile communication systems due to its high flexibility and efficiency. In the CDMA systems, there are two different operation modes, namely frequency division duplex (FDD) and time division duplex (TDD). Comparing to the FDD-CDMA system with a pair of separated frequency bands used for downlink and uplink transmissions, the uplink and downlink transmissions in the TDD/CDMA systems multiplex the uplink and downlink time slots on the same frequency band. By exploiting the inherent time division component, time division duplex (TDD) mode is very suitable to provide asymmetric traffic services. [2, 3].

However, to support the asymmetric traffic in the TDD/CDMA system, the different asymmetric traffic conditions among cells may cause heavy *cross-slot interference*, which will seriously degrade the system performance [3–5]. Take the TDD/CDMA systems specified in the Universal Mobile Telecommunications System as an example (UMTS) [6, 7]. A TDD frame has 15 time slots, where the first one is usually used for signaling, and the others can be allocated for either the uplink or the downlink traffic channels as shown in Fig. 1.1. The boundary between the uplink and downlink time slots within a transmission frame is called the switching point. When two neighboring cells have different switching points due to distinct

uplink-to-downlink traffic ratios, some time slots may be used for downlink transmissions in one cell, while being used for uplink transmissions in other cells. The opposite uplink and downlink transmissions in some time slots for two neighboring cells is called the cross-slot interference in this chapter. Note that in Fig. 1.1, there are two kinds of cross-slot interference: base-to-base cross-slot interference in the uplink and the mobile-to-mobile cross-slot interference in the downlink. Because the transmission power of a base station is much higher than that of a mobile terminal, the base-to-base cross-slot interference is quite significant. Meanwhile, as a mobile terminal approaches to another mobile of an adjacent cell at the cell boundary, the mobile-to-mobile cross-slot interference can not be ignored. Both types of cross-slot interference will degrade the system performance seriously [8, 9], since it is usually suggested that a time slot should be used for the same transmission direction either uplink or downlink for two neighboring cells. This constraint, however, obviously wastes time slots if traffic asymmetric ratio of two neighboring cells differs significantly. Apparently, this approach may lose the key advantages of the TDD systems in supporting asymmetric traffic services [3,10]. The key to relax this restriction is to find an effective approach to overcome the cross-slot interference in the TDD/CDMA system.

In the literature, there are three research directions to avoid the cross-slot interference. The first one is to apply the dynamic channel assignment (DCA) techniques [11–13]. In [11], the authors proposed an ordered DCA algorithm to reduce the probability to use the time slot that may have a higher chance of experiencing the cross-slot interference. When the traffic load or the traffic asymmetric ratio is high, this method may have difficulty in overcoming the cross-slot interference. The authors in [12] and [13] proposed the region-based and path gain division DCA. In these algorithms, the users close to the home base station are assigned to use the time slots even having the cross-slot interference, whereas the users near the cell boundary

are assigned the clean time slots without the cross-slot interference. The performance of this system will highly depend on the way of separating the inner and the outer regions. In the time-varying traffic condition, it is usually hard to accurately separate two regions with one being robust to the cross-slot interference and the other being untolerant to the cross-slot interference.

Another research direction of overcoming cross-slot interference is to adopt advanced antenna techniques [17, 27, 50]. The authors in [17] and [50], focusing on the TDD/CDMA system and TDD-TDMA system, respectively, suggested to adopt the sectorized antennas combined with time slot allocation methods to suppress the inter-cell cross-slot interference. In [27], the authors applied the minimum variance distortionless response (MVDR) beamformer technique to eliminate the cross-slot interference in the uplink. However, the mobile-to-mobile cross-slot interference in the downlink was not considered in [27].

Third direction of overcoming the cross-slot interference in TDD/CDMA systems is to combine DCA with antenna techniques. The link proportional DCA (LP-DCA) algorithm combined with the sectorized antennas was proposed in [51]. The LP-DCA algorithm is similar to [12] but has more flexibility. Nevertheless, most DCA algorithms including the LP-DCA in [11] can not effectively alleviate the base-to-base cross-slot interference.

In this chapter, for supporting asymmetric traffic in the TDD/CDMA system, we propose a cross-slot interference-based dynamic channel assignment scheme combined with the MVDR beamformer. In the proposed scheme, the DCA is focused on reducing the mobile-to-mobile cross-slot interference, while the MVDR beamformer is aiming to suppress the base-to-base cross-slot interference. To alleviate the mobile-to-mobile cross-slot interference, the basic idea of the cross-slot interference-based DCA is to allocate time slots to users in a specific order. Specifically, for reducing the base-to-base cross-slot interference, both receiving and transmitting beamforming

weights are designed according to the MVDR beamformer criterion and the fourier beamformer criterion, respectively. According to our numerical results, the cross-slot interference-based DCA can improve system performance in both downlink and uplink, while providing asymmetric traffic services with a great deal of flexibility.

The rest of this chapter is organized as follows. Section 6.2 describes the system model. In Section 6.3, we discuss the signal quality and capacity of the TDD/CDMA system with beamforming techniques. In Section 6.4, we describe the proposed integration DCA and beamforming scheme. Numerical results will be provided in Section 6.5. We give our conclusion remarks in Section 6.6.

6.2 System Model

In this section, we introduce the cellular system model and the propagation model. We consider a TDD/CDMA hexagonal cellular system and the mobiles are assumed to be uniformly distributed over the system. It is assumed that power control is conducted in both the downlink and the uplink transmission.

6.2.1 Propagation Model

We define the propagation loss between two wireless entities (a mobile or a base station) i and j as

$$G_{i,j} = G(r_{i,j}, \alpha_{i,j}) = \min\left(\frac{G_i G_j h_i^2 h_j^2}{r_{i,j}^4} \cdot 10^{\frac{\alpha_{i,j}}{10}}, MCL_{i \to j}\right) \tag{6.1}$$

where G_i and G_j are the antenna gains of communication entities i and j; h_i and h_j are the antenna heights, $r_{i,j}$ is the distance between i and j, and $\alpha_{i,j}$ is the log-normally distributed shadowing component with standard deviation $\sigma_{i,j}$. Furthermore, we introduce the minimum coupling loss (MCL) as the minimum propagation loss including antenna gain measured between antenna connectors [46]. We defined

$MCL_{b\to m}$ as the MCL between the base station and the mobile and $MCL_{m\to m}$ as the MCL between two mobiles. In [47], the value of $MCL_{b\to m}$ is defined as $10^{-5.3}$, and $MCL_{m\to m}$ is equal to 10^{-4}.

6.2.2 Uplink SINR

Let $P_{m,i}$ be the transmit power level of the target mobile i. Then the different kinds of the interference received for mobile i at any time slot can be categorized as

(1) Intra-cell interference

$$I_{h,i}^{(u)} = \sum_{j=1, j\neq i}^{N_h} P_{m,j} \cdot G(r_{h,j}, \alpha_{h,j}) \tag{6.2}$$

where N_h is the number of interfering mobiles observed in the uplink direction at the home base station h, and $G(r_{h,j}, \alpha_{h,j})$ is defined in (6.1).

(2) Inter-cell interference from the mobiles in the neighboring cell k

$$I_{m\to b,i}^{(u)} = \sum_{k\in B^{(u)}} \sum_{i_k=1}^{N_k} P_{m,i_k} \cdot G(r_{h,i_k}, \alpha_{h,i_k}) \tag{6.3}$$

where $B^{(u)}$ is the set of adjacent cells in the uplink transmission, and N_k is the number of interfering mobiles in cell k.

(3) Base-to-base cross-slot interference

$$I_{b\to b,i}^{(u)} = \sum_{k\in B^{(d)}} G(r_{h,k}, \alpha_{h,k}) \sum_{i_k=1}^{N_k} P_{b,i_k} \tag{6.4}$$

where $B^{(d)}$ is the set of neighboring cells in the downlink transmission, and P_{b,i_k} is the transmission power form the neighboring cell k to the mobile i_k.

Combining all types of interference, the signal-to-interference and noise ratio (SINR) of user i can be written as

$$\gamma_i = \frac{P_{m,i} \cdot G(r_{h,i}, \alpha_{h,i})}{I_{h,i}^{(u)} + I_{m\to b,i}^{(u)} + I_{b\to b,i}^{(u)} + \eta} \tag{6.5}$$

where η is the white thermal noise power, and $I_{h,i}^{(u)}$, $I_{m\to b,i}^{(u)}$, and $I_{b\to b,i}^{(u)}$ are defined in (6.2), (6.3), and (6.4).

For simplicity, let

$$I_{b\to b,i}^{(u)} = I_{b\to b}^{(u)}, \text{ for } i = 1, 2, \ldots, N_{k'}, \ k' \in B^{(d)}, \tag{6.6}$$

$$I_{m\to b,i}^{(u)} = I_{m\to b}^{(u)}, \text{ for } i = 1, 2, \ldots, N_k, \ k \in B^{(u)}, \tag{6.7}$$

and

$$I_a = I_{m\to b}^{(u)} + I_{b\to b}^{(u)} + \eta. \tag{6.8}$$

Then the system adjust the power of user i iteratively to achieve its target SINR γ_t. We can obtain the power in $(n+1)$-th step as

$$P_{m,i}^{(n+1)} = \gamma_t \cdot \left[\sum_{j=1, j\neq i}^{N_h} P_{m,j}^{(n)} \frac{G_{h,j}}{G_{h,i}} + \frac{I_a^{(n)}}{G_{h,i}} \right]. \tag{6.9}$$

where γ_t is the target SINR for each user, and then

$$\mathbf{P}_m^{(n+1)} = \gamma_t \cdot \left(\mathbf{F} \cdot \mathbf{P}_m^{(n)} + \mathbf{I}^{(n)} \right), \tag{6.10}$$

where $\mathbf{P}_m = [P_{m,1}, P_{m,2}, \ldots, P_{m,N_h}]^T$, $\mathbf{I} = [\frac{I_a^{(n)}}{G_{h,1}}, \frac{I_a^{(n)}}{G_{h,2}}, \ldots, \frac{I_a^{(n)}}{G_{h,N_{u,h}}}]$, and $\mathbf{F}$ is a nonnegative matrix, defined as

$$[\mathbf{F}]_{ij} = \begin{cases} 0, & \text{if } j = i \\ \frac{G_{h,j}}{G_{h,i}} > 0, & \text{if } j \neq i \end{cases} \tag{6.11}$$

6.2.3 Downlink SINR

Three different kinds of received interference in the downlink transmission for mobile i at any time slot are defined as

(1) Intra-cell interference

$$I_{h,i}^{(d)} = \sum_{j=1, j\neq i}^{N_h} (1-\rho) \cdot P_{b,j} \cdot G(r_{h,i}, \alpha_{h,i}), \tag{6.12}$$

where ρ is the orthogonal factor between the codes used in the downlink of the same cell.

(2) Inter-cell mobile-to-mobile cross-slot interference

$$I_{m\to m,i}^{(d)} = \sum_{k\in B^{(u)}} \sum_{i_k=1}^{N_k} P_{m,i_k} \cdot G(r_{i,i_k}, \alpha_{i,i_k}). \tag{6.13}$$

(3) Inter-cell interference from the neighboring cell k in the downlink transmission

$$I_{b\to m,i}^{(d)} = \sum_{k\in B^{(d)}} \sum_{i_k=1}^{N_k} P_{b,i_k} \cdot G(r_{k,i}, \alpha_{k,i}) \tag{6.14}$$

Similarly, we can express the SINR of the target user i in the downlink as

$$\gamma_i = \frac{P_{b,i} \cdot G(r_{h,i}, \alpha_{h,i})}{I_{h,i}^{(d)} + I_{m\to m,i}^{(d)} + I_{b\to m,i}^{(d)} + \eta} \tag{6.15}$$

From (6.12)to(6.15), the allocated power for user i at the $(n+1)$-th step can be written as

$$P_{b,i}^{(n+1)} = \gamma_t \cdot \left\{ \sum_{j=1,j\neq i}^{N_h} (1-\rho) \cdot P_{b,j}^{(n)} + \sum_{k\in B^{(u)}} \sum_{i_k=1}^{N_k} P_{m,i_k} \cdot \frac{G_{i,i_k}}{G_{h,i}} + \sum_{k\in B^{(d)}} \sum_{i_k=1}^{N_k} P_{b,i_k}^{(n)} \cdot \frac{G_{k,i}}{G_{h,i}} + \frac{\eta}{G_{h,i}} \right\}^{-1}. \tag{6.16}$$

6.3 Interference Analysis with Antenna Array

In this section, we discuss the method of analyzing interference for TDD-CDMA systems with antenna array. We first derive the expression of the received signal to interference plus noise ratio with a generic antenna beamformer. Assume an M-element uniform circular array (UCA) is employed at a base station. The array

manifold vector (or steering vector) of an UCA is written as

$$\mathbf{a}(\theta,\phi) = \begin{pmatrix} e^{j2\pi l/\lambda \sin\phi\cos\theta} \\ e^{j2\pi l/\lambda \sin\phi\cos(\theta-2\pi/M)} \\ \vdots \\ e^{j2\pi l/\lambda \sin\phi\cos(\theta-2\pi(M-1)/M)} \end{pmatrix} \tag{6.17}$$

where l is the radius of the circular antenna array, λ is the wavelength, θ is the azimuth angle, and ϕ is the vertical angle. In this chapter, l is assumed to be equal to half the wavelength and the azimuth angle ϕ is equal to $\pi/2$. While employing antenna arrays at the base station, the transmitted and received signal of the array elements are first combined with the beamformers, as shown in Figure 6.1. To produce a desired main beam and adjustable nulls, the weight factors $\mathbf{w}_i$ will be calculated for each user i.

6.3.1 Uplink SINR with Antenna Array

In [27], we have investigated three different kinds of received interference in the uplink transmission for the mobile i at any time slots as follows

$$I_{h,i}^{(u)} = \sum_{j=1,j\neq i}^{N_h} P_{m,j} \cdot G(r_{h,j},\alpha_{h,j}) \|\mathbf{w}_i^H \mathbf{a}_{h,j}\|^2 \ , \tag{6.18}$$

$$I_{m\to b,i}^{(u)} = \sum_{k\in B^{(u)}} \sum_{i_k=1}^{N_k} P_{m,i_k} \cdot G(r_{h,i_k},\alpha_{h,i_k}) \|\mathbf{w}_i^H \mathbf{a}_{h,i_k}\|^2 \ , \tag{6.19}$$

and

$$I_{b\to b,i}^{(u)} = \sum_{k\in B^{(d)}} \sum_{i_k=1}^{N_k} P_{b,i_k} \cdot G(r_{h,k},\alpha_{h,k}) \|\mathbf{w}_{i_k}^H \mathbf{b}_{k,h}\|^2 \|\mathbf{w}_i^H \mathbf{a}_{h,k}\|^2 \ . \tag{6.20}$$

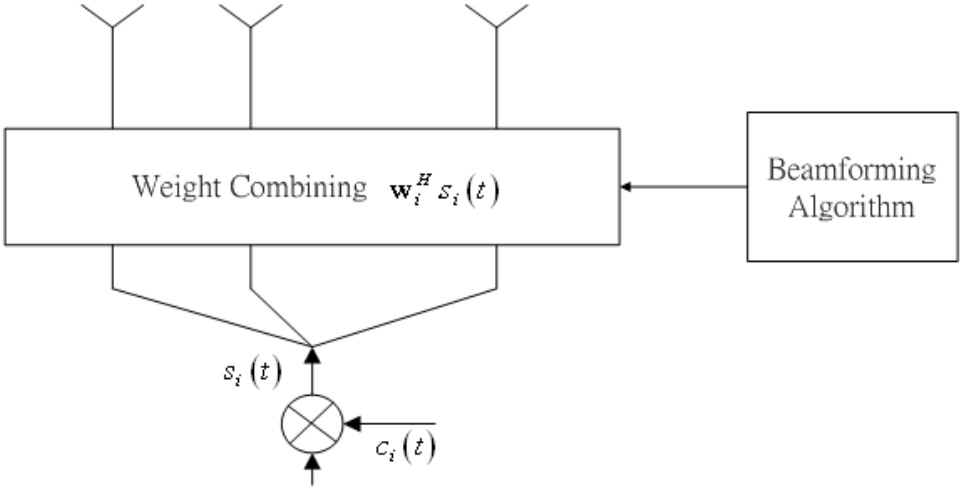

(a) a transmitter block diagram with antenna beamformer

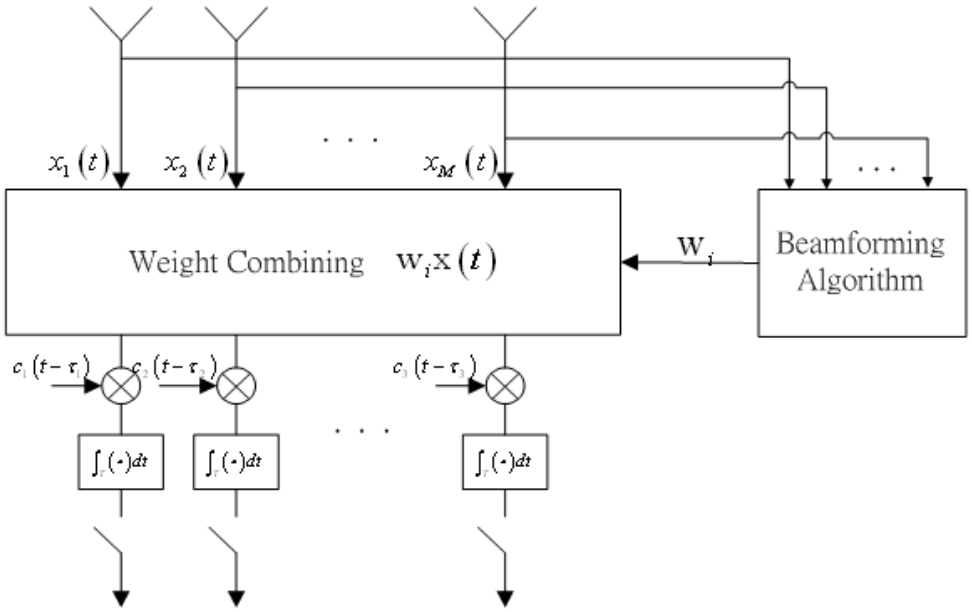

(b) a receiver block diagram with antenna beamformer

Figure 6.1: The block diagrams with antenna beamformers.

By substituting (6.18), (6.19), and (6.20) into (6.5), the SINR of mobile i in the uplink transmission with antenna beamforming becomes

$$\gamma_i^{(u)} = P_{t,i}\|\mathbf{w}_i^H\mathbf{a}_{h,i}\|^2 \quad \cdot \quad \left\{ \sum_{j=i,j\neq i}^{N_h} P_{m,j} \cdot \frac{G_{h,j}}{G_{h,i}}\|\mathbf{w}_i^H\mathbf{a}_{h,j}\|^2 + \sum_{k\in B^{(u)}}\sum_{i_k=1}^{N_k} P_{m,i_k} \cdot \frac{G_{h,i_k}}{G_{h,i}}\|\mathbf{w}_i^H\mathbf{a}_{h,i_k}\|^2 \right.$$
$$\left. + \sum_{k\in B^{(d)}}\sum_{i_k=1}^{N_k} P_{b,i_k} \cdot \frac{G_{h,k}}{G_{h,i}}\|\mathbf{w}_{i_k}^H\mathbf{b}_{k,h}\|^2\|\mathbf{w}_i^H\mathbf{a}_{h,k}\|^2 + \frac{\eta}{G_{h,i}} \right\}^{-1} \tag{6.21}$$

6.3.2 Downlink SINR with Antenna Array

Using the same methods, the received interference in the downlink transmission for mobile i at any time slot as

$$I_{h,i}^{(d)} = \sum_{j=1,j\neq i}^{N_h} (1-\rho) \cdot P_{b,j} \cdot G(r_{h,i},\alpha_{h,i})\|\mathbf{w}_j^H\mathbf{b}_{h,i}\|^2 \ , \tag{6.22}$$

$$I_{m\to m,i}^{(d)} = \sum_{k\in B^{(u)}}\sum_{i_k=1}^{N_k} P_{m,i_k} \cdot G(r_{i,i_k},\alpha_{i,i_k}) \ , \tag{6.23}$$

and

$$I_{b\to m,i}^{(d)} = \sum_{k\in B^{(d)}}\sum_{i_k=1}^{N_k} P_{b,i_k} \cdot G(r_{k,i},\alpha_{k,i})\|\mathbf{w}_{i_k}^H\mathbf{b}_{k,i}\|^2 \ . \tag{6.24}$$

Then we can obtain SINR of mobile i in the downlink transmission as

$$\gamma_i^{(d)} = P_{b,i}\|\mathbf{w}_i^H\mathbf{b}_{h,i}\|^2 \quad \cdot \quad \left\{ \sum_{j=1,j\neq i}^{N_k} (1-\rho) \cdot P_{b,j}\|\mathbf{w}_j^H\mathbf{b}_{h,i}\|^2 + \sum_{k\in B^{(u)}}\sum_{i_k=1}^{N_k} P_{m,i_k} \cdot \frac{G_{i,i_k}}{G_{h,i}} \right.$$
$$\left. + \sum_{k\in B^{(d)}}\sum_{i_k=1}^{N_k} P_{b,i_k} \cdot \frac{G_{k,i}}{G_{h,i}}\|\mathbf{w}_{i_K}^H\mathbf{b}_{k,i}\|^2 + \frac{\eta}{G_{h,i}} \right\}^{-1} \ . \tag{6.25}$$

6.3.3 Uplink Receive Beamformer

To investigate how to effectively apply antenna beamforming techniques with DCA algorithm to improve the system performance and suppress base-to-base cross-slot

interference, two types of antenna beamformers are considered in the uplink received signals: the conventional beam-steering technique and the minimum variance distortionless response (MVDR) beamformers. In [52], the authors demonstrated that remarkable capacity gain can be achieved for FDD-CDMA systems by the beam-steering beamformer. While the beam-steering beamformer can't alleviate the base-to-base cross-slot interference efficiently [27], we encourage to employ the MVDR beamformer in the proposed algorithm. In the rest of this section, we will introduce the beamformers employed in this work.

According to the beam-steering method, we know that the beamformer weight $\mathbf{w}_i$ is equal to its array manifold vector, i.e.,

$$\mathbf{w}_i = \frac{1}{M}\mathbf{a}_{h,i} \tag{6.26}$$

where the factor $1/M$ in (6.26) is a normalization factor such that $\mathbf{w}_i^H \mathbf{a}_{h,i} = 1$.

As a result, the signal-to-interference plus noise ratio after applying beam-steering becomes

$$\gamma_i^{(u)} = \frac{P_{m,i}}{M^2} \cdot \left\{ \sum_{j=i,j\neq i}^{N_h} P_{m,j} \cdot \frac{G_{h,j}}{G_{h,i}} \|\mathbf{a}_{h,i}^H \mathbf{a}_{h,j}\|^2 + \sum_{k\in B^{(u)}} \sum_{i_k=1}^{N_k} P_{m,i_k} \cdot \frac{G_{h,i_k}}{G_{h,i}} \|\mathbf{a}_{h,i}^H \mathbf{a}_{h,i_k}\|^2 \right.$$
$$\left. + \sum_{k\in B^{(d)}} \sum_{i_k=1}^{N_k} P_{b,i_k} \cdot \frac{G_{h,k}}{G_{h,i}} \|\mathbf{b}_{k,i_k}^H \mathbf{b}_{k,h}\|^2 \|\mathbf{a}_{h,i}^H \mathbf{a}_{h,k}\|^2 + \frac{\eta}{G_{h,i}} \right\}^{-1}, \tag{6.27}$$

The goal of the MVDR criteria is to minimize the output power, while maintaining signal strength equal to one in the desired direction [53]. The MVDR beamformer will determine the weight factor $\mathbf{w}_{mv}$ of the combining scheme according to the following rule:

$$\mathbf{w}_{mv} = \arg\min_{\mathbf{w}_i} E\left\{ \|\mathbf{w}_i^H \mathbf{x}\|^2 \right\}$$
$$s.t. \quad \mathbf{w}_i^H \mathbf{a}_{h,i} = 1 \tag{6.28}$$

where $\mathbf{x}(t) = [x_1(t), x_2(t), \ldots, x_M(t)]^T$ is the received signal vector in an M-element antenna array. In (6.28) the term $E\{\|\mathbf{w}_i^H \mathbf{x}\|^2\}$ can be expressed as

$$E\{\|\mathbf{w}_i^H \mathbf{x}\|^2\} = \mathbf{w}_i^H \Phi_x \mathbf{w}_i \ . \tag{6.29}$$

where Φ_x is the sampled covariance matrix of the received signal $\mathbf{x}(t)$ i.e., $\Phi_x = E\{\mathbf{x}(t)\mathbf{x}(t)^H\}$.

Applying the Lagrange multiple approach, we can obtain the MVDR beamformer weight $\mathbf{w}_{mv,i}$ of the user i as follows

$$\mathbf{w}_{mv,i} = \frac{\Phi_x^{-1}\mathbf{a}_{h,i}}{\mathbf{a}_{h,i}^H \Phi_x^{-1}\mathbf{a}_{h,i}} \tag{6.30}$$

According to (6.30), the total output power after the MVDR beamforming is equal to

$$E\|\mathbf{w}_{mv,i}^H \mathbf{x}\| = (\mathbf{a}_{h,i}^H \Phi_x^{-1}\mathbf{a}_{h,i})^{-1} \tag{6.31}$$

Then similar to the derivation of (6.27), we can first substitute the weight $\mathbf{w}_{mv,i}$ of (6.30) into (6.25) and then refer to (6.31) to obtain the signal-to-interference and noise ratio $\gamma_{mv,i}$ with the MVDR beamformer as following:

$$\gamma_{mv,i} = \frac{P_{m,i} \cdot G(r_{h,i}, \alpha_{h,i})}{(\mathbf{a}_i^H \Phi_x^{-1}\mathbf{a}_{h,i})^{-1} - P_{m,i} \cdot G_(r_{h,i}, \alpha_{h,i})} \tag{6.32}$$

6.3.4 Downlink Transmit Beamformer

Downlink transmit beamformer can enhance the performance by minimizing the induced interference to other users [23]. However, the downlink MVDR transmit beamforming may cause strong interference to other mobiles because of the higher amplitude in the side lobes [27]. Hence, we only consider the conventional beam-steering downlink transmit beamformer.

Similar to the received beam-steering beamformer in (6.26), the weight factor of mobile i in the downlink transmission can be denoted as

$$\mathbf{w}_i = \frac{1}{M}\mathbf{b}_{h,i} \tag{6.33}$$

From (6.25), the received downlink SINR for the mobile i in the downlink can de described as

$$\gamma_i^{(d)} = \frac{P_{b,i}}{M^2} \cdot \left\{ \sum_{j=1,j\neq i}^{N_h} (1-\rho) \cdot P_{b,j} \|\mathbf{b}_{h,j}^H \mathbf{b}_{h,i}\|^2 + \sum_{k\in B^{(u)}} \sum_{i_k=1}^{N_k} P_{m,i_k} \cdot \frac{G_{i,i_k}}{G_{h,i}} + \sum_{k\in B^{(d)}} \sum_{i_k=1}^{N_k} P_{b,i_k} \cdot \frac{G_{k,i}}{G_{h,i}} \|\mathbf{b}_{k,i_k}^H \mathbf{b}_{k,i}\|^2 + \frac{\eta}{G_{h,i}} \right\}^{-1} . \quad (6.34)$$

6.4 The Proposed Cross-slot Interference-based DCA algorithm

6.4.1 DCA algorithm

To improve the system capacity of the TDD-CDMA systems, we propose a cross-slot interference-based dynamic channel assignment algorithm. The proposed algorithm has the following steps:

Algorithm:

(1) Determining the ratio of downlink time slots to uplink time slots:
Let the aggregated requested rates in the downlink and the uplink be $\overline{R}^{(d)}$ and $\overline{R}^{(u)}$, respectively. Then the number of time slots for downlink and uplink transmissions, denoted by $T^{(d)}$ and $T^{(u)}$, can be calculated by $T^{(d)} = \text{round}\left(T \cdot \frac{\overline{R}^{(d)}}{\overline{R}^{(d)}+\overline{R}^{(u)}}\right)$ and $T^{(u)} = T - T^{(d)}$, where $T = T^{(d)} + T^{(u)}$ is the total number of time slots in each frame.

(2) Resource allocation for downlink users:
Since the mobile-to-mobile cross-slot interference can be very serious at the cell

boundary [13], the proposed DCA algorithm allocates downlink users near the cell boundary with the time slots without cross-slot interference.

– User grouping determination

  Each user will be classified to either the outer group or the inner group, denoted by G_{out} and G_{in}, according to the path loss to the serving base station. For any user i, the determination rule is described as follows:

$$\begin{aligned} i \quad &\in G_{out}, \text{if } G(r_{h,i}, \alpha_{h,i}) < G((R \cdot f_s), 0) \\ i \quad &\in G_{in}, \text{Otherwise.} \end{aligned} \tag{6.35}$$

  where R is the cell radius, f_s is the factor of separating the inner and outer region, choose $0 \leq f_s \leq 1$.

– Time Slot allocation

  If user i belongs to G_{in}, the link quality is usually better. Therefore,it can choose time slot from $S_c^{(d)}$, the set of time slots with higher probability having mobile-to-mobile cross-slot interference. Denote s_i as the time slot allocated for user i. Then, for the target SIR γ_t,

$$s_i = \arg \min_{s \in S_c^{(d)}} (\gamma_i(s) \mid \ \gamma_i(s) \geq \gamma_t + \gamma_m) \tag{6.36}$$

  where $\gamma_i(s)$ is the SIR of user i in time slot s, and γ_m is the SIR margin to guarantee the received signal quality. In the same way, the users in G_{out} will be designed to use the time slots with the lower probabilities having the mobile-to-mobile cross-slot interference $S_n^{(d)}$, i.e.,

$$s_i = \arg \min_{s \in S_n^{(d)}} (\gamma_i(s) \mid \ \gamma_i(s) \geq \gamma_t + \gamma_m), \tag{6.37}$$

  If there is no time slot in $S_c^{(d)}$ or $S_n^{(d)}$ can support user i to achieve the SIR equal to $\gamma_{t,i} + \gamma_m$, the system will try to find some other time slots requiring

the least transmit power to achieve the target SIR γ_t, i.e.

$$s_i = \arg \min_{s_i \in \left(S_c^{(d)} \cup S_n^{(d)}\right)} \left\{ \frac{\gamma_t}{\|\mathbf{w}_i^H(s)\mathbf{b}_{h,i}\|^2} \cdot \left[\sum_{j=1,j\neq i}^{N_h(s)} (1-\rho) \cdot P_{b,i} \frac{G_{h,j}}{G_{h,i}} \|\mathbf{w}_j^H \mathbf{b}_{h,i}\|^2 \right.\right.$$

$$\left.\left. + \sum_{k \in B^{(u)}(s)} \sum_{i_k=1}^{N_k(s)} P_{m,i_k} \cdot G_{i,i_k} + \sum_{k \in B^{(d)}(s)} \sum_{i_k=1}^{N_k(s)} P_{b,i_k} \frac{G_{k,i}}{G_{h,i}} \|\mathbf{w}_{i_k}^H \mathbf{b}_{k,i}\|^2 + \frac{\eta}{G_{h,i}} \right] \right\} \quad (6.38)$$

where $\mathbf{w}_i(s)$ is the weight factor for user i in the sth time slot, $\left(S_c^{(d)} \cup S_n^{(d)}\right)$ is the union of the time slots with cross-slot interference and those without cross-slot interference, $B^{(d)}(s)$ and $B^{(u)}(s)$ are the sets of adjacent cell at the sth time slot in the uplink and downlink individually, $N_h(s)$ and $N_k(s)$ are the number of users at the sth time slot in the home cell and that in the adjacent cell k, respectively. In the downlink case, we suggest using the conventional beam-steering beamformer. That is, the beam-steering weight $\mathbf{w}_i(s) = \frac{1}{M} b_{h,i}$, for any $s \in \left(S_c^{(d)} \cup S_n^{(d)}\right)$.

– Power update

Then we apply the joint beam-steering and the iterative SIR-based power control scheme to determine the base station power for user i $P_{b,i}$ at the $(n+1)$-th step as follows:

$$P_{b,i}^{(n+1)} = \frac{\gamma_t}{M^2} \cdot \left\{ \sum_{j=1,j\neq i}^{N_h} (1-\rho) \cdot P_{b,j}^{(n)} \|\mathbf{b}_{h,j}^H \mathbf{b}_{h,i}\|^2 + \sum_{k \in B^{(u)}} \sum_{i_k=1}^{N_k} P_{m,i_k}^{(n)} \cdot \frac{G_{i,i_k}}{G_{h,i}} \right.$$

$$\left. + \sum_{k \in B^{(d)}} \sum_{i_k=1}^{N_k} P_{b,i_K}^{(n)} \cdot \frac{G_{k,i}}{G_{h,i}} \|\mathbf{b}_{k,i_k}^H \mathbf{b}_{k,i}\|^2 + \frac{\eta}{G_{h,i}} \right\} \quad (6.39)$$

(3) Resource Allocation for uplink users

– Time slot allocation

For the uplink users, we will apply the MVDR beamformer to overcome the

most serious base-to-base cross-slot interference. The time slot s_i allocated to user i can be determined by the following criterion.

$$\begin{aligned} s_i &= \arg\min_{s\in S^{(u)}} \left\{ \frac{\gamma_t}{\|\mathbf{w}_i^H(s)\mathbf{a}_{h,i}\|^2} \left[\sum_{j=1,j\neq i}^{N_h(s)} P_{m,j}\cdot\frac{G_{h,j}}{G_{h,i}}\|\mathbf{w}_i^H(s)\mathbf{a}_{h,j}\|^2 \right.\right. \\ &+ \sum_{k\in B^{(u)}(s)}\sum_{i_k=1}^{N_k(s)} P_{m,i_k}\cdot\frac{G_{h,i_k}}{G_{h,i}}\cdot\|\mathbf{w}_i^H(s)\mathbf{a}_{h,i_k}\|^2 \\ &+ \left.\left. \sum_{k\in B^{(d)}(s)}\sum_{i_k=1}^{N_k(s)} P_{b,i_k}\cdot\frac{G_{h,k}}{G_{h,i}}\|\mathbf{w}_{i_k}^H\mathbf{b}_{k,h}\|^2\|\mathbf{w}_i^H(s)\mathbf{a}_{h,k}\|^2 + \frac{\eta}{G_{h,i}} \right] \right\} \end{aligned} \quad (6.40)$$

where $S^{(u)}$ is the set of all the time slots in the uplink. Note that (6.40) is similar to (6.38) except that the downlink interference is replaced with the uplink interference, and the beamformer weight. The adopted MVDR beamformer weight is in (6.30).

– Joint beamforming weights and power update

We suggest applying the MVDR beamformer to reduce base-to-base cross-slot interference. According to the MVDR criteria, the beamformer weights are updated as follows:

$$\mathbf{w}_{mv,i}^{(n+1)} = \frac{(\Phi_x^{(n)})^{-1}\mathbf{a}_{h,i}}{\mathbf{a}_{h,i}^H(\Phi_x^{(n)})^{-1}\mathbf{a}_{h,i}} \quad (6.41)$$

where Φ and $\mathbf{a}$ are defined in Section 6.3. As the weight factor for the beamformer is determined, the power allocation for user i will also be updated as follows:

$$P_{m,i}^{(n+1)} = P_{m,i}^{(n)}\cdot\gamma_t\cdot\left\{\mathbf{a}_i^H(\Phi_x^{(n)})^{-1}\mathbf{a}_i\right\} \quad (6.42)$$

The proposed cross-slot interference-based DCA algorithm can sufficiently reduce the impact of cross-slot interference through exploiting the flexibility of allocating resources in both space and time domains. In the downlink transmissions, the

users that may suffer from the serious mobile-to-mobile cross-slot interference are first assigned to utilize the edge time slots in a frame, which have the lower probability to be affected by the cross-slot interference. On the other hand, the users near the base station with better received signal quality are preferred to utilize the time slots in the middle portion of time slots in a frame, which have a higher probability experiencing the cross-slot interference. That is, the key idea of the cross-slot interference-based DCA algorithm is to preserve the time slots without cross-slot interference for the users near the cell boundary. For the uplink users, the base-to-base cross-slot interference is the major source to degrade the system capacity. The proposed scheme integrates iterative power control and the MVDR beamformer to reduce the cross-slot interference and other co-channel interference.

6.4.2 Parameter Design in the cross-slot interference-based DCA

In this subsection, we discuss how to design the factor of separating the inner and the outer region, the parameter f_s of the proposed DCA. Because the users are uniformly distributed, the probability that two mobiles run into each other from different base stations may not be very high. As a result, we analyze the received mobile-to-mobile cross-slot interference with only one interfering source as shown in Fig. 6.2. We assume that mobile b is at the cell boundary of cell n served by base station n while the target user a is served by the home base station h. Considering of MCL defined in subsection 6.2.1, the received mobile-to-mobile cross-slot interference can be expressed as

$$\begin{aligned} I_{m\to m} &= [P_{m,b}\cdot G_{a,b}\cdot\varphi(G_{a,b},(MCL_{m\to m})) \\ &+ P_{m,b}\cdot(MCL_{m\to m})\cdot\varphi((MCL_{m\to m}),G_{a,b})]\cdot\varphi(G_{h,b},G_{n,b}) \end{aligned} \quad (6.43)$$

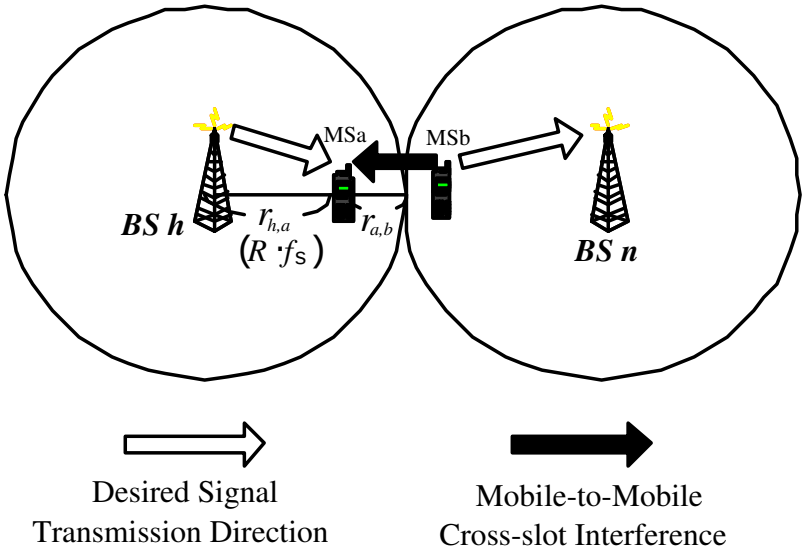

Figure 6.2: The environment for the mobile-to-mobile cross-slot interference analysis.

where $MCL_{m\to m}$ is the minimum coupling loss between two mobiles, and the function $\varphi(u,v)$ is used to indicate whether $u \le v$ or not, i.e.,

$$\varphi(u,v) = \begin{cases} 1, & \text{if } u \le v \ . \\ 0, & \text{otherwise} \ . \end{cases} \tag{6.44}$$

As shown in Fig. 6.2, we assume $r_{h,a} = R \cdot f_s$ and $r_{a,b} = R(1-f_s)$, R is the cell radius defined in subsection 6.4.1. Then we can obtain the mean received mobile-to-mobile interference as follows

$$\begin{aligned} E[I_{m\to m}] &= \frac{1}{2}\Big[P_{m,b}\cdot k_{a,b}\cdot[R(1-f_s)]^{-4}\cdot e^{\frac{1}{2}\eta^2\sigma_m^2} \\ &\cdot\ Q\left(\eta\sigma_m - \frac{\ln\{(MCL_{m\to m})\cdot[R(1-f_s)]^4\}}{\eta\sigma_m}\right) \\ &+\ P_{t,b}\cdot(MCL_{m\to m})\cdot\ Q\left(\frac{\ln\{(MCL_{m\to m})\cdot[R(1-f_s)]^4\}}{\eta\sigma_m}\right)\Big] \end{aligned} \tag{6.45}$$

where $k_{a,b} = G_a G_b h_a^2 h_b^2$, $\eta = \frac{\ln 10}{10}$, σ_m is the standard deviation of the shadowing effect between two mobiles, and $Q(x) = \int_x^\infty \frac{1}{\sqrt{2\pi}} e^{-\frac{t^2}{2}} dt$.

On the other hand, we evaluate the mean received power level for the mobile near the cell boundary. Similarly, the received power of mobile a can be denoted as

$$P_{r,a} = P_{b,a} \cdot G(r_{h,a}, \alpha_{h,a}) \cdot \varphi(G(r_{n,a}, \sigma_{n,a}), G(r_{h,a}, \sigma_{h,a})). \tag{6.46}$$

Similar as (6.45), the mean received power level in mobile station a is expressed as

$$\begin{aligned} E[P_{r,a}] &= P_{b,a} \cdot k_{h,a} \cdot (R \cdot f_s)^{-4} \cdot \frac{1}{\sqrt{2\pi}} e^{\frac{1}{2}\eta^2\sigma_s^2} \\ &\cdot \int_{-\infty}^{\infty} Q\left(\frac{\sigma_n}{\sigma_s} z - \eta\sigma_s - \frac{4}{\eta\sigma_s} \ln\left(\frac{2 - f_s}{f_S}\right)\right) e^{-\frac{1}{2}z^2} \, dz \end{aligned} \tag{6.47}$$

where $k_{h,a} = G_h G_a h_h^2 h_a^2$, σ_s is the standard deviation of the shadowing effect between the mobile and its home base station, and σ_n is the standard deviation of the shadowing effect between the mobile and its adjacent base station,

By comparing (6.45) and (6.47), we can determine the suitable value of f_S. Figure 6.3 shows the ratio between the mean received desired signal power level and the mean received cross-slot interference according to the position of the target user at different normalized radius of the inner region f_s. The impact of the mobile-to-mobile cross-slot interference will be reduced as the distance between the target user and the interfering mobiles increases. To promise the mobile-to-mobile cross-slot interference will not cause heavy performance degradation to the target user, we defined that the mobile-to-mobile cross-slot interference should be less than the received signal quality over a threshold τ. i.e.

$$\frac{E[I_{m\to m}]}{PG \cdot E[P_{r,a}]} \leq \tau. \tag{6.48}$$

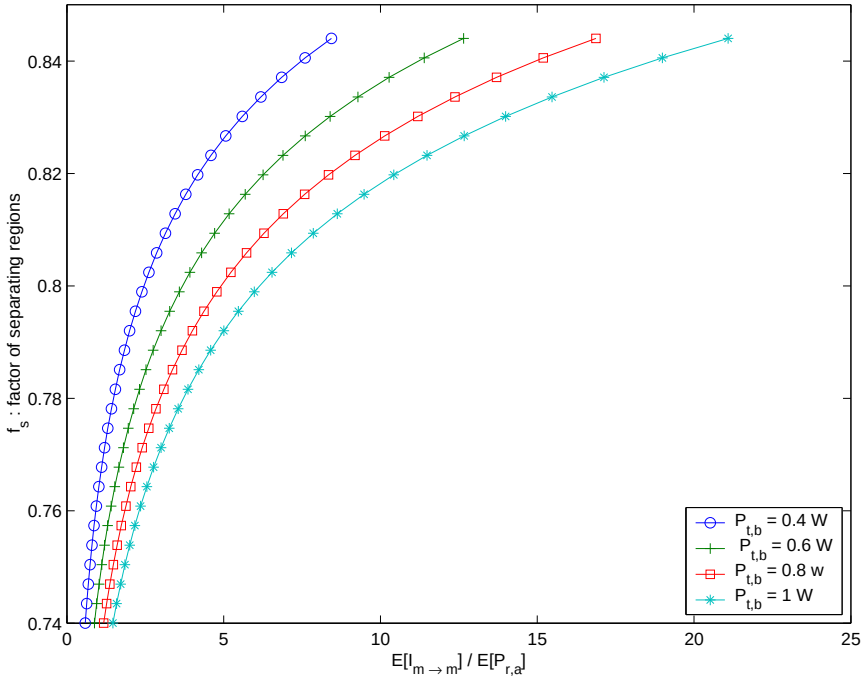

Figure 6.3: Effect of mobile-to-mobile cross-slot interference on the normalized radius of the inner region

6.5 Numerical Results

This section demonstrates the performance of the proposed cross-slot interference-based DCA algorithms. For comparison, we also investigate the performance of three other different schemes:

- Scheme I: the conventional DCA with the uplink and downlink beam-steering;
- Scheme II: the conventional DCA with the uplink MVDR beamformer and the downlink beam-steering;
- Scheme III: the cross-slot interference-based DCA with the uplink MVDR beamformer and downlink beam-steering;
- Scheme IV: the cross-slot interference-based DCA with the uplink MVDR beamformer and downlink beam-steering (the proposed scheme).

Note that in [27], Schemes I and II have been investigated for TDD-CDMA system, but without DCA and only considered the uplink performance. Our performance results include mobile-to-mobile cross-slot interference in the downlink and base-to-base cross-slot interference in the uplink. We will demonstrate that the cross-slot interference-based DCA combining with a suitable antenna array technique can effectively reduce both mobile-to-mobile and base-to-base cross-slot interferences in TDD-CDMA systems, thereby flexibly providing asymmetric services.

6.5.1 Cellular System Model

We consider a TDD-CDMA system with 19 cells, where all cells provide asymmetric traffic services based on their own traffic requirements. To investigate the system performance in various asymmetric traffic conditions, we defined the traffic load factor

and the degree of traffic asymmetry. The traffic load factor (T_F) is defined as

$$\text{Traffic Load } (T_F) = \frac{\text{the utilized codes}}{\text{the total number of available codes}}, \tag{6.49}$$

In our simulations, there are 32 codes available in each time slot [43]. To consider the impact of traffic asymmetry we assume every three adjacent cells have different asymmetric traffic conditions. For simplicity, it is assumed that the pattern of asymmetric traditions of the three adjacent cells is repeated in the entire cellular system, as shown in Fig.5. To define the degree of traffic asymmetry (DA), we first choose the cell with the most symmetric load between the downlink and the uplink as the referenced cell. Denote

$$IND = \min_i \{\|T_i^{(d)} - T_i^{(u)}\|,\ i \in \text{the all cells in the system}\}; \tag{6.50}$$

Then we set the degree of traffic asymmetry for the the referenced cell to be zero and define the number of downlink time slots of the referenced cell as $T_{IND}^{(d)}$. Then we set the degree of traffic asymmetry for any cell i as

$$\Lambda_i = T_i^{(d)} - T_{IND}^{(d)}. \tag{6.51}$$

In the following example, referring to Fig. 6.4, we assume that $\Lambda_A = 0$, $\Lambda_B = 3$, and $\Lambda_C = -3$. Other system parameters used are listed in Table I.

6.5.2 Effect of Traffic Asymmetry

Figure 6.5 shows the overall outage probability performance of the four schemes in the different traffic asymmetry conditions. The outage probability is defined as $Prob\{\gamma_i < \gamma_t\}$. Consider the traffic load factor $T_F = 0.8$ and the system parameters in Table I. As shown in the figure, the increased degree of traffic asymmetry degrades the overall outage performance. One can find that the proposed Scheme IV outperforms other schemes. Furthermore, the performances of Schemes II and IV are better than those

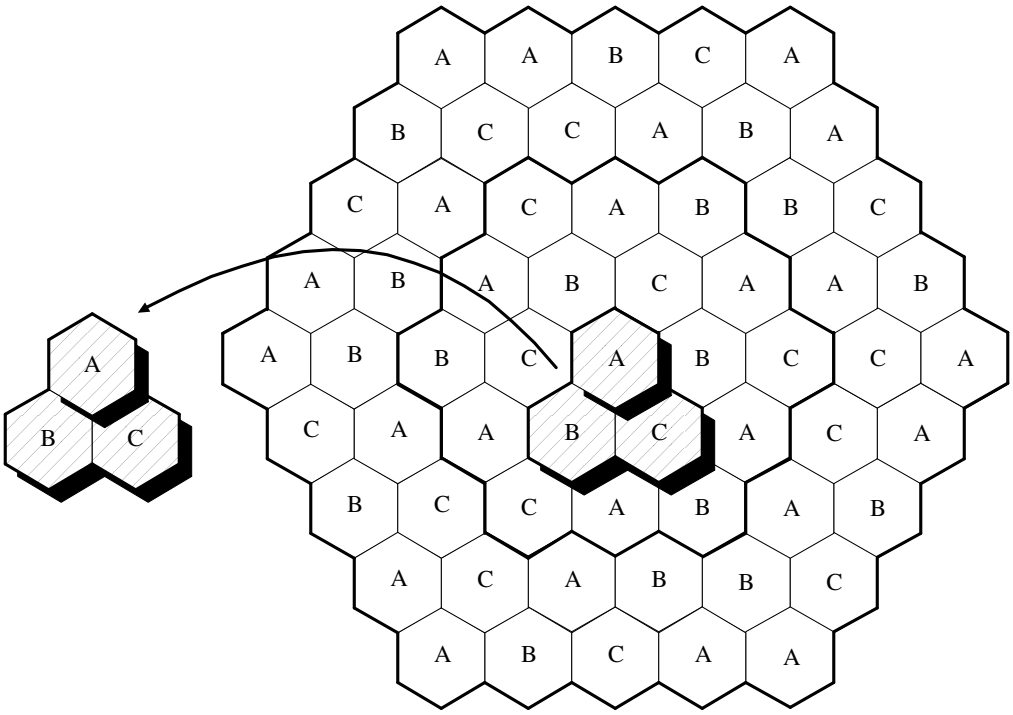

Figure 6.4: The cellular system with grouped cells, where cell A has a symmetric load, cell B has more downlink traffic than uplink traffic, and cell B has more uplink traffic than downlink traffic.

Table I : System Parameters

Cell radius	R=577 m
Base station antenna hight	h_b = 15 m
Mobile antenna height	h_m =2 m
Shadowing standard deviation between home base station and mobile	σ_s = 6 dB
Shadowing standard deviation between adjacent base station and mobile	σ_n = 8 dB
Shadowing standard deviation between base station and base station	σ_b = 3 dB
Shadowing standard deviation between mobile and mobile	σ_m = 10 dB
Processing Gain	$PG = 32$
Number of Antennas	$M = 5$
Normalized inner region radius	$f_s = 0.8$
SNR	20dB
Max. allocatable power per user	1 w
Target downlink SIR	$\gamma_t^{(d)}$ = -6 dB
Target uplink SIR	$\gamma_t^{(u)}$ = -9 dB

of Schemes I and III. This is because the impact of base-to-base cross-slot interference is much higher than that of mobile-to-mobile cross-slot interference. Using the MVDR beamformer, the base-to-base cross-slot interference can be effectively alleviated.

Figure 6.6 evaluates the outage probability for the downlink users in the outer region. The outage probability of these users will increase significantly when the degree of traffic asymmetry increases. With the help of the proposed DCA algorithm, the time slots that hace less cross-slot interference are reserved for these users. With $\Lambda = 5$, this figure demonstrates that Scheme IV can reduce at least 8 times of outage probability compared to Scheme II, while Scheme III improves the outage probability by 4 times compared to Scheme I.

Figure 6.7 illustrates the effect of traffic asymmetry on the outage performance for all the downlink users in the system. For Scheme I, the outage probability increase from 0.5 % to 4.5 % as degree of traffic asymmetry changes from 0 to 5. By using the cross-slot interference-based algorithm with uplink and downlink beam-steering (Scheme III), the outage probability van be improved to 2.5 % when the degree of traffic asymmetry is equal to 5. By adopting the uplink MVDR beamforming and downlink beam-steering in the cross-slot interference-based DCA (Scheme IV), the outage probability for the downlink users can be further reduced to 0.4 %.

Figure 6.8 illustrates the outage probability against the degree of asymmetry for the four different schemes. From the figure, one can see that the cross-slot interference-based DCA with the uplink and downlink beam-steering (Scheme III) can not significantly improve the uplink outage performance. This phenomenon is different from the downlink case. As seen previously in Fig. 6.7, Scheme III can significantly improve the downlink outage performance as compared to Schemes I and II. However, in the uplink case, Scheme III only performs slightly better than Scheme I and ever worse than Scheme II. This is because the base-to-base cross-slot interference can effectively reduced by the MVDR beamformer. As shown in the figure,

at the degree of asymmetry equal to 5, the uplink outage probability of Scheme II can be reduce to 3 % as compared with 15% of outage probability of Schemes I and III. By using MVDR beamformer and cross-slot interference based DCA, the uplink outage probability can be reduced to 0.5 % in the same traffic asymmetry condition.

From the above results, it has been shown that the proposed cross-slot interference-based DCA algorithm combining with MVDR beamformer can significantly reduce both the mobile-to-mobile and base-to-bas cross-slot interference. The MVDR beamformer can suppress the base-to-base cross-slot interference significantly. However, the mobile-to-mobile cross-slot interference will cause high outage probability for the mobiles near the cell boundary, thereby reducing the cell coverage area. The proposed cross-slot interference-based DCA algorithm can avoid the mobile-to-mobile cross-slot interference by reserving good channels for the potential users having mobile-to-mobile cross-slot interference.

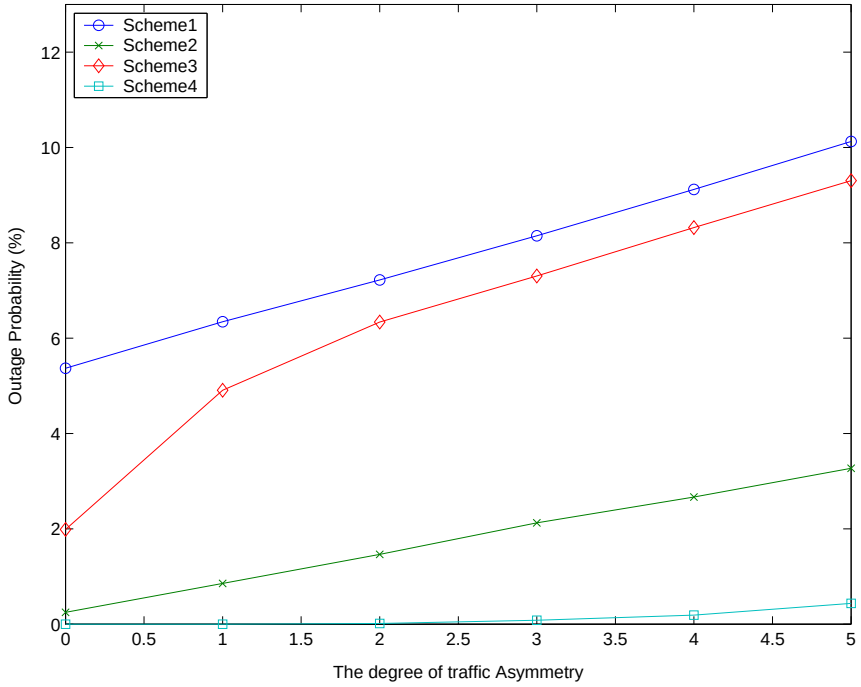

Figure 6.5: Effect of traffic asymmetry on the overall outage performance with both downlink and uplink users.

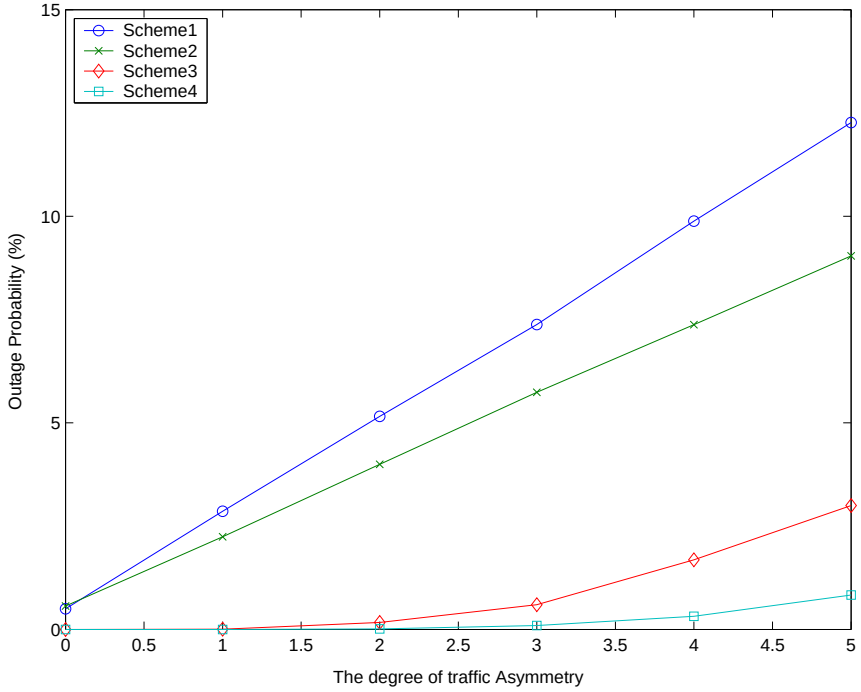

Figure 6.6: Effect of traffic asymmetry and mobile-to-mobile cross-slot interference on the outage performance for the downlink users in the outer region.

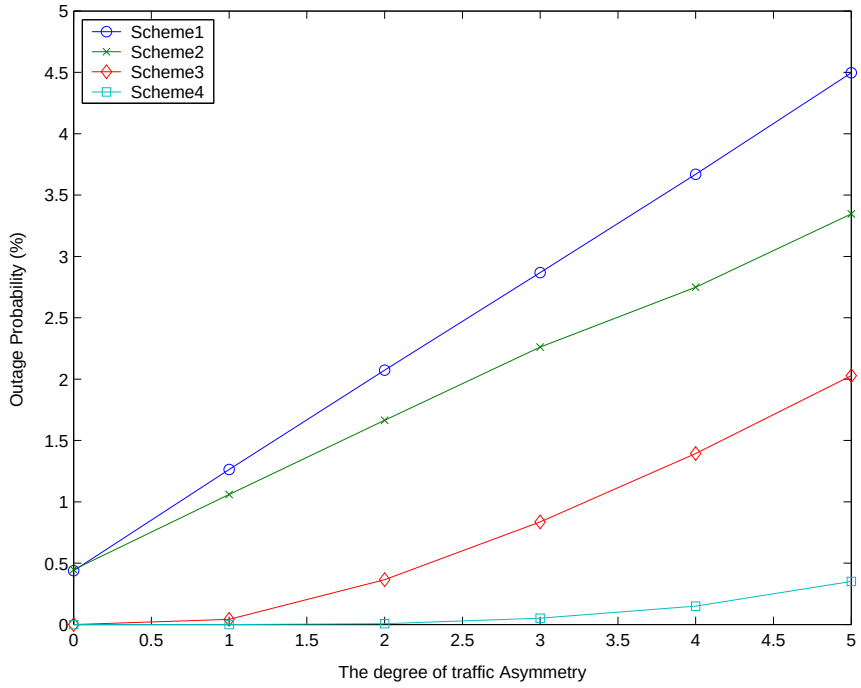

Figure 6.7: Effect of traffic asymmetry and the mobile-to-mobile cross-slot interference on the outage performance of all the downlink users in the system.

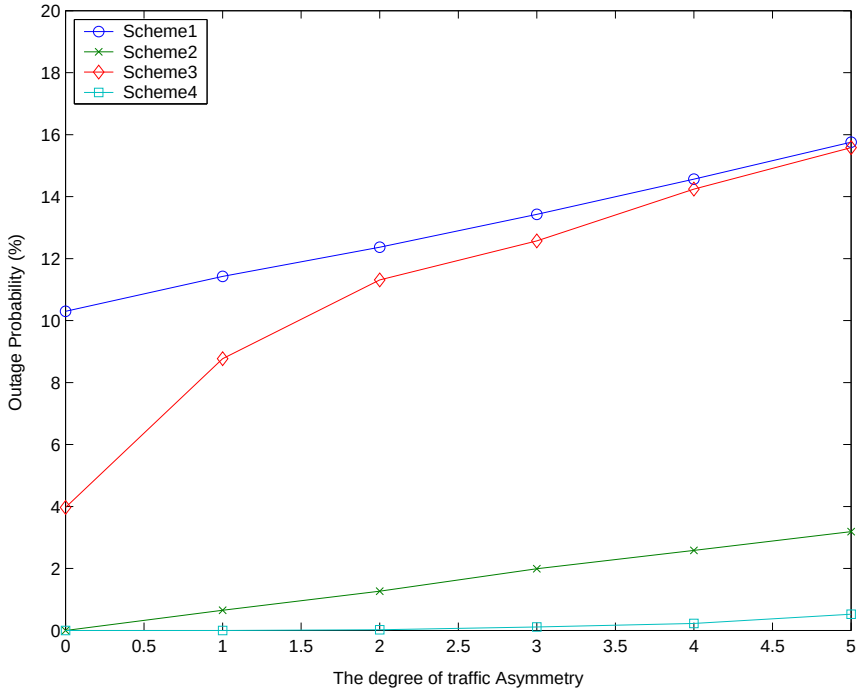

Figure 6.8: Effect of traffic asymmetry and base-to-base cross-slot interference on the outage performance for all the uplink users.

CHAPTER 7

A Hierarchical TDD Microcell/FDD Macrocell CDMA System Using Antenna Arrays and Power Ratio Adjustments

In this chapter, we present a new hierarchical cellular system with an underlaid TDD/CDMA microcell and overlaying FDD/CDMA macrocells. With an objective to exploit the underutilized FDD uplink capacity due to traffic asymmetry, the TDD/CDMA mircocell is operated within *the uplink frequency band* of the overlaying FDD/CDMA macrocells. By jointly applying the proposed antenna arrays at the cell site and a new power ratio adjustment technique, we evaluate the outage probabilities of the macrocell and the microcell. From the simulation results, we demonstrate that the full capacity of the TDD/CDMA mircocell can be obtained without degrading the performance of FDD/CDMA marcocells.

7.1 Introduction

In future wireless Internet services, the traffic volume in the downlink transmission is expected to be much higher than that in the uplink transmission. The frequency division duplex (FDD) systems have difficulty providing asymmetric traffic because uplink and downlink operate in one pair of equal-sized frequency bands. The time

division duplex (TDD) systems can resolve the asymmetric traffic issue by allocating different numbers of time slots to uplink and downlink in single unpaired frequency band [2, 17].

In this chapter, with an aim to exploit the underutilized FDD uplink capacity due to traffic asymmetry, we present a hierarchical cell system with an underlaid TDD/CDMA microcell and overlaying FDD/CDMA macrocells. In the proposed system, the TDD/CDMA mircocell is operated within the uplink frequency band of the overlaying FDD/CDMA macrocells. To make such a heterogeneous system become feasible, not only both the uplink and downlink performance of the microcell should be satisfied simultaneously, but also the uplink performance of the macrocell should be degraded as little as possible. In the literature, some papers have performed feasibility studies on the FDD/TDD heterogeneous system [54–56]. In general, these papers concluded that it is not easy to share the same spectrum between the FDD/CDMA system and the TDD/CDMA system without any limitation. However, to our best knowledge, few papers have proposed solutions to resolve the frequency sharing issue in the FDD/TDD heterogeneous system.

In [52], Naguib *et al* concluded that the capacity can be improved by employing antenna arrays (AA) in the homogenous FDD/CDMA system. However, under the FDD/TDD heterogeneous system, the interference analysis for the antenna array system becomes much more complicated. More importantly, we will see in this chapter that it does not suffice to support the co-existence of the FDD/TDD heterogeneous system by simply employing the AA at the cell site. Therefore, we propose a new power ratio adjustment (PRA) technique combining with the AA to alleviate the mutual interference between the TDD microcell and the FDD macrocell. With the synergy of the proposed joint AA and PRA, we will show that the TDD microcell capacity can be obtained without degrading the FDD macrocell performance.

In the next section, we describe the system model and analyze the performance

of the macrocell and the microcell with the AA. In Section 7.3, we derive the outage probabilities of the macrocell and the microcell. In Section 7.4, we present some simulation results. Finally, we conclude this work in Section 7.5.

7.2 The Hierarchical CDMA System Model

7.2.1 System Description

As shown in Fig. 7.1, our hierarchical CDMA system consists of $K+1$ overlaying FDD mode CDMA macrocells and one TDD mode CDMA microcell underlaid to the center macrocell with distance d. Let the cell M or the cell 0 denote the center macrocell and the cell μ denote the microcell. Then let R_M and R_μ be the radius of the macrocell and the microcell, respectively. Assume that in each macrocell and microcell, N_M and N_μ users are uniformly distributed, respectively. The mobile in the microcell is assumed to operate in TDD/CDMA mode and shares the uplink frequency of the overlaying FDD/CDMA mode macrocells. Therefore, there exists four types of interference between the heterogeneous system as shown in Fig. 7.2:

1. Interference from a macrocell mobile station (MS) to a microcell base station (BS);
2. Interference from a microcell MS to a macrocell BS;
3. Interference from a microcell BS to a macrocell BS;
   (Base station-to-Base station co-channel interference)
4. Interference from a macrocell MS to a microcell MS.
   (mobile-to-mobile co-channel interference)

The type 3 and type 4 interference result from the frequency sharing between the heterogeneous system. To alleviate the mutual interference between the microcell

and the macrocells, we propose to employ the AA at the cell site and the PRA technique.

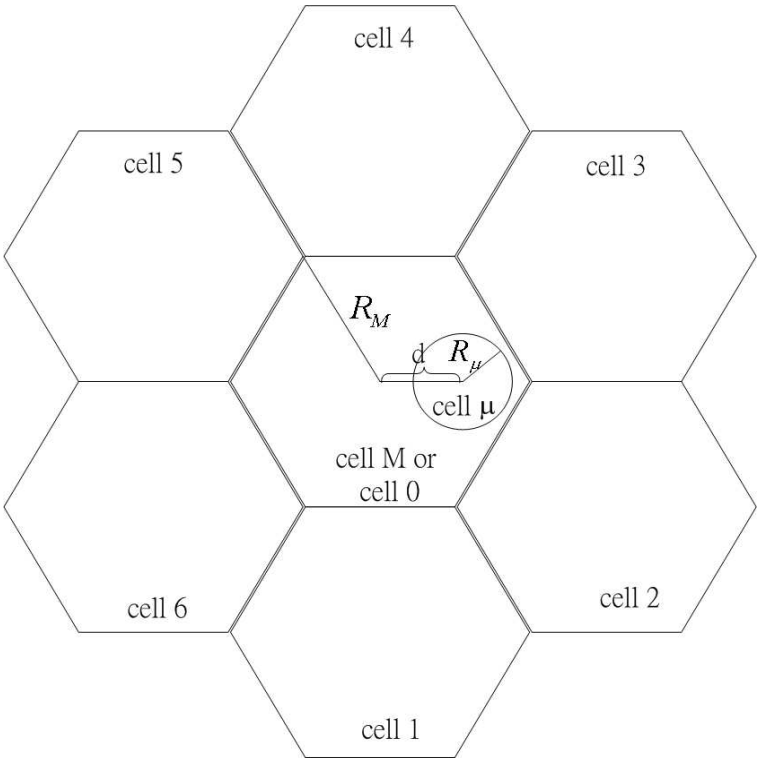

Figure 7.1: The hierarchical CDMA system model.

Figure 7.3 shows the frame structure of the TDD/CDMA system. There are S_U uplink time slots and S_D downlink time slots in a frame. We assume each mobile in the TDD/CDMA microcell uses one uplink time slot and S_D/S_U downlink time slots for traffic asymmetry. Let $N_s = \lceil N_\mu/S_U \rceil$ denote the number of used codes per time slot. And let the $\{S_U(i-1)+j\}$-th mobile $(i = 1, \cdots N_s, j = 1, \cdots S_U)$ be sequentially allocated to the j-th uplink time slot in one frame. Therefore, for the microcell base station, there are N_S code channels receiving over S_U slots and transmitting over S_D slots in each frame, respectively.

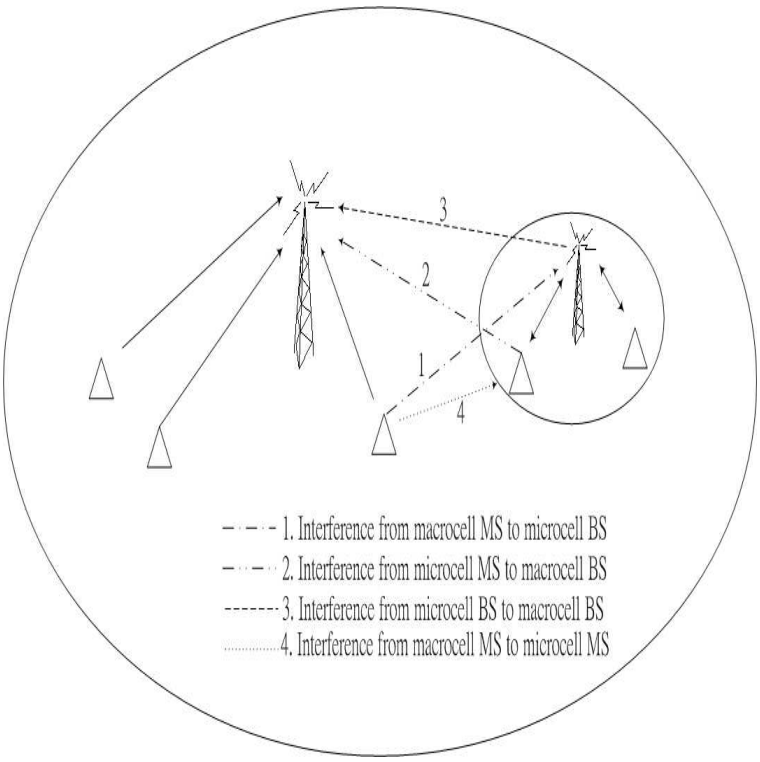

Figure 7.2: Mutual interference in the hierarchical CDMA system.

For clarity, we will use the notations in the following manners. When M and μ are used as either superscripts or subscripts, they denote the center macrocell and the microcell respectively. U and D represent the uplink and downlink respectively. And r and t are used as superscripts to denote the receiving and transmitting respectively from the base station. For example, $P_{o,M}^{U}$ denotes the uplink outage probability of the macrocell, and $P_{o,\mu}^{D}$ for the downlink outage probability of the microcell.

7.2.2 Power Ratio Adjustments

We assume ideal power control in the uplink. Let P_M^r and P_μ^r denote the received power level controlled by the base station of the macrocell and microcell, respectively.

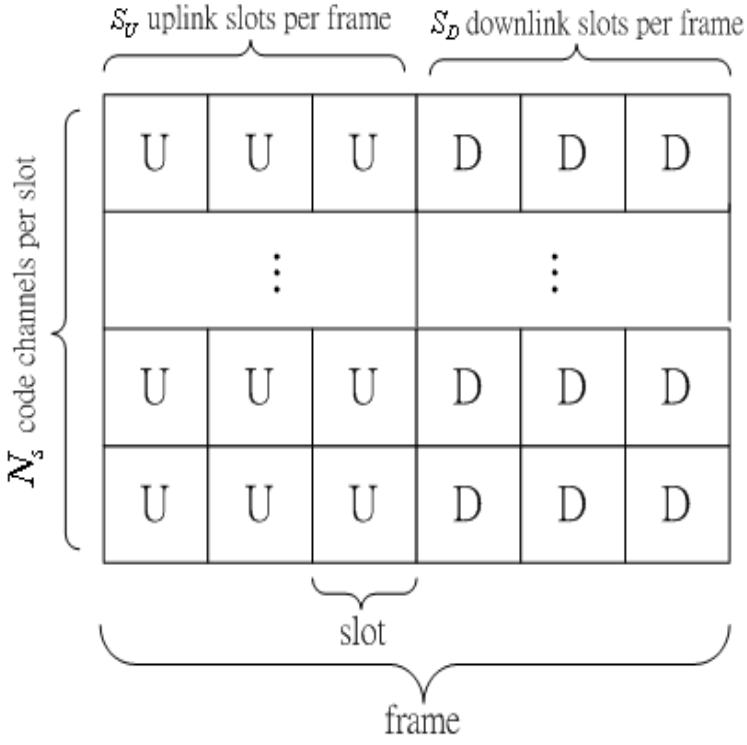

Figure 7.3: Frame structure of the TDD/CDMA system.

Here, we define the first power ratio adjustment K_1 as

$$K_1 = \frac{P_\mu^r}{P_M^r} \ . \tag{7.1}$$

It will be seen in Section 7.3 that the adjustment of the K_1 can be used to balance the influence of type 1 and type 2 interference.

The link gain $G(r, \alpha)$ between the transmitter and the receiver with distance r is modelled by propagation loss and lognormal shadowing

$$G(r, \alpha) = \min(\kappa_0 r^{-m} \cdot 10^{\alpha/10}, (MCL)) \ . \tag{7.2}$$

where κ_0 is a constant, m is the path loss exponent and α is a normal random variable with zero mean and standard deviation σ dB. Otherwise, we introduce minimum

coupling loss (MCL) as the minimum distance loss including antenna gain measured between antenna connectors [46]. The value of σ and MCL are different with the distinct environment conditions. We assume that MCL between base station and mobile is equivalent to $10^{-5.3}$ and MCL between base station and mobile is equal to 10^{-4} [47].

Let P_{μ}^{t} denote the transmitted power from the base station for each mobile in the microcell. After propagating over a distance of the cell radius, the received signal power at the boundary of the microcell equals $P_{\mu}^{t} \cdot (\kappa_0 {R_{\mu}}^{-m})$ without considering the lognormal shadowing. Therefore, we define the second power ratio adjustment K_2 as

$$K_2 = \frac{P_{\mu}^{t}}{P_{M}^{r}} \cdot (\kappa_0 {R_{\mu}}^{-m}) \ . \tag{7.3}$$

In the following section, we will show that the adjustment of K_2, when combined with the AA, is effective to cope with the type 4 interference without aggravating type 3 interference.

7.2.3 Antenna Array and Beamforming

In this chapter, we propose that the L-element uniform circular array (UCA) is adopted at both macrocell and microcell sites to enhance signal-to-interference ratio by using uplink and downlink beamforming. Assume the narrowband siganl model and perfect power control in the uplink. If $\mathbf{a}_{ij}$ is the $L \times 1$ receiving array response vector for the signal arriving from the mobile j, the received interference power from the mobile j for the desired mobile i at the cell site (e.g. the macrocell M) is given by

$$I_{ij} = P_{M}^{r} \|\mathbf{w}_{i}^{H} \mathbf{a}_{ij}\|^2 \ . \tag{7.4}$$

where H is the Hermitian transpose operation, $\| \cdot \|$ is the norm operation and $\mathbf{w}_i$ is a $L \times 1$ weight vector to combine the output of L-element antenna array. Similarly,

if $\tilde{\mathbf{w}}_i$ is a $L \times 1$ transmitting weight vector for the desired mobile i, $\mathbf{b}_{ij}$ is the $L \times 1$ transmitting array response vector of the mobile j seen by the base station (e.g. the microcell μ), the received interference due to leakage from the transmitted power of the base station to the mobile j is given by

$$I_{ij} = P_{\mu}^{t} \| \tilde{\mathbf{w}}_i^H \mathbf{b}_{ij} \|^2 \ . \tag{7.5}$$

There are several ways to derive the weight vector under different criterions. We adopt the maximum ratio combining (MRC) in this chapter. As a result, the receiving weight vector is equal to its receiving array response vector [35]. Moreover, thanks to the channel reciprocity in TDD system, the weight vector obtained in the uplink can be applied to the downlink beamforming provided that the channel remains stationary between uplink and downlink during a time frame [57].

7.2.4 Bit Energy-to-Noise Density Ratio of FDD Cells

Now, we can obtain the uplink bit energy-to-noise density ratio of the mobile i in the center macrocell. By neglecting the thermal noise, from [52] $(E_b/N)_{M,i}^{U}$ is given by

$$\left(\frac{E_b}{N} \right)_{M,i}^{U} = \frac{P_M^r}{I_1 + I_2 + I_3} \cdot PG_M \ . \tag{7.6}$$

where

$$I_1 = \sum_{j \neq i}^{N_M} P_M^r \psi_j \| \mathbf{w}_i^H \mathbf{a}_{ij}^{(M)} \|^2 \ , \tag{7.7}$$

$$I_2 = \sum_{k=1}^{K} \sum_{j=1}^{N_M} P_M^r \psi_{k_j} \frac{G(r_{k_j}^{(M)}, \alpha_{k_j}^{(M)})}{G(r_{k_j}^{(k)}, \alpha_{k_j}^{(k)})} \| \mathbf{w}_i^H \mathbf{a}_{ik_j}^{(k)} \|^2 \ , \tag{7.8}$$

and

$$I_3 = \sum_{j=1}^{N_s} P_{\mu}^r \frac{G(r_j^{(M)}, \alpha_j^{(M)})}{G(r_j^{(\mu)}, \alpha_j^{(\mu)})} \| \mathbf{w}_i^H \mathbf{a}_{ij}^{(\mu)} \|^2 \ . \tag{7.9}$$

From (7.7) to (7.9), PG_M is the processing gain for the macrocell, ψ_j is a Bernoulli variable with probability v to model the voice activity, $r_j^{(k)}$ is the distance between the mobile j and the base station k, $\alpha_j^{(k)}$ is the path shadowing between the mobile j and the base station k, $\mathbf{a}_{ij}^{(k)}$ is the receiving array response vector for signal arriving from the mobile j in the cell k. Thus, I_1 denotes the intracell interference from the mobiles in the center macrocell, I_2 denotes the intercell interference from the mobiles in adjacent macrocells, and I_3 denotes the type 2 intersystem interference. When the base station in the microcell is transmitting instead of receiving, the intersystem interference turns out to be the type 3 interference I_3', which is given by

$$I_3' = \sum_{j=1}^{N_s} P_\mu^t G(d,\alpha) \|\tilde{\mathbf{w}}_j^H \mathbf{b}\|^2 \|\mathbf{w}_i^H \mathbf{a}\|^2 \ . \tag{7.10}$$

where $\mathbf{a}$ is the receiving array response vector for signal arriving from the microcell base station, $\mathbf{b}$ is the transmitting array response vector for signal transmitting from the microcell base station to the macrocell base station, and $\tilde{\mathbf{w}}_j$ is the transmitting weight vector for any mobile j in the microcell.

7.2.5 Bit Energy-to-Noise Density Ratio of TDD Cells

In the following, we derive the uplink and downlink bit energy-to-noise density ratio of the TDD microcell. For the desired mobile i in the microcell, the uplink bit energy-to-noise density ratio of the microcell can be obtained as

$$\left(\frac{E_b}{N}\right)_{\mu,i}^{U} = \frac{P_\mu^r}{I_1 + I_2} \cdot PG_\mu \ . \tag{7.11}$$

where

$$I_1 = \sum_{j \neq i}^{N_s} P_\mu^r \|\mathbf{w}_i^H \mathbf{a}_{ij}^{(\mu)}\|^2 \ . \tag{7.12}$$

is the intracell interference from the mobiles in the microcell and

$$I_2 = \sum_{k=0}^{K} \sum_{j=1}^{N_M} P_M^r \psi_{k_j} \frac{G(r_{k_j}^{(\mu)}, \alpha_{k_j}^{(\mu)})}{G(r_{k_j}^{(k)}, \alpha_{k_j}^{(k)})} \|\mathbf{w}_i^H \mathbf{a}_{ij}^{(k)}\|^2 \ . \tag{7.13}$$

is the type 1 interference from the mobiles in the macrocells.

On the other hand, when the mobile i in the mircocell is receiving, the interference then comes from I_1 and I_2. I_1 in this case denotes the interference from the microcell base station and I_2 denotes the type 4 intersystem interference. Thus, the downlink bit energy-to-noise density ratio of the microcell can be obtained as

$$\left(\frac{E_b}{N}\right)_{\mu,i}^{D} = \frac{P_\mu^t G(r_i^{(\mu)}, \alpha_i^{(\mu)})}{I_1 + I_2} \cdot PG_\mu \ . \tag{7.14}$$

where

$$I_1 = \sum_{j \neq i}^{N_s} P_\mu^t G(r_i^{(\mu)}, \alpha_i^{(\mu)}) \|\tilde{\mathbf{w}}_i^H \mathbf{b}_{ij}^{(\mu)}\|^2 \ , \tag{7.15}$$

and

$$I_2 = \sum_{k=0}^{K} \sum_{j=1}^{N_M} P_M^r \psi_{k_j} \frac{G(r_{k_j}^{i}, \alpha_{k_j}^{i})}{G(r_{k_j}^{(k)}, \alpha_{k_j}^{(k)})} \ . \tag{7.16}$$

In (7.14)-(7.16), r_j^i and α_j^i are the distance and the path shadowing between the desired mobile i in the microcell and other mobile j in the macrocell, respectively.

7.3 Outage Probability

The outage probability P_o is defined as the probability of the bit energy-to-noise density ratio below a certain threshold γ

$$P_o = Pr\left(\frac{E_b}{N} < \gamma\right) \ . \tag{7.17}$$

Then, substituting (7.6)-(7.10) to (7.17), we have the uplink outage probability of the macrocell

$$\begin{aligned} P_{o,M}^{U} &= Pr\left(J_1 + J_2 + J_3 > \frac{PG_M}{\gamma_M^U}\right) \cdot \frac{S_U}{S_U + S_D} \\ &+ Pr\left(J_1 + J_2 + J_3' > \frac{PG_M}{\gamma_M^U}\right) \cdot \frac{S_D}{S_U + S_D} \ . \end{aligned} \tag{7.18}$$

where

$$J_1 = \sum_{j \neq i}^{N_M} \psi_j \|\mathbf{w}_i^H \mathbf{a}_{ij}^{(M)}\|^2 \ , \tag{7.19}$$

$$J_2 = \sum_{k=1}^{K} \sum_{j=1}^{N_M} \psi_{k_j} \frac{G(r_{k_j}^{(M)}, \alpha_{k_j}^{(M)})}{G(r_{k_j}^{(k)}, \alpha_{k_j}^{(k)})} \|\mathbf{w}_i^H \mathbf{a}_{ik_j}^{(k)}\|^2 \ , \tag{7.20}$$

$$J_3 = K_1 \sum_{j=1}^{N_s} \frac{G(r_j^{(M)}, \alpha_j^{(M)})}{G(r_j^{(\mu)}, \alpha_j^{(\mu)})} \|\mathbf{w}_i^H \mathbf{a}_{ij}^{(\mu)}\|^2 \ , \tag{7.21}$$

and

$$J_3' = K_2 {R_\mu}^m \cdot G(d, \alpha) \|\mathbf{w}_i^H \mathbf{a}\|^2 \sum_{j=1}^{N_s} \|\tilde{\mathbf{w}}_j^H \mathbf{b}\|^2 \ . \tag{7.22}$$

Similarly, substituting (7.11)-(7.13) to (7.17), we have the uplink outage probability of the microcell

$$P_{o,\mu}^{U} = Pr\left(\left(\frac{E_b}{N}\right)_\mu^U < \gamma_\mu^U\right) = Pr\left(J_1 + J_2 > \frac{PG_\mu}{\gamma_\mu^U}\right) \ . \tag{7.23}$$

where

$$J_1 = \sum_{j \neq i}^{N_s} \|\mathbf{w}_i^H \mathbf{a}_{ij}^{(\mu)}\|^2 \ , \tag{7.24}$$

and

$$J_2 = \frac{1}{K_1} \sum_{k=0}^{K} \sum_{j=1}^{N_M} \psi_{k_j} \frac{G(r_{k_j}^{(\mu)}, \alpha_{k_j}^{(\mu)})}{G(r_{k_j}^{(k)}, \alpha_{k_j}^{(k)})} \|\mathbf{w}_i^H \mathbf{a}_{ij}^{(k)}\|^2 \ . \tag{7.25}$$

Finally the downlink outage probability of the micrcell is given by substituting (7.14)-(7.16) to (7.17)

$$P_{o,\mu}^{D} = Pr\left(\left(\frac{E_b}{N}\right)_{\mu}^{D} < \gamma_{\mu}^{D}\right) = Pr\left(J_1 + J_2 > \frac{PG_{\mu}}{\gamma_{\mu}^{D}}\right) \quad . \tag{7.26}$$

where

$$J_1 = \sum_{j\neq i}^{N_s} \|\tilde{\mathbf{w}}_i^H \mathbf{b}_{ij}^{(\mu)}\|^2 \quad , \tag{7.27}$$

and

$$J_2 = \frac{1}{K_2} R_{\mu}^{-m} G(r_i^{(\mu)}, \alpha_i^{(\mu)}) \sum_{k=0}^{K} \sum_{j=1}^{N_M} \psi_{k_j} \frac{G(r_{k_j}^{i}, \alpha_{k_j}^{i})}{G(r_{k_j}^{(k)}, \alpha_{k_j}^{(k)})}. \tag{7.28}$$

As mentioned in Section 7.1, the outage probabilities in (7.18), (7.23) and (7.26) should be simultaneously examined to guarantee the feasibility of such a hierarchical system. On one hand, the effect of forming a receiving beam towards the desired mobile is to reduce the effective numbers of the interfering mobiles that fall within the beam [52]. At the same time, forming a transmitting beam can concentrate the power towards the desired mobile by reducing the leaking interference. Therefore, by virtue of uplink and downlink beamforming, the interference in (7.19)-(7.22), (7.24)-(7.25) and (7.27) will be reduced.

On the other hand, increasing the PRA constant K_1 and K_2 (defined in (7.1) and (7.3)) can reduce the type 1 interference in (7.25) and type 4 interference in (7.28) whcih degrade the performance of the heterogeneous system. These two types of interference become serious when a mobile belonging to the macrocell moves close the boundary of the microcell. However, large K_1 and K_2 increase the type 2 interference in (7.21) and type 3 interference in (7.22), respectively. As a result, the uplink performance of the macrocell will be seriously degraded. By jointly applying our proposed AA and PRA technique, thanks to the interference suppression by the AA, the majority of mobiles in the macrocell will receive the negligible type 2 and type 3 interference even with large K_1 and K_2. Because the radius of the microcell is much

smaller than that of the macrocell, we are allowed to choose a larger value of K_1 and K_2.

7.4 Environment Analysis And Numerical Results

We evaluate the impact of mobile-to-mobile co-channel interference (type 4 interference) and describe why the proposed the power ratio adjustments can alleviate the type 1 and type 4 interference. Finally, the outage probability is performed to demonstrate the system performance improvement with the assistance of AA and PRA.

7.4.1 Worst Case Analysis with the impact of the mobile-to-mobile interference

In this subsection, we will evaluate the impact of the mobile-to-mobile co-channel interference and describe how the proposed power ratio adjustments can alleviate type 1 and type 4 interference between the heterogeneous systems. In some issues of the radio resource management in the TDD/CDMA systems, the mobile-to-mobile co-channel interference is considered to significantly degrade the system performance [13, 58]. To alleviate this kind of interference, we suggest employing a power ratio adjustment method in subsection 7.2.2. Here we will describe how to adjust the power level to alleviate the impact of type 4 interference.

At first, we analyze the impact of type 4 interference in a worst case to define the required received signal quality for the mobiles. The worst case about the most serious interference is illustrated in (7.4). This condition will happen when the interfering source is approaching the cell boundary with the maximum transmit power. The interfering mobile a is at the right side cell boundary of the microcell μ

and served by the macrocell. With the usage of the MCL, the received co-channel interference from the interfering mobile to the different positions can denoted as

$$\begin{aligned} I_{m\to m} &= \frac{P_M^r}{G\left(r_a^{(M)}, \alpha_a^{(M)}\right)} \cdot G\left(r_a^b, \alpha_a^b\right) \cdot \varphi\left(G\left(r_a^b, \alpha_a^b\right), (MCL_{m\to m})\right) \\ &+ \frac{P_M^r}{G\left(r_a^{(M)}, \alpha_a^{(M)}\right)} \cdot (MCL_{m\to m}) \cdot \varphi\left((MCL_{m\to m}), G\left(r_a^b, \alpha_a^b\right)\right) \end{aligned}$$

where $MCL_{m\to m}$ is the minimum coupling loss between two mobiles, $\alpha_a^{(M)}$ and α_a^b are the shadowing components between the interfering mobile a to the base-station of the macrocell M and target mobile b with standard deviation $\sigma_a^{(M)}$ and σ_a^b, respectively. The function $\varphi(u, v)$ is used to indicate whether $u \leq v$ or not, i.e.,

$$\varphi(u, v) = \begin{cases} 1, & \text{if } u \leq v \ . \\ 0, & \text{otherwise} \ . \end{cases} \tag{7.29}$$

Then we can obtain the mean received mobile-to-mobile interference by taking average over $\alpha_a^{(M)}$ and α_a^b, i.e.

$$\begin{aligned} E[I_{m\to m}] &= P_M^r \cdot (\frac{r_a^{(M)}}{r_a^b})^4 \cdot e^{\frac{1}{2}\eta^2(\sigma_a^{(M)})^2} \cdot \mathrm{Q}\left(\frac{\eta^2\sigma_b^{a2} - k}{\eta\sigma_b^a}\right) \\ &+ P_M^r \cdot (r_a^{(M)})^4 \cdot (MCL_{m\to m}) \cdot e^{\frac{1}{2}\eta^2(\sigma_a^{(M)})^2} \cdot \mathrm{Q}(\frac{k}{\sqrt{2}\eta\sigma_b^a}). \end{aligned} \tag{7.30}$$

where $\eta = \frac{\ln 10}{10}$, and $k = \ln\left[MCL_{m\to m} \cdot (r_a^b)^4\right]$.

Figure 5 illustrates the mean received mobile-to-mobile interference corresponding to the different locations in the microcell. The system parameters are outlined in Table 7.1, and we set $R_\mu/R_M = 0.1$, $d = 700$ m, and $\alpha_a^{(M)} = \alpha_a^b = 5$ dB. From the fig. 5, the mean received mobile-to-mobile co-channel interference from the interfering mobile only dominates around the cell boundary. The central position of the microcell (base station) only receive much less interference. In the

other words, the impact of the type 1 interference can be easily reduced by slightly increasing $K1$ of the PRA. While the mean received interference will be much serious around a circular-region of the interfering mobile, the mobiles in this region may be blocked easily. In this way, we should define a larger $K2$ to compensate the type 4 (mobile-to-mobile) interference.

To design a proper parameter $K2$ in (7.2), we evaluate the mean received power level for a mobile b in the microcell as follows

$$\begin{aligned} P_r^b &= P_\mu^t \cdot G(r_b^{(\mu)}, \alpha_b^{(\mu)}) \cdot \varphi(G(r_b^{(\mu)}, \alpha_b^{(\mu)}), (MCL_{b\to m})) \\ &+ P_\mu^t \cdot (MCL_{b\to m}) \cdot \varphi((MCL_{b\to m}), G(r_b^{(\mu)}, \alpha_b^{(\mu)})). \end{aligned} \tag{7.31}$$

where $MCL_{b\to m}$ is minimum coupling loss between the base station and mobile, $\alpha_b^{(\mu)}$ is the shadowing component with the standard deviation $\sigma_b^{(\mu)}$. Then we can obtain the mean received power level for the target mobile b as By taking average over $\alpha_b^{(\mu)}$, we can obtain

$$\begin{aligned} E[P_r^b] &= P_\mu^t \cdot r_b^{(M)-4} \cdot e^{\frac{1}{2}\eta^2{\sigma_b^{(\mu)}}^2} \cdot \mathrm{Q}(\frac{\eta^2{\sigma_b^{(\mu)}}^2 - k'}{\eta\sigma_b^{(\mu)}}) \\ &+ P_\mu^t \cdot (MCL_{b\to m}) \cdot \mathrm{Q}(\frac{k'}{\eta\sigma_b^{(\mu)}}). \end{aligned} \tag{7.32}$$

where $P_\mu^t \propto K2$ in (7.2), and $k' = \ln\left[MCL_{b\to m} \cdot (r_b^{(\mu)})^4\right]$.

Figure 6 illustrates the ratio between the mean received mobile-to-mobile interference to the mean received signal quality corresponding to the different distance between the interfering mobile and the target mobile. We move the location of the target mobile along a direct line between the interfering mobile of the worst case to the base station of the microcell. With the increase of the $K2$ and the distance between two mobiles, the received mobile-to-mobile interference decreases rapidly. The impact of mobile-to-mobile interference can be limited into a circular-region about 35

m around the interfering mobile when $K2$ is larger than 1500. While the mobiles are uniformly distributed, the probability for an approaching interfering mobile to cause heavy mobile-to-mobile interference will to much smaller.

7.4.2 Numerical Results

The outage probabilities in (7.18), (7.23) and (7.26) are evaluated by Monte Carlo simulation. In Fig. 7.7, we set $L = 7$, $N_M = 36$ (which is approximate 80% capacity of the homogenous macrocell without the embedded microcell), $R_\mu/R_M = 0.1$, $d = 700$ m, $K_1 = 180$ and $K_2 = 1800$. One can see that, by jointly applying the AA and PRA, the uplink and downlink outage probabilities of the microcell are controlled to be below around 0.02 and 0.015, respectively. And the uplink outage probability of the macrocell increases slightly as N_μ increases. It is obvious that, the co-existence of such a heterogeneous system is feasible by using the proposed joint AA and PRA technique. Although not shown in the simulation, similar results can be obtained with different L, R_μ or d.

Figure 7.8 and Figure 7.9 show the the tradeoff between the outage probabilities of the macrocell and the microcell by adjusting the PRA constant K_1 and K_2. In Fig. 7.8, it is shown that when the K_1 increases, the uplink outage probability of the microcell decreases and the uplink outage probability of the macrocell increases slightly. Fig. 7.9 shows that the the uplink outage probability of the macrocell is traded off against the downlink outage probability of the microcell with the increasing K_2.

Finally in Fig. 7.10, the worst one among the uplink outage probability of the macrocell, uplink outage probability of the microcell and downlink outage probability of the microcell is plotted with or without applying the AA and PRA. It is important to see that, only by jointly employing AA and PRA, we can obtain the full microcell

capacity without degrading the performance of the macrocells.

Table 7.1: System Parameters

PG_M, PG_μ	128
$\gamma_M^U, \gamma_\mu^U, \gamma_\mu^D$	5 dB
S_U, S_D	3
R_M	1000 m
K	6
σ	8 dB
v	3/8
m	4

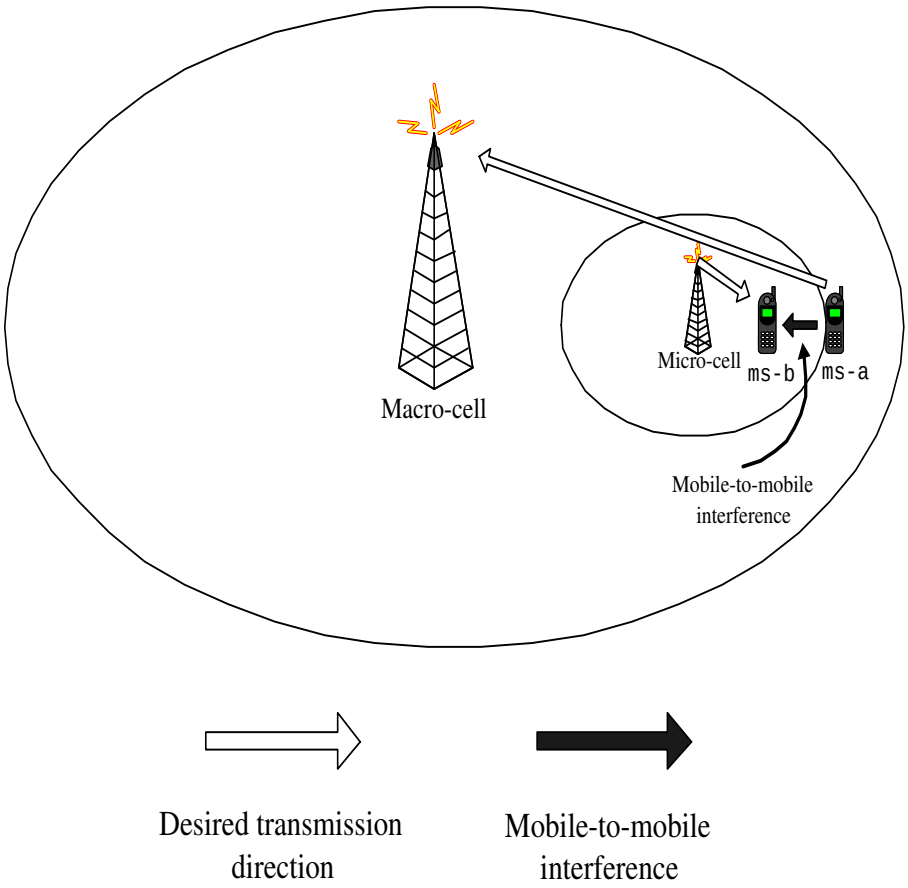

Figure 7.4: The worst case corresponding to the impact of mobile-to-mobile co-channel interference.

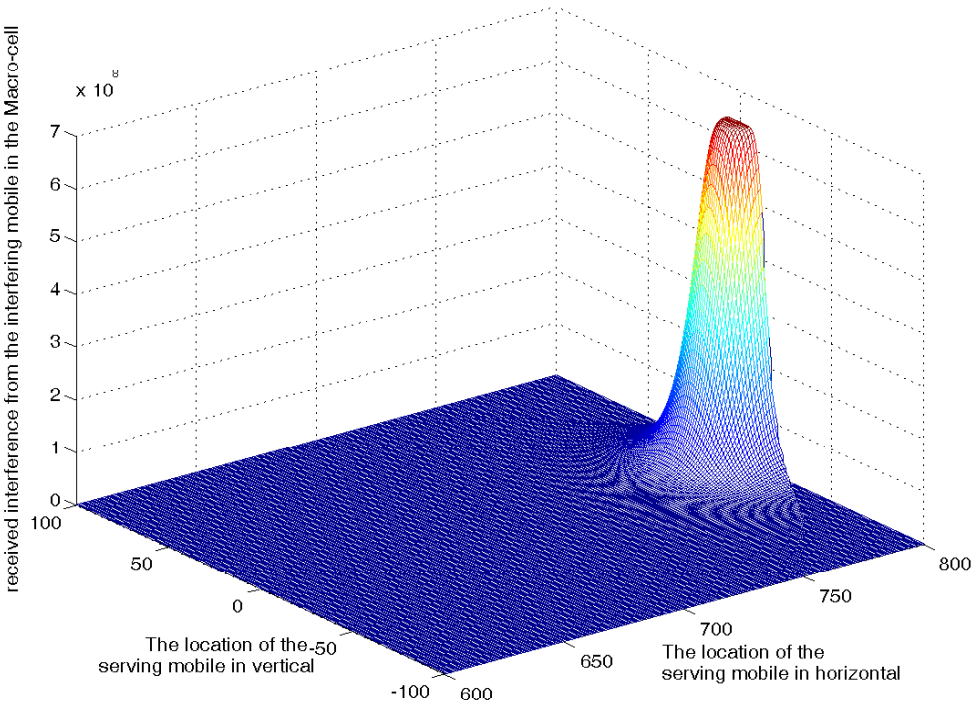

Figure 7.5: The mean received interference from the interfering mobile of the macro-cell to the different positions of microcell.

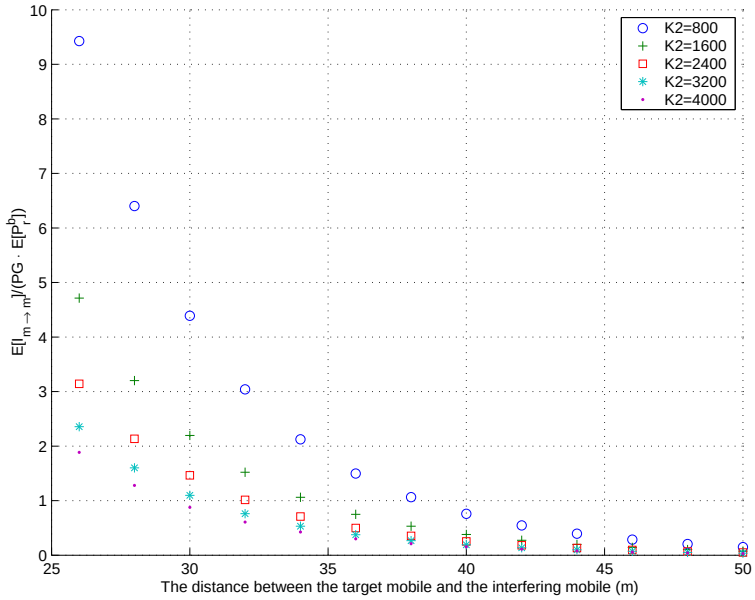

Figure 7.6: The ratio between the mean received mobile-to-mobile interference to the mean received desired power level correaponds to the distance between two mobiles.

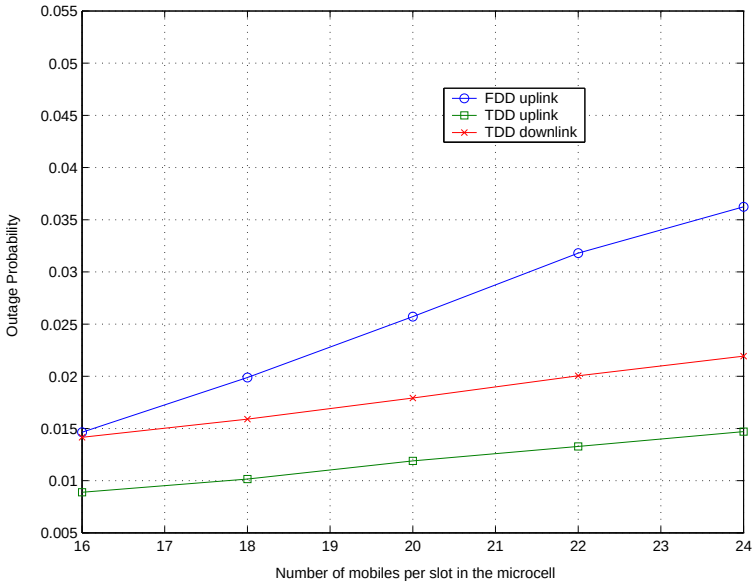

Figure 7.7: Outage probabilities as a function of N_μ for $L = 7$.

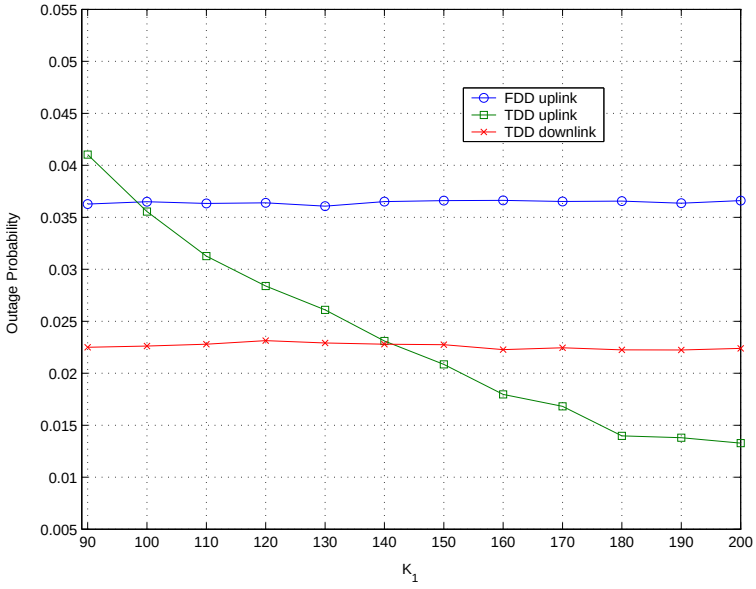

Figure 7.8: Outage probabilities as a function of K_1.

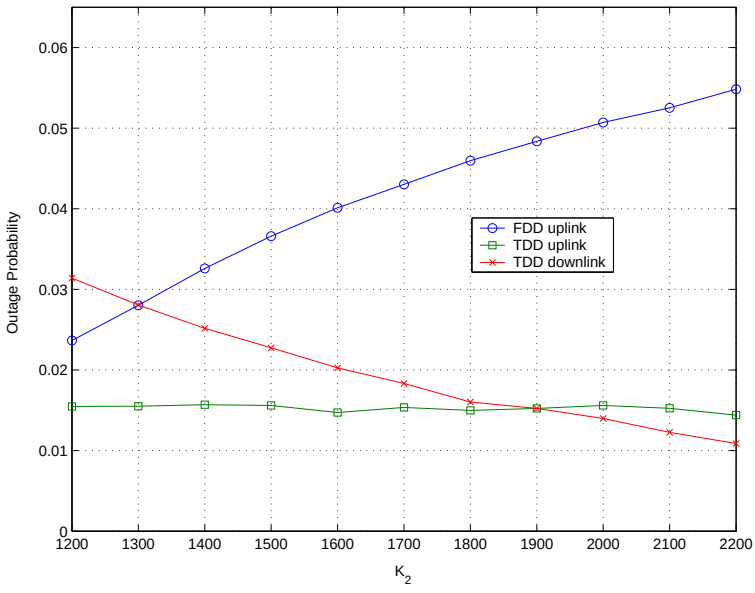

Figure 7.9: Outage probabilities as a function of K_2.

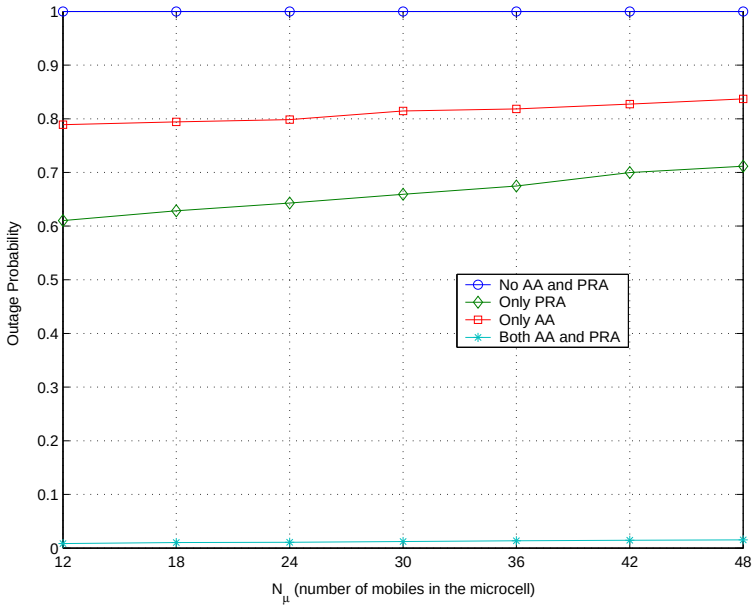

Figure 7.10: Comparison of the outage probabilities for (a) no AA and PRA; (b) only PRA; (c) only AA; and (d) joint AA and PRA are used.

CHAPTER 8

Concluding Remarks

The objective of this project is to efficiently utilize the two dimensions of radio resource - time and space - to support the traffic asymmetry and enhance the system performance in the TDD-CDMA systems.This thesis includes the following research topics:

1. Exact analysis of interference in TDD-CDMA systems with directional antennas;
2. A distributed code/time slot allocation scheme for TDD-CDMA systems to take advantage of the directional antennas;
3. From a system perspective of TDD/CDMA cellular network, to investigate how to effectively apply antenna beamforming techniques to suppress cross-slot interference;
4. To investigate how to simultaneously using transmitting and receiving beamformers in the TDD/CDMA systems from a system perspective;
5. A virtual-cell based link-proportional dynamic channel assignment (LP-DCA) mechanism in the TDD/CDMA systems with asymmetric traffic;
6. Taking the characteristics of users' locations and sectorized antennas to reduce the overall received interference;

7. Investigated different DCA algorithms and antenna beamforming techniques to overcome the cross-slot interference in the TDD/CDMA systems;

8. Propose the synergy of combining the cross-slot interference-based DCA and the MVDR beamformer to support asymmetric services with various degrees of traffic asymmetry in different cells;

9. Present a new hierarchical cell system with an underlaid TDD/CDMA microcell and overlaying FDD/CDMA macrocells;

10. By jointly applying the proposed antenna arrays at the cell site and a new power ratio adjustment technique, we demonstrate that the full capacity of the TDD/CDMA mircocell can be obtained without degrading the performance of FDD/CDMA marcocells.

8.1 Interference Analysis and Resource Allocation for TDD-CDMA Systems to Support Asymmetric Services by Using Directional Antennas

In Chapter 3 and [17, 45, 59], we have developed an analytic framework to evaluate the interference of the TDD-CDMA system with directional antennas and asymmetric services. Our results show that the strong cross-slot interference in the TDD-CDMA system will be restricted into a small area, namely a virtual cell, if a trisector directional antennas are employed at base stations. It is found that the directivity of sector antennas can provide additional degree of freedom for allocating radio resources, which inspires us to design a virtual cell-based code/time slot assignment

scheme to allocate radio resource in the TDD-CDMA system. Through simulation, we have demonstrated that by coordinating the switching point setting of only three sectors in a virtual cell, the proposed simple code/time slot allocation algorithm can substantially reduce the strong base-to-base and mobile-to-mobile cross-slot interference, while maintaining good call blocking performance. Therefore, through the virtual cell-based code/time slot assignment algorithm in the trisector cellular structure, the TDD-CDMA system can have a greater flexibility in supporting asymmetric service by allowing independently setting on the rates of asymmetry in every small area within the entire system.

8.2 Suppressing Opposite Direction Interference in TDD/CDMA Systems with Asymmetric Traffic by Antenna Beamforming

In Chapter 4 and [27,60], we have investigated the effects of beamforming techniques from the perspective of suppressing the opposite direction interference to improve the uplink performance of TDD/CDMA systems. We exploit the synergy of combining the downlink transmitting and uplink receiving beamforming to search a feasible scheme to resolve the opposite direction interference from a network viewpoint. Based on our numerical results, we can draw the following conclusions:

- Schemes IV, which adopts the MVDR beamformer in the uplink and the beam-steering in the downlink, can effectively suppress the strong opposite direction interference of TDD/CDMA systems, thereby allowing every cell to provide asymmetric traffic services with different rates of traffic asymmetry.

- Scheme III, which adopts the beam-steering method in both the downlink trans-

mission and uplink reception, can provide satisfactory performance when the number of cells generating the opposite direction interference is not large. When combined with other sectorization or channel assignment techniques, Scheme III can be a very effective mechanism to overcome the opposite direction interference in the TDD/CDMA system with lower implementation costs.

- If only the uplink beamforming is considered, the MVDR beamformer (Scheme II) instead of the conventional beamforming method (Scheme I) should be adopted since the conventional beam-steering can not effectively suppress the opposite direction interference.

While we have sketched some potential advantages of using antenna beamforming to enhance the downlink performance of TDD/CDMA systems in Section 4.5, it is still worth further investigating the downlink performance improvement in the future studies. In summary, this work has demonstrated the great potential of applying antenna beamforming techniques in the TDD/CDMA system. Even with the severe impact of the opposite direction interference, we find that there exists a feasible and economical beamforming mechanism (e.g. Scheme III suggested in the chapter 3), which can enable the TDD/CDMA system to deliver asymmetric traffic services within the entire service area with greater flexibility.

8.3 A Novel Link Proportional Dynamic Channel Assignment for a Virtual-cell Based TDD/CDMA System with Asymmetric Traffic

In Chapter 5 and [51], we propose a novel link-proportional dynamical channel assignment scheme in TDD/CDMA systems with directional antennas. The proposed

scheme can achieve higher system performance and outperform other DCA algorithms. To design an efficient DCA algorithm, we first analyze the received inter-cell interference in both the uplink and the downlink. Following the analysis results, we propose a novel virtual-cell based DCA mechanism to reduce the overall received interference. The key idea of our proposed scheme is to categorize the cross-slot interference based on the users' locations and then allocate radio resource depending on the users' locations. The performance gain comes from the alleviation of the serious cross-slot interference, intra-cell interference, and same directional inter-cell interference. The proposed approach ensures that the TDD/CDMA system can reliably and flexibly support the asymmetric traffic services.

8.4 Joint Cross-Slot Interference-Based Dynamic Channel Assignment and Antenna Beamforming for the TDD/CDMA Systems with Asymmetric Traffic

In Chapter 6 and [61], we have investigated different DCA algorithms and antenna beamforming techniques to overcome the cross-slot interference in the TDD/CDMA systems with asymmetric traffic. In such a system, both the base-to-base and mobile-to-mobile cross-slot interferences are the major factors to degrade the system performance. With respect to reduce the mobile-to-mobile cross-slot interference, we suggested the improved-region separation method to allocate the users near the cell boundary with the time slots in the edge of a frame, which has less cross-slot interference. As for the base-to-base cross-slot interference, we suggest employing the MVDR beamformer to alleviate base-to-base cross-slot interference. Our numerical

results show that the synergy of combining the cross-slot interference-based DCA and the MVDR beamformer can allow TDD/CDMA system to support asymmetric services with various degrees of traffic asymmetry in different cells.

8.5 A Hierarchical TDD Microcell/FDD Macrocell CDMA System Using Antenna Arrays and Power Ratio Adjustments

In Chapter 7 and [62], we have presented a new hierarchical cell system with an underlaid TDD/CDMA microcell and overlaying FDD/CDMA macrocells. We propose to jointly use the antenna arrays and power ratio adjustment technique to support the co-existence of the FDD/TDD heterogeneous system. In terms of the derived outage probability, we demonstrate that the additional capacity of the TDD/CDMA mircocell can be obtained without degrading the FDD/CDMA marcocell performance.

8.6 Suggestions for Future Research

In the future, some interesting research topics that can be extended from this work includes time-vary fading channel and code reuse with the space/time separation. In the time-varying channel, we can furthermore combine time diversity characteristic to alleviate the co-channel interference and enhance system capacity by adaptive rate allocation. For the code reuse issue, we have considered to apply the same code in the different time slots. However, with the space division between users by beamformer techniques, different users may apply the same code at the same time without experiencing the heavy co-channel interference. Since the available number of codes are limited in the CDMA systems, the space/time code reuse can significantly

improve the system capacity. The results of this thesis have demonstrated the great potential for combining space/time resource allocation in the wireless network. This methodology provides a great deal of flexibility in supporting diverse asymmetric traffic services and improves performance significantly for the TDD/CDMA systems.

Bibliography

[1] 3rd Generation Partnership Project (3GPP) Technical Specification Group Radio Access Network, "Feasibility study for enhanced uplink for utra fdd," *3G TS 25.896 V1.2.1 (2004-01)*, Jun. 2004.

[2] M. Haardt, A. Klein, R. Koehn, S. Oestreich, M. Purat, V. Sommer, and T. Ulrich, "The TD-CDMA based UTRA TDD mode," *IEEE Journal on Selected Areas in Communications*, vol. 18, no. 8, pp. 1375–1385, August 2000.

[3] W. S. Jeon and D. G. Jeong, "Comparison of time slot allocation strategies for CDMA/TDD systems," *IEEE Journal on Selected Areas in Communications*, vol. 18, no. 7, pp. 1271–1278, July 2000.

[4] D. G. Jeong and W. S. Jeon, "CDMA/TDD systems for wireless multimedia services with traffic unbalance between uplink and downlink," *IEEE Journal on Selected Areas in Communications*, vol. 17, no. 5, pp. 939–946, May 1999.

[5] Y. Cao, B. Zhou, and C. Li, "A novel channel allocation scheme to enhance resource utilization in CDMA/TDD," *International Conference on Communication Technology Proceedings* , vol. 2, pp. 821–824, April 2003.

[6] G. J. R. Povey and M. Nakagawa, "A review of Time Division Duplex - CDMA techniques," *in Proc. ISSSTA'98*, vol. 2, pp. 630–633, Sept. 1998.

[7] H. Holma and A. Toskla, WCDMA `for` UMTS. John Wiley & Sons, 2000.

[8] H. Holma, S. Heikkinen, O.-A. Lehtinen, and A. Toskala, "Interference considerations for the time division duplex mode of UMTS terrestrial radio access," *IEEE Journal on Selected Areas in Communications*, vol. 18, no. 8, pp. 1386–1393, August 1998.

[9] G. J. R. Povey, "Effects of synchronization and asymmetry in UTRA TDD," *Proceedings of 3G Mobile Communication Technolohies Conference*, pp. 86–88, March 2000.

[10] W. S. Jeon and D. G. Jeong, "Time slot allocation in CDMA/TDD systems for mobile multimedia services," *IEEE Communication Letters*, vol. 4, no. 7, pp. 1271–1278, July 2000.

[11] H. Yomo and S. Hara, "An uplink/downlink asymmetric slot allocation algorithm in CDMA/TDD-based wireless multimedia communications systems," *IEEE Vehicular Technology Conference*, vol. 2, pp. 797–801, Oct. 2001.

[12] S. H. Wie and D. H. Cho, "Time slot allocation schemes based on a region division in CDMA/TDD systems," *IEEE Vehicular Technology Conference*, vol. 4, pp. 2445–2449, May 2001.

[13] J. Nasreddine and X. Lagrange, "Time slot allocation based on a path gain division scheme for TD-CDMA TDD systems," *IEEE Vehicular Technology Conference*, vol. 2, pp. 1410–1414, April 2003.

[14] W. Jeong and M. Kavehrad, "Cochannel interference reducation in dynamic-TDD fixed wireless applications using time slot allocation algorithms," *IEEE Transactions on Communications*, vol. 50, pp. 1627–1636, Oct. 2002.

[15] R. L.-U. Choi and R. D. Murch, "Evaluation of a pre-rake smart antenna system for TDD CDMA systems," *IEEE Vehicular Technology Conference*, vol. 2, pp. 1543–1547, Oct. 2001.

[16] E. Mitjana, X. Song, L. Lu, M. Haardt, C. Gessner, G. Lehmann, and M. Vollmer, "Performance of smart antenna in TD-SCDMA system," *Proc. International Conference on Communication Technology*, vol. 1, pp. 152–155, 2000.

[17] L. C. Wang, S. Y. Huang, and Y. C. Tseng, "A novel interference-resolving algorithm to support asymmetric services in TDD-CDMA systems with directional antennas," *IEEE Vehicular Technology Conference*, vol. 1, pp. 327–330, May. 2002.

[18] S. S. Choi and D. H. Cho, "Coordinated resource allocation scheme for forward link in sectorized CDMA systems," *IEEE Vehicular Technology Conference*, vol. 4, pp. 2356–2360, Sept. 2002.

[19] L. C. Godara, "Application of antenna arrays to mobile communications, part i: performance improvements, feasibility, and system considerations," *Proceedings of IEEE*, vol. 85, pp. 1031–1060, July 1997.

[20] P. V. Rooyen, M. P. Lötter, and D. V. Wyk, *Space-Time Processing for* CDMA *Mobile Communications.* Kluwer, 2000.

[21] L. C. Godara, "Performance analysis of CDMA mobile communication systems using antenna arrays," *IEEE Proc. ICASSP*, vol. 85, pp. 153–156, July 1993.

[22] A. F. Naguib, A. Paulraj, and T. Kailath, "Capacity improvement with base-station antenna arrays in cellular CDMA," *IEEE Transactions on Vehicular Technology*, vol. 43, pp. 691–698, Aug. 1994.

[23] F. Rashid-Farrokhi, K. Liu, and L. Tassiulas, "Transmit beamforming and power control for cellular wireless systems," *IEEE Journal on Selected Areas in Communications*, vol. 16, pp. 1437–1450, Oct. 1998.

[24] H. Boche and M. Schubert, "Analysis of sir based-downlink beamforming," *IEICE*, vol. E85-B, pp. 1160–1168, June 2002.

[25] X. Wu, L. L. Yang, and L. Hanzo, "Uplink capacity investigations of TDD/CDMA," *IEEE Vehicular Technology Conference*, vol. 2, pp. 997–1001, May 2002.

[26] H. Holma, G. Povey, and A. Toskala, "Evaluation of interference between uplink and downlink in UTRA/TDD," *IEEE Vehicular Technology Conference*, vol. 5, pp. 2616–2620, Sept. 1999.

[27] C. J. Chen and L. C. Wang, "Supressing opposite direction interference in TDD/CDMA systems with asymmetric traffic by antenna beamforming," *will appear on IEEE Transactions on Vehicular Technology*, 2004.

[28] H. Haas, S. McLaughlin, and G. J. R. Povey, "A novel interference resolving algorithm for the TDD TD-CDMA mode in UMTS," *IEEE Personal, Indoor and Mobile Radio Communications*, pp. 1231–1235, Sep. 2000.

[29] O. Lehtinen and J. Kurjenniemi, "UTRA TDD dynamic channel allocation in uplink with slow reallocation."

[30] K. Pahlavan and A. Levesque, *Wireless information networks.* John Wiley & Sons, 1995.

[31] K. S. Gilhousen, I. M. Jacobs, R. Padovani, A. J. Viterbi, L. A. Weaver, and C. Wheatly, "On the capacity of a cellular CDMA system," *IEEE Transactions on Vehicular Technology*, vol. 40, pp. 303–312, May 1991.

[32] J. P. Linnartz, *Narrowband Land-Mobile Radio Networks.* Artech House, 1993.

[33] H. Haas and S. McLaughlin, "A dynamic channel assignment algorithm for a hybrid TDMA/CDMA-TDD interface using the novel TS-opposing technique," *IEEE Journal on Selected Areas in Communications*, vol. 19, pp. 1831–1846, Oct. 2001.

[34] A. J. Viterbi, A. M. Viterbi, and E. Zehavi, "Other-cell interference in cellular power-controlled CDMA," *IEEE Transactions on Communications*, vol. 42, pp. 1501–1504, Apr. 1994.

[35] R. A. Monzingo and T. W. Miller, *Introduction to Adaptive Arrays.* John Wiley & Sons, 1980.

[36] J. Litva and T. K. Y. Lo, *Digital Beamforming in Wireless Communications*. Artech House, 1996.

[37] L. C. Godara, "Application of antenna arrays to mobile communications, part ii: beam-forming and direction-of-arrival considerations," *Proceedings of IEEE*, vol. 85, pp. 1195–1245, Aug. 1997.

[38] B. H. Khalaj, A. J. Paulraj, and T. Kailath, "2D rake receivers for cdma cellular systems," *Proceedings of IEEE Global Telecommunications Conference* , vol. 1, pp. 400–404, Nov. 1994.

[39] A. J. Paulraj and C. B. Papadias, "Space-time processing for wireless communications," *IEEE Signal Processing Magazine*, vol. 1, pp. 49–83, Nov. 1997.

[40] J. H. Chang, L. Tassiulas, and F. R. Farrokhi, "Joint transmitter receiver diversity for efficient space division multiaccess," *IEEE Transactions on Communications*, vol. 1, pp. 16–27, Jan. 2002.

[41] F. R. Farrokhi, A. Lozano, G. J. Foschini, and R. A. Valenzuela, "Spectral efficiency of FDMA/TDMA wireless systems with transmit and receive antenna arrays," *IEEE Transactions on Communications*, vol. 1, pp. 591–599, Oct. 2002.

[42] I. Forkel, B. Wegmann, and E. Schulz, "On the capacity of a UTRA-TDD network with multiple services," *IEEE International Conference on Communications*, vol. 1, pp. 585–598, May 2002.

[43] 3rd Generation Partnership Project (3GPP) Technical Specification Group Radio Access Network, "Physical channels and mapping of transport channels onto physical channels (TDD)," *3G TS 25.221 V3.1.1 (1999-12)*, Dec. 1999.

[44] H. Haas, B. Wegmann, and S. Flanz, "Interference diversity through random time slot opposing (RTO) in a cellular TDD system," *IEEE Vehicular Technology Conference*, vol. 3, pp. 24–28, Sept. 2002.

[45] L.-C. Wang, S.-Y. Huang, and Y.-C. Tseng, "Interference analysis of TDD-CDMA systems with directional antennas," *IEEE Vehicular Technology Conference*, vol. 2, pp. 2445–2449, Oct. 2003.

[46] 3rd Generation Partnership Project (3GPP) Technical Specification Group Radio Access Network, "TDD base station classification," *3G TS 25.952 (Release 4)*, 2001.

[47] ETSI, "Selection procedures for the choice of radio transmission technologies of the UMTS," *ETSI/SMG2 TR 101 112, UMTS 30.03 version 3.2.0*, April 1998.

[48] J. Nasreddine and X. Lagrange, "Power control and slot allocation in TD-CDMA system," *IEEE Vehicular Technology Conference*, vol. 2, pp. 880–884, May 2002.

[49] J. Liu, Y. Yuan, L. Xu, R. Wu, Y. Dai, Y. Li, L. Zhang, M. Shi, and Y. Du, "Research on smart antenna technology terminals for the TD-SCDMA system," *IEEE Communications Magazine*, pp. 116–119, June 2003.

[50] W. Jeong and M. Kavehrad, "Cochannel interference reduction in dynamic-TDD fixed wireless applications, using time slot allocation algorithms," *IEEE Communications Magazine*, vol. 50, pp. 1627–1636, Oct. 2002.

[51] L. C. Wang and Y. C. Chen, "A novel link proportional dynamic channel assignment for TDD-CDMA systems with directional antennas," *IEEE International Conference on Networking, Sensing And Control*, pp. 164–169, March 2004.

[52] A. Naguib, A. Paulraj, and T. Kailath, "Capacity improvement with base-station antenna arrays in cellular CDMA," *IEEE Transactions on Vehicular Technology*, vol. 43, pp. 691–698, Aug. 1994.

[53] H. V. Trees, *Optimum Array Processing*. John Wiley & Sons, 2002.

[54] D. Kim, P. Song, and C. Kang, "Capacity analysis of TDD cell sharing underutilized FDD uplink," *IEEE Vehicular Technology Conference*, vol. 4, pp. 24–28, May 2001.

[55] W. Wong and E. S. Sousa, "Feasibility study of TDD- and FDD-CDMA frequency sharing cellular networks," *IEEE ICUPC*, vol. 1, pp. 531–535, Oct. 1998.

[56] H. Haas and G. J. R. Povey, "A capacity investigation on UTRA-TDD utilising underused UTRA-FDD uplink resources," *IEE Colloquium*, pp. 7/1–7/6, Apr. 1999.

[57] J. C. Liberti and T. Rappaport, *Smart Antennas for Wireless Communications*. Prentice Hall, 1999.

[58] M. Lindstrom, "Improved TDD resource allocation through inter-mobile interference avoidance," *IEEE Vehicular Technology Conference*, vol. 2, pp. 1027–1031, May 2001.

[59] L.-C. Wang, S.-Y. Huang, and Y.-C. Tseng, "Interference analysis and resource allocation for TDD-CDMA systems to support asymmetric services by using directional antennas," *IEEE Transactions on Vehicular Technology (accepted)*.

[60] C.-J. Chen and L.-C. Wang, "Interference suppression in TDD/CDMA cellular systems with asymmetric traffic using MVDR beamforming," *IEEE Vehicular Technology Conference*, vol. 1, pp. 24–28, Sept. 2002.

[61] L. C. Wang and Y. C. Chen, "Joint cross-slot interference-based dynamic channel assignment and antenna beamforming for the TDD/CDMA systems with asymmetric traffic," *to be submitted*.

[62] C.-J. Chen and L.-C. Wang, "A hierarchical TDD microcell/FDD macrocell CDMA system using antenna arrays and power ratio adjustments," *Proceedings of IEEE Global Telecommunications Conference* , vol. 2, pp. 1945–1949, Nov. 2002.